

Comments by **reviewer #1** are reproduced in a black font below. Our responses follow each comment in a blue font. Text additions to the manuscript, for example, significantly modified sentences, appear in the revised manuscript in red color. Deletions from the manuscript are not explicitly shown but are described in the responses below. Minor editorial edits to the text are not explicitly shown to prevent a cluttered view.

We thank the reviewer for the comments, which we have addressed in a point by point fashion below.

Urban organic aerosol composition in Eastern China differs from North to South: Molecular insight from a liquid chromatography-Orbitrap mass spectrometry study Wang et al.

This paper describes the results from the analysis of organic aerosol collected at three Chinese cities during haze events using a high resolution method. The paper is within the scope of ACP and is well written and easy to follow. A very careful analysis of the data is presented and the methods applied for formula assignment are appropriate. I agree that the organic aerosol in the North is likely to be more influenced by coal combustion and the warmer cities in the South more affected by photochemistry. However, I don't think that the data in this paper is sufficient to draw those conclusions. Far too much weight is given to very small differences in O:C and DBE based on peak area only, without any discussion about the impact of structure on ionization efficiency or any estimate of the uncertainty in these values. For instance on page 11, line 335, is a difference of 0.11 between the DBE from Shanghai and Guangzhou a meaningful difference? Nitrophenol species can have vastly different ionisation efficiencies in ESI- depending on the position of the constituents on the ring (see Schmidt et al., 2006. <https://onlinelibrary.wiley.com/doi/full/10.1002/rcm.2591>). These nitrophenols are some of the dominant species detected in this study and thus their peak area will have a significant impact on the calculation of DBE and O:C. They also effect the calculation of Xc since they give incorrect values using $p=0.5$. The ionization efficiency of carboxylic acids also depends on structure and can vary by several orders of magnitude. Compounds with the same formula such as an unsaturated hydroxy-acids and a carbonyl-acid are likely to have very different ionisation efficiencies (Leito et al., 2008. <https://onlinelibrary.wiley.com/doi/pdf/10.1002/rcm.3371>, Krueve et al., 2014 <https://pubs.acs.org/doi/full/10.1021/ac404066v>). The data presented is interesting and shows there are differences in composition between the three locations. But I would not recommend publication in ACP without major changes to the way the average peak area weighted metrics are used to draw conclusions.

Response: We thank the reviewer for pointing out the uncertainties existing in the peak abundance weighted comparison caused by the different ionization efficiencies among different compounds. Actually, we mentioned these uncertainties in Page 7, Line 202-204 in the original manuscript as well as in the original SI. Because OA is highly complex and authentic standards are limited, the identification and quantification of OA components are a challenging analytical task and it is very difficult to avoid ionization efficiency related

uncertainties. Since the conclusions drawn in this study are mainly based on the peak abundance weighted comparison, we now emphasize the uncertainties in the sections of Abstract (Page 2, Line 50-53) and Limitations (Page 18, Line 555-571) in the revised manuscript as follows:

Abstract: "...It should be noted that the conclusions drawn in this study are mainly based on comparison of molecular formulas weighted by peak abundance, and thus, are associated with inherent uncertainties due to different ionization efficiencies for different organic species."

Limitations: "In this study, we used the peak abundance-weighted method to illustrate the difference in chemical formulas assigned by Orbitrap mass spectrometry. This comparison was made based on the assumption that the measured organic compounds have same peak abundance response in the mass spectrometer. However, this assumption can bring some uncertainties because the ionization efficiencies vary between different compounds (Schmidt et al., 2006; Leito et al., 2008; Perry et al., 2008; Krueve et al., 2014). For example, the ionization efficiencies of nitrophenol species detected in negative ESI mode can vary by a large degree depending on the position of the substituents at the nitrobenzene ring (Schmidt et al., 2006; Krueve et al., 2014) and the ionization efficiencies of carboxylic acids can also vary by several orders of magnitude depending on the structures (Krueve et al., 2014). Nonetheless, it is a challenging analytical task to identify and quantify all compounds in ambient OA due to the high chemical complexity of OA and the limits in authentic standards of OA. Despite the inherent uncertainties, the peak abundance-weighted comparison of molecular formulas provides an overview of the difference in chemical composition of OA in these three representative Chinese cities. In particular, the chemical formulas assigned in this study can be validated in future studies by authentic standards and the difference in ionization efficiencies can be further evaluated."

Specific comments

Abstract: There needs to be a comment in the abstract about the uncertainties of using this approach.

Response: A statement about the uncertainties has been now added in the Abstract (Page 2, Line 50-53 in the revised manuscript) as follows:

"It should be noted that the conclusions drawn in this study are mainly based on comparison of molecular formulas weighted by peak abundance, and thus, are associated with inherent uncertainties due to different ionization efficiencies for different organic species."

Chromatography: This paper uses UPLC to separate the species and where isomers are found, they are recombined to produce the reconstructed mass spectra and various figures. It seems a waste to have so much

isomeric speciation and then not use any of it. For instance, how many isomers were found on average per molecular formula? A similar analysis could have been achieved by direct injection into the source. While using chromatography may minimise matrix effects, the lack of information on whether structure effects ionisation efficiency counteracts its usefulness.

Response: The important advantage of the application of UPLC in this study is that compounds are separated by the LC-column before they enter the ionization source, minimizing the matrix effects. Meanwhile, the compounds are concentrated in the LC-column, which can increase the sensitivity of the measurement. In addition, it can provide separation of some compounds and information of retention time of the compounds, which is useful for the identification of the compounds and the separation of isomers. This statement is now added in Page 5, Line 142-147 (also see it below). Since the numbers of isomer vary a lot depending molecular formulas, we have added the term named isomer number fraction (meaning the percentage of formula numbers that have isomers among all assigned formulas) in the revised Table 1. It shows that 31-34% and 30-56% of formulas have isomers in negative mode and positive mode, respectively. In addition, we now define the common formulas observed in all samples as the formulas that have the same molecular formulas and the same retention time (retention time difference ≤ 0.1 min).

“Compared to the direct infusion method applied in other UHRMS studies (Lin et al., 2012a; Lin et al., 2012b; Rincón et al., 2012; Kourtchev et al., 2016; Fleming et al., 2018), the UHPLC technique was used in this study, which could separate and concentrate the compounds before they entered the ion source, reducing the ionization suppression and increasing the sensitive of the measurement. In addition, it can provide separation of some compounds and information of retention time of the compounds, which is useful for the identification of the compounds and the separation of isomers.”

Page 6, line 162: When first reading this I struggled to understand how the values for p and q were derived. I found the information in the SI, but this needs to be included in the main paper, alongside a discussion of the uncertainties and issues using this approach.

Response: The detailed description of the aromaticity equivalent (X_c) and the values of p and q in the equation is now stated in Page 6, line 171-185 in the main paper as follows:

“The aromaticity equivalent (X_c) as a modified index for aromatic compounds was obtained using the equation: $X_c = [3(\text{DBE} - (p \times o + q \times n)) - 2] / [\text{DBE} - (p \times o + q \times n)]$, where p and q, respectively, refer to the fraction of oxygen and sulfur atoms involved in the π -bond structure of a compound. As such the values of p and q vary between compound categories (Yassine et al., 2014). For example, carboxylic acids and esters are

characterized using $p = q = 0.5$, while $p = q = 1$ and $p = q = 0$ are used for carbonyl and hydroxyl, respectively. Since it is impossible to identify the structures of the hundreds of formulas observed in this study, we cannot know the exact values of p and q in an individual compound. Therefore, in this study, $p = q = 0.5$ was applied for compounds detected in ESI⁻ as carboxylic compounds are preferably ionized in negative mode. However, because of the high complexity of the mass spectra in ESI⁺, $p = q = 1$ was used in ESI⁺ to avoid an overestimation of the amount of aromatics. Moreover, for $\text{DBE} \leq (p \times o + q \times n)$ or $X_c \leq 0$, X_c was defined as zero. Furthermore, in ESI⁻, for odd numbers of $(p \times o + q \times n)$, the value of $(p \times o + q \times n)$ was rounded down to the lower integer. $X_c \geq 2.50$ and $X_c \geq 2.71$ have been suggested as unambiguous minimum criteria for the presence of monoaromatics and polyaromatics, respectively (Yassine et al., 2014).”

Page 7, line 189-200: The authors need to be careful with the use of the word significant here. It is impossible to tell if the values are significantly different without an estimate of the uncertainty in the values. An H:C of 1.03 does not seem “significantly lower” than a value of H:C = 1.05. What is the spread in the values between the three replicates? Again, this whole section assumes that peak area = abundance and that the differences in OC are driven by oxidation and not different sources.

Response: The word ‘significant’ is now carefully used and the sentences related to ‘significant difference’ is now rephrased throughout the manuscript. The effect of OA sources on the chemical composition (e.g., the different O/C ratio) is now added in the discussion throughout the revised manuscript (also see it below).

Page 2, Lines 44-47: “Moreover, the ESI⁻ analysis showed higher H/C and O/C ratios for organic compounds in Shanghai and Guangzhou compared to samples from Changchun, indicating that OA undergoes more intense photochemical oxidation processes in lower latitude regions of China and/or is affected to a larger degree by biogenic sources.”

Page 8, Lines 235-240: “The different chemical composition of the samples is probably caused by... or by different biogenic/anthropogenic precursors.”

Page 10, Lines 307-309: “Altogether, these results indicate that CHO⁻ compounds in urban OA from East and Southeast China experienced more intense oxidation and aging processes and/or were affected to a larger degree by biogenic sources.”

Page 10-11, Lines 313-315: “Again, these average formulas show that CHO⁻ in Shanghai⁻ and Guangzhou⁻ experienced more intense oxidation processes and/or were affected to a larger degree by biogenic precursors, indicated by the larger abundance-weighted MM_{avg} with a higher degree of oxygenation.”

Page 8, line 230: In the reconstructed mass spectra in figure 1, the ESI+ spectra from Shanghai and Guangzhou seem to be dominated by a single ion. What is this ion and how does this affect the calculation of the % abundance of CHN+? Page 8, line 250: Are the 52 common formulas the same chromatographic peak, or is it just the formula that is common? Page 9, line 258: The Van Krevelen plots in S1 look fairly similar for compounds of high O:C, I don't really see any substantial difference. Page 9, line 266. I don't agree that these average abundance weighted formulas can be used to state that the Shanghai and Guangzhou OA experienced "more intense oxidation". Certainly the MF have a higher amount of O and a lower amount of C but this could also be related to the sources of the OA, with more biogenic/aliphatic material in the south.

Response:

1. In Shanghai and Guangzhou samples, the ion with molecular formula of $C_{10}H_{14}N_2$ is dominant among all CHN+ compounds, which is probably due to its high concentration and/or high ionization efficiency in ESI+. This ion accounts for 63% and 52% in terms of peak abundance in Shanghai and Guangzhou CHN+ compounds, respectively. The discussion about this ion is now added to Page 14, line 438-442 in the revised manuscript, as follows:

"Remarkably, as can be seen in Fig. 6, the abundance of CHN+ compounds in Changchun+ distribute evenly among different individual CHN+ compounds, while in Shanghai+ and Guangzhou+ they are dominated by the formula of $C_{10}H_{14}N_2$ (the biggest purple circle in Fig. 6) with DBE value of 5, which probably has high concentration and/or high ionization efficiency in the positive ESI mode."

2. In the original manuscript, the common formulas just refer to the same formula and do not refer to the same chromatographic peaks. Now, in the revised manuscript we define the common formulas observed in all samples as the formulas that have both the same molecular formulas and the same retention time (retention time difference ≤ 0.1 min). It shows that most of compounds with the same molecular formulas have similar retention time. And the Figure 2 about the new definition of common formulas is now redrawn in the revised manuscript (please see the revised Figure 2 below).

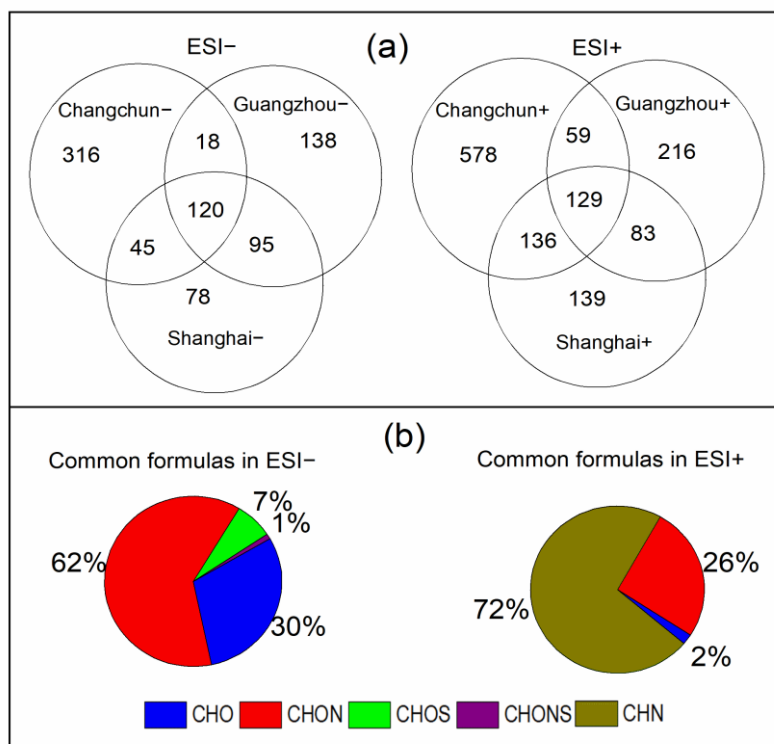


Figure 2. (a) Venn diagrams showing the number distribution of all molecular formulas detected in ESI⁻ and ESI⁺ for all sample locations. The overlapping molecular formulas refer to the compounds detected in each city with the same molecular formulas and with the same retention times (retention time difference ≤ 0.1 min). (b) Peak abundance contribution of each elemental formula category to the total common formulas.

3. Since the Van Krevelen diagram is plotted by the O/C and H/C, it hides the compounds with different formulas but with the same O/C and H/C and is not the best tool to present the difference of compounds with high O/C in these three samples. Therefore, we have calculated the relative peak abundance fraction of CHO⁻ compounds with O/C ≥ 0.6 (which are considered as highly oxidized compounds, please see the reference ‘Tu et al., 2016, Analytical Chemistry’) in all samples measured in the negative mode. It shows that 14% of compounds in terms of peak abundance in Changchun⁻ have O/C ratio larger than 0.6, while they are relatively higher in Shanghai⁻ and Guangzhou⁻ samples, accounting for 34% in Shanghai and 45% in Guangzhou. The Figure S1 in Supporting Information is now removed and the following discussion is now added in Page 10, line 304-307 in the revised manuscript.

“Furthermore, the relative peak abundance fraction of CHO⁻ compounds with O/C ≥ 0.6 , which are considered as highly oxidized compounds (Tu et al., 2016), is 14% in Changchun and somewhat higher in Shanghai⁻ (34%) and Guangzhou⁻ (45%).”

Tu, P., Hall, W. A. t., and Johnston, M. V.: *Characterization of Highly Oxidized Molecules in Fresh and Aged Biogenic Secondary Organic Aerosol*, *Anal. Chem.*, 88, 4495-4501, 10.1021/acs.analchem.6b00378, 2016

4. Yes, we agree that the sources of SOA may also affect the chemical composition of aerosols. Therefore, the conclusion is now modified in Page 10, line 313-315 in the revised manuscript as follows:

“these average formulas show that CHO– compounds in Shanghai– and Guangzhou– experienced more intense oxidation processes and/or were affected to a larger degree by biogenic sources, indicated by the larger abundance-weighted MM_{avg} with a higher degree of oxygenation.”

Page 10, line 289: When discussing “individual” compounds, do you mean peaks? For these formulas, how many peaks were observed? For these species discussed, i.e. $C_8H_8O_3$, why have you chosen these specific oxidation products of estragole? Surely this could also be biomass burning emissions such as vanillin?

Response: 1. They refer to individual formulas. For clarification, we have rephrased the sentence from “through mass spectrometric analysis of individual compounds” to “through the analysis of individual formulas”. There are 3-4, 1-2, 1-4, 1-5, 2-8 peaks were observed for formulas of $C_8H_6O_4$, $C_7H_6O_2$, $C_7H_6O_3$, $C_8H_8O_2$, and $C_8H_8O_3$, respectively, in these three cities. 2. For the discussion about the source of these specific compounds, we checked these compounds in the aerosol-related literatures, in which these compounds were also observed. Yes, the compounds with formula of $C_8H_8O_3$ could also be suggested to vanillin emitted from biomass burning. We have now considered ‘vanillin’ as one possible compound of $C_8H_8O_3$ and the related discussion is now revised in Page 11, Line 343-345 as follows:

“ $C_8H_8O_2$ is likely 4-hydroxy acetophenone, which could be derived from estragole (Pereira et al., 2014), while $C_8H_8O_3$ is suggested to be either 4-methoxybenzoic acid generated from estragole (Pereira et al., 2014) or vanillin emitted from biomass burning (Li et al., 2014).”

Page 25, figure 2: In the upper panel, the Venn diagrams need to be labelled as ESI+ and ESI-. Also, the Guangzhou circle in the Venn Diagram has 304 compounds but in the table there are 488 compounds. Why are they different?

Response: The label of ESI+ and ESI- is now added in the revised Venn diagram in Figure 2. The number in the Venn diagram refers to the number of the formulas. However, the number of compounds in Table 1 refer to the number of peaks, which is higher compared to the number of formulas due to the isomers. In addition, the information of formula numbers for each compound group is now added in the revised Table 1.

Page 26, Figure 3: Can you explain why the dots are scaled to the fourth root of the peak area? I assume it is to reduce the size of the largest peaks. However, this is not mentioned in the text and could be easily missed in the caption. This should be clearly stated in the text. I would also like to see these figures with the observed peak area for comparison in the SI.

Response: Yes, the purpose for the use of the fourth root of the peak area is to reduce the size difference of the dots related to different formulas, because the peak areas vary a lot between different formulas. For clarification, the following statement is now added in Page 10, line 284-288 in the revised manuscript (also see it below). Meanwhile, the figures with the size of dot related to the absolute peak area are now added in the SI (also see them below: Figure S2 of DBE vs. C-atom numbers for CHO⁻; Figure S6 of DBE vs. C-atom numbers for CHON⁻; Figure S8 of DBE vs. C-atom numbers for CHON⁺; Figure S10 of H/C vs. N/C for CHN⁺; Figure S11 of DBE vs. C-atom numbers for CHOS⁻).

“In addition, since peak abundances for the formula can vary by orders of magnitude, the area of the circles presented in the Figure 3 and Figures 5–7 is proportional to the fourth root of the peak abundance of each formula to reduce the size difference of the circles. For a more detailed comparison, figures with the circle size related to the absolute peak abundances are presented in the SI.”

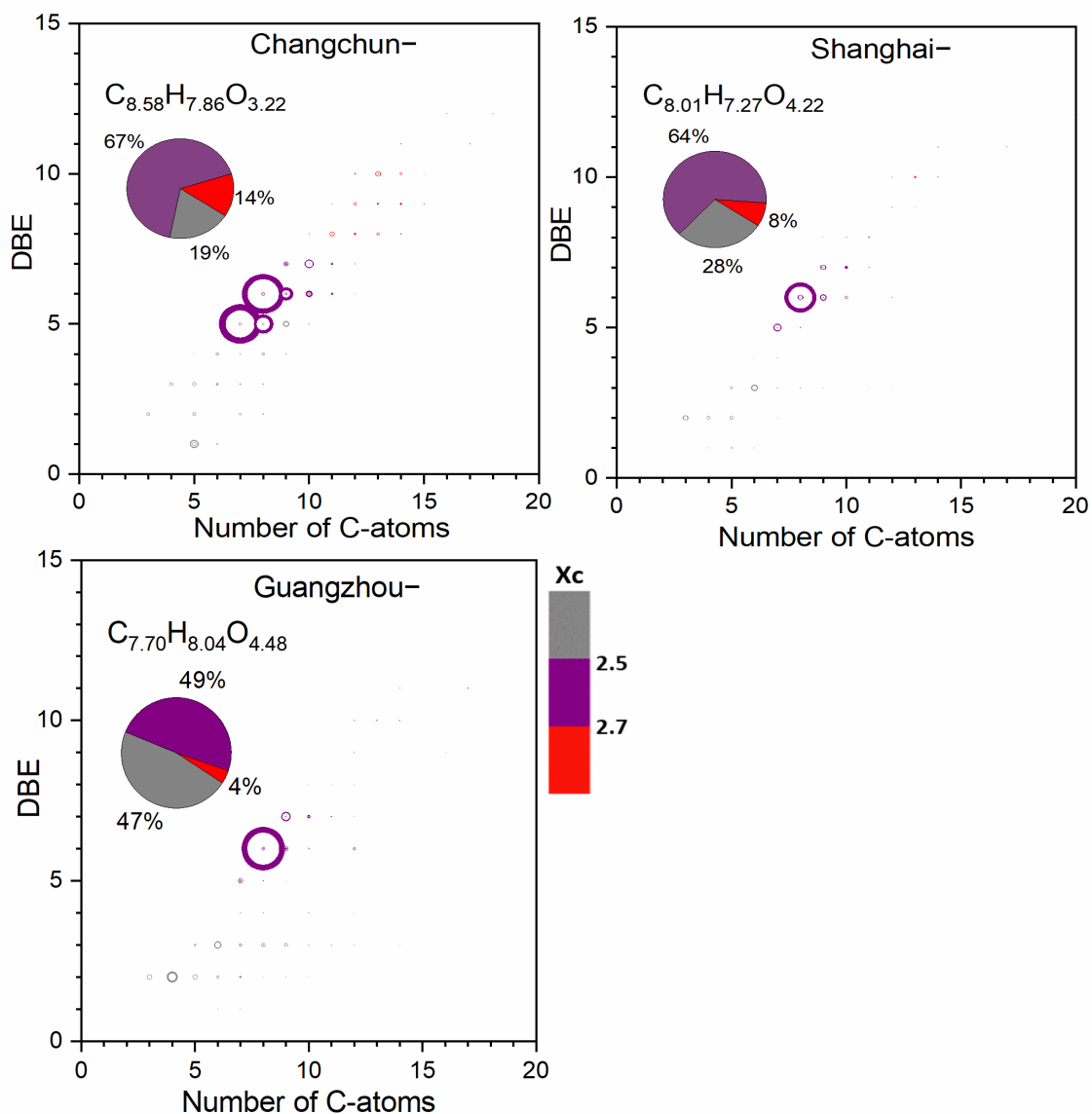


Figure S2. Double bond equivalent (DBE) versus carbon number for all CHO⁻ compounds for all sample locations. The molecular formula represents the abundance-weighted average CHO⁻ formula and the area of the circles is proportional to the absolute peak abundance of an individual compound. The color bar denotes the aromaticity equivalent (gray with X_c < 2.50, purple with 2.50 ≤ X_c < 2.70 and red with X_c ≥ 2.70). The pie charts show the percentage of each X_c category (i.e., gray color-coded compounds, purple color-coded compounds and red color-coded compounds) in each sample in terms of peak abundance.

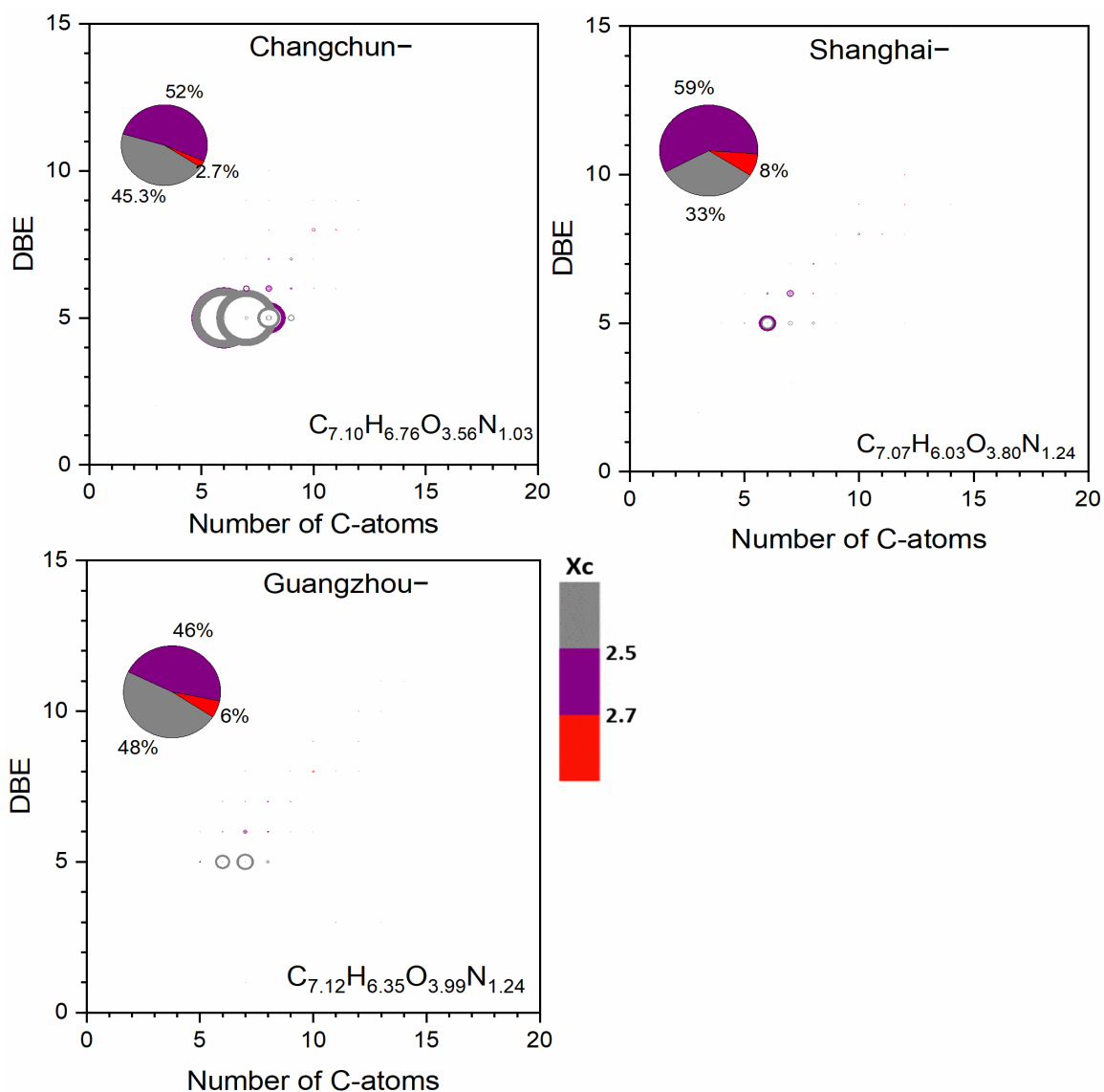


Figure S6. Double bond equivalent (DBE) versus carbon number for all CHON- compounds for all sample locations. The molecular formula represents the abundance-weighted average CHON- formula and the area of circles is proportional to the absolute peak abundance of an individual compound. The color bar denotes the aromaticity equivalent (gray with $X_c < 2.50$, purple with $2.50 \leq X_c < 2.70$ and red with $X_c \geq 2.70$). The pie charts show the percentage of each X_c category (i.e., gray color-coded compounds, purple color-coded compounds and red color-coded compounds) in each sample in terms of peak abundance.

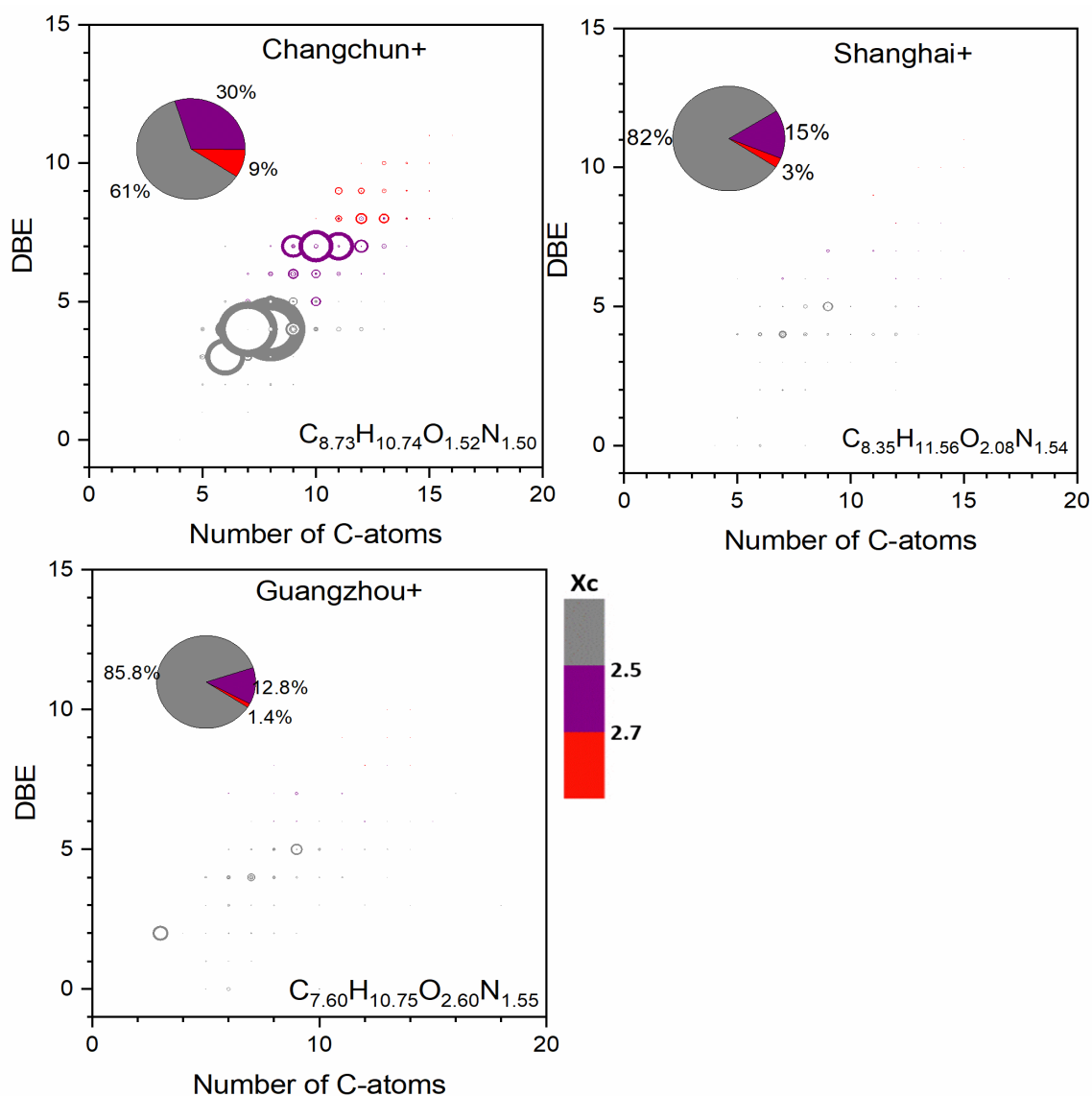


Figure S8. Double bond equivalent (DBE) vs C number for all CHON+ compounds of all samples. The molecular formula represents the abundance-weighted average CHON+ formula and the area of the circles is proportional to the absolute peak abundance of an individual compound. The color bar denotes the aromaticity equivalent (gray with $X_c < 2.50$, purple with $2.50 \leq X_c < 2.70$ and red with $X_c \geq 2.70$). The pie charts show the percentage of each X_c category (i.e., gray color-coded compounds, purple color-coded compounds and red color-coded compounds) in each sample in terms of peak abundance.

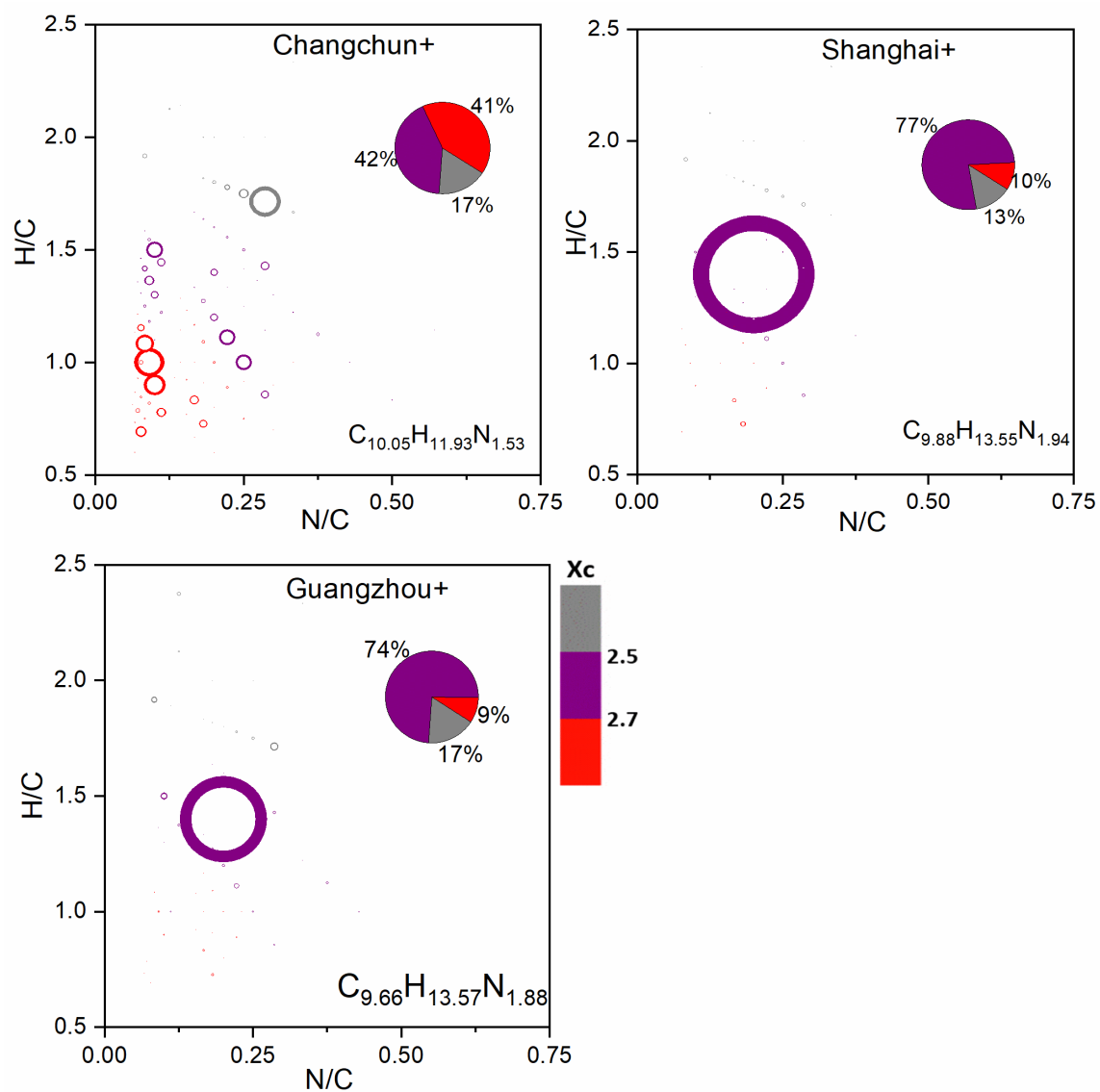


Figure S10. Van Krevelen diagrams for CHN+ compounds in Changchun, Shanghai and Guangzhou samples. The area of circles is proportional to the absolute peak abundance of an individual compound and the color bar denotes the aromaticity equivalent (gray with $X_c < 2.50$, purple with $2.50 \leq X_c < 2.70$ and red with $X_c \geq 2.70$). The pie charts show the percentage of each Xc category (i.e., gray color-coded compounds, purple color-coded compounds and red color-coded compounds) in each sample in terms of peak abundance.

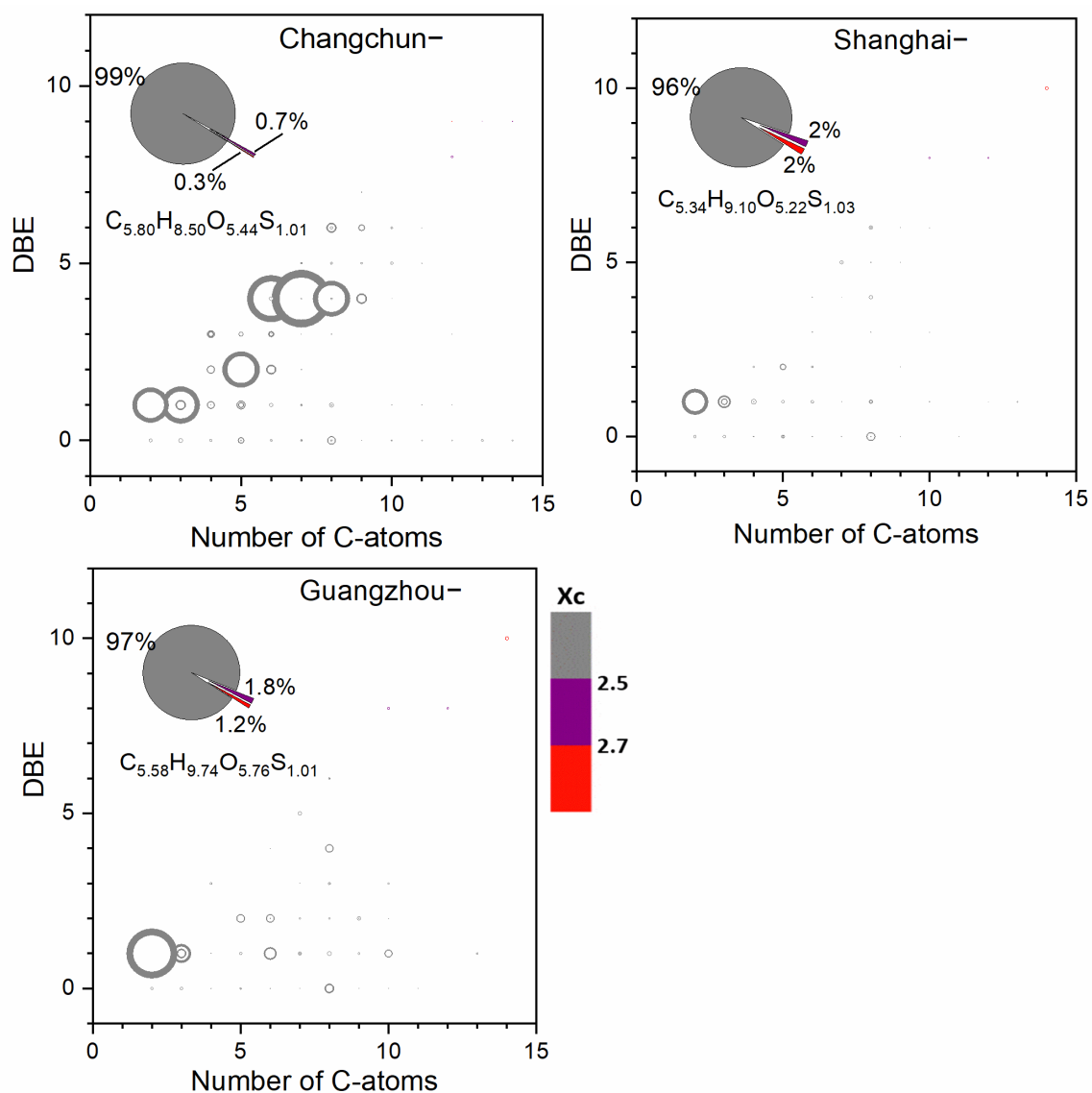


Figure S11. Double bond equivalent (DBE) versus carbon number for all CHOS⁻ compounds for all sample locations. The molecular formula represents the abundance-weighted average CHOS⁻ formula and the area of circles is proportional to the absolute peak abundance of an individual compound. The color bar denotes the aromaticity equivalent (gray with $X_c < 2.50$, purple with $2.50 \leq X_c < 2.70$ and red with $X_c \geq 2.70$). The pie charts show the percentage of each X_c category (i.e., gray color-coded compounds, purple color-coded compounds and red color-coded compounds) in each sample in terms of peak abundance.

Minor comments

Page 3, line 64: Change “comprehended” to “understood”.

Response: “comprehended” is now changed to “understood”.

Page 4, line 104: I would help the reader to know a little bit more about the differences in industrial structure, energy etc.

Response: The city of Changchun is located in Northeast of China, which was used to be the center of heavy industry of China (Zhang, Chinese Geographical Science, 2008). The heavy industries like the coal chemistry industry and steelworks can produce a large amount of air pollutants (e.g., NO_x and SO₂), which can affect the chemical composition of aerosols in this area. However, the cities of Shanghai and Guangzhou are located in the East Coast of China, where there are much less of heavy industries. Moreover, another important factor is that residential heating (i.e. coal combustion) is extensively used in wintertime in Northeast of China, which can make a large contribution to the PM_{2.5} mass (Huang et al., Nature 2014; An et al., PNAS 2019). And, these statements are now added in Page 4, line106-111, in the revised manuscript as follows:

“In addition, the industrial structure, energy consumption and energy sources in these three cities are different, such as much more heavy industries (e.g., coal chemical industry and steelworks) in Northeast China (Zhang, 2008), which can cause difference in anthropogenic emissions, and can therefore influence the chemical composition of urban OA. Moreover, OA is strongly affected by residential coal combustion during winter in Northeast China (Huang et al., 2014; An et al., 2019).”

Zhang, P.: *Revitalizing old industrial base of Northeast China: Process, policy and challenge*, *Chin. Geogra. Sci.*, 18, 109-118, 10.1007/s11769-008-0109-2, 2008

Huang, R. J., Zhang, Y., Bozzetti, C., Ho, K. F., Cao, J. J., Han, Y., Daellenbach, K. R., Slowik, J. G., Platt, S. M., Canonaco, F., Zotter, P., Wolf, R., Pieber, S. M., Bruns, E. A., Crippa, M., Ciarelli, G., Piazzalunga, A., Schwikowski, M., Abbaszade, G., Schnelle-Kreis, J., Zimmermann, R., An, Z., Szidat, S., Baltensperger, U., El Haddad, I., and Prevot, A. S.: *High secondary aerosol contribution to particulate pollution during haze events in China*, *Nature*, 514, 218-222, 10.1038/nature13774, 2014.

An, Z., Huang, R. J., Zhang, R., Tie, X., Li, G., Cao, J., Zhou, W., Shi, Z., Han, Y., Gu, Z., and Ji, Y.: *Severe haze in northern China: A synergy of anthropogenic emissions and atmospheric processes*, *Proc Natl Acad Sci U S A*, 116, 8657-8666, 10.1073/pnas.1900125116, 2019.

Page 11, line 317: I don't understand this sentence. What data does the 59 % relate to?

Response: This sentence means that in terms of peak abundance, 59% of all CHON compounds detected in the negative mode in Guangzhou samples can be assigned with formulas with oxygen to nitrogen ratio higher than or equal to 4. And, this sentence is now clarified in Page 12, Line 369-371 as follows:

“In terms of the peak abundance, 59% of CHON⁻ compounds observed in Guangzhou⁻ exhibited formulas with O/N ratios ≥ 4 , ...”

Page 12, line 371: Is the 83 -87% the percentage of the peak area?

Response: Yes, the value of 83-87% refers to the percentage of the peak area. For clarification, we have added “in terms of peak abundance” right after the “83-87%”.

Page 15, line 461: this should say “mononitrate organosulfate”

Response: “pinanediol mononitrate” is now changed to “mononitrate organosulfate”.

Page 23, table 1: Does the “number of compounds” mean number of formulas or number of peaks?

Response: “number of compounds” in Table 1 refers to the number of peaks detected in this study. In addition, the number of formulas assigned for these compounds is now added in the revised Table 1.

Page 7, line 190: change to “detected”

Response: It is now corrected.

Comments by **reviewer #3** are reproduced in a black font below. Our responses follow each comment in a blue font. Text additions to the manuscript, for example, significantly modified sentences, appear in the revised manuscript in red color. Deletions from the manuscript are not explicitly shown but are described in the responses below. Minor editorial edits to the text are not explicitly shown to prevent a cluttered view.

General comments:

This manuscript presents the application of UHPLC/Orbitrap MS to three sets of samples collected in urban locations in China. The observed molecular formula are classified according to the components (CHO, CHON, CHOS, etc.) and overall trends in the abundance and characteristics of these molecular formulas are compared between the three samples. The paper is well written and the results are clearly communicated. I appreciate the careful and detailed break down of trends by compound class. The largest gap that I see is a lack of discussion/consideration for the information provided by the chromatography itself. I recommend publication after the following concerns are addressed.

Response: We thank the reviewer for the comments. We have revised and improved the manuscript according to these comments.

Specific comments:

1. Throughout the manuscript, a comparison is made between overlapping molecular formula. However, no reference to the LC data set is provided. The separation should provide some information on whether the observed molecular formulas actually correspond to the same chemical structure.

Response: Compared to direct infusion in other studies, the UHPLC technique used in this study could separate and concentrate the compounds before they enter the ion source, reducing the ionization suppression and increasing the sensitive of the measurement. We have now added this description in the Sample Analysis section in Page 5, Line 142-147 in the revised manuscript (also see it below). Meanwhile, it can provide additional information of isomers that have the same molecular formulas but different retention time. In the revised manuscript, we have added the term named isomer number fraction (meaning the percentage of formula numbers that have isomers among all assigned formulas) in the revised Table 1. It shows that 31-34% and 30-56% of formulas have isomers in the negative mode and positive mode, respectively.

“Compared to the direct infusion method applied in other UHRMS studies (Lin et al., 2012a; Lin et al., 2012b; Rincón et al., 2012; Kourtchev et al., 2016; Fleming et al., 2018), the UHPLC technique was used in this study,

which could separate and concentrate the compounds before they entered the ion source, reducing the ionization suppression and increasing the sensitive of the measurement. In addition, it can provide separation of some compounds and information of retention time of the compounds, which is useful for the identification of the compounds and the separation of isomers.”

a. What fraction of the overlapping formulas in Figure 2 (and discussed throughout the document) have the same or very similar retention times in the column?

Response: It is true that compounds with the same molecular formulas may not have the same retention time. Therefore, the Figure 2 is now redrawn (please see the revised Figure 2 below) and the overlapping molecular formulas now refer to the compounds detected in each city with the same molecular formula as well as with the same retention time (retention time difference ≤ 0.1 min). It shows that most of compounds with the same molecular formulas have similar retention time. Therefore, the changes of the definition of overlapping molecular formulas do not change the main conclusions drawn in the manuscript. Furthermore, the values of the number and peak abundance of the overlapping molecular formulas according to the revised Figure 2 have been updated in the revised manuscript.

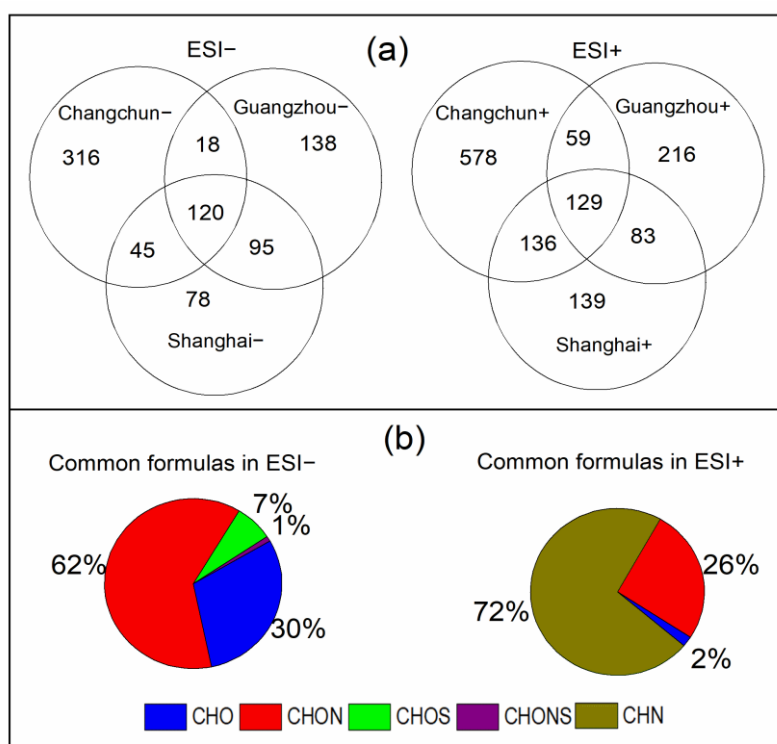


Figure 2. (a) Venn diagrams showing the number distribution of all molecular formulas detected in ESI- and ESI+ for all sample locations. The overlapping molecular formulas refer to the compounds detected in each

city with the same molecular formulas and with the same retention times (retention time difference ≤ 0.1 min).
(b) Peak abundance contribution of each elemental formula category to the total common formulas.

b. Possible identities for some compounds are given (e.g. page 10 lines 289-330 and page 11 lines 342-355).
How do the retention times of these compounds compare to standards run with the same column settings?

Response: In this study, the possible identities for these compounds are based on their molecular formulas and published data in the literatures. It will be very interesting to check/verify these compounds by adding some standards in future studies. Related discussion has been added in the section of Limitations on Page 18, Line 569-571 as follows:

“In particular, the chemical formulas assigned in this study can be validated in future studies by authentic standards and the difference in ionization efficiencies can be further evaluated.”

2. How clean was the separation? Were multiple ions observed under each chromatography peak? Were there differences in this between the three sample locations? It looks like there are a lot more compounds in the Changchun samples as a whole. If there was more charge competition during ionization (especially in positive ion mode) in specific samples, it would be good to clarify this because you are using the signal to directly correlate to abundance.

Response: 1. Since there were hundreds of different compounds detected in each measurement, it was very difficult to completely separate all these compounds using one UHPLC method. However, as a high-resolution Orbitrap MS was applied in this study, these compounds can be efficiently distinguished by the m/z ratios, even though they had same/similar retention time. 2. Yes, the charge competition during ionization can be different for samples of different mass loadings and organic components. To reduce the uncertainties from charge competition, we set the particle mass concentration in the extract to $600 \mu\text{g mL}^{-1}$ for all samples (please see Page 5, Line 139-140 in the revised manuscript). In addition, we have now added a discussion about uncertainties caused by using the signal to directly correlate to abundance in Page 6-7, Line 186-193 in the revised manuscript as well as in the section of Limitations (Page 18, Line 555-571) as follows:

“Comparing the peak abundance has been used in UHRMS recent studies (Wang et al., 2017; Fleming et al., 2018; Song et al., 2018; Ning et al., 2019) to illustrate the relative importance of specific types of compounds. However, it should be noted that different organic compounds have different signal responses in the mass spectrometer due to the differences in ionization and transmission efficiencies (Schmidt et al., 2006; Leito et

al., 2008; Perry et al., 2008; Krueve et al., 2014). Therefore, uncertainties may exist when comparing the peak areas among compounds. In this work, we assume that all organic compounds have the same peak abundance response in the mass spectrometer.”

Limitations: “In this study, we used the peak abundance-weighted method to illustrate the difference in chemical formulas assigned by Orbitrap mass spectrometry. This comparison was made based on the assumption that the measured organic compounds have same peak abundance response in the mass spectrometer. However, this assumption can bring some uncertainties because the ionization efficiencies vary between different compounds (Schmidt et al., 2006; Leito et al., 2008; Perry et al., 2008; Krueve et al., 2014). For example, the ionization efficiencies of nitrophenol species detected in negative ESI mode can vary by a large degree depending on the position of the substituents at the nitrobenzene ring (Schmidt et al., 2006; Krueve et al., 2014) and the ionization efficiencies of carboxylic acids can also vary by several orders of magnitude depending on the structures (Krueve et al., 2014). Nonetheless, it is a challenging analytical task to identify and quantify all compounds in ambient OA due to the high chemical complexity of OA and the limits in authentic standards of OA. Despite the inherent uncertainties, the peak abundance-weighted comparison of molecular formulas provides an overview of the difference in chemical composition of OA in these three representative Chinese cities. In particular, the chemical formulas assigned in this study can be validated in future studies by authentic standards and the difference in ionization efficiencies can be further evaluated.”

3. The positive ion mode data for Guangzhou and Shanghai are interesting in that they appear to be dominated by (one?) very high abundance peak. The fact that amines can ionize very well in ESI+ is discussed in the manuscript. However, it would be helpful to provide more context/information on these samples. In particular, I suggest including (possibly in the supplemental) the reconstructed MS for Shanghai+ and Guangzhou+ with a zoom in on the lower abundance ions (indicate those CHN+ ions are off scale). I also recommend making comparisons in the CHN+ section both in terms of numbers of chemical formula and in terms of abundances (as is currently provided).

Response: Yes, the organic compounds detected in ESI+ in Guangzhou and Shanghai samples are dominated by several CHN+ compounds. This is probably because that these CHN+ have high concentrations and/or have high ionization efficiencies in the positive ESI mode. To display other ions (CHO+, CHON+, CHONS+ and other CHN+ with low intensity) more obviously, the positive mass spectra figures for Shanghai+ and Guangzhou+ has been modified by inserting a break in the Y-axis (please see the revised Figure 1 below). In addition, more information/discussion related to the chemical formula numbers has been now added in the CHN+ section in Page 13-14, Lines 406-442 in the revised manuscript (also see it below).

“696 CHN+ compounds were detected in Changchun+ samples in ESI+, which is higher than in Shanghai+ (253) and Guangzhou (205). These CHN+ compounds are likely assignable to amines according to previous studies (Rincón et al., 2012; Wang et al., 2017; Wang et al., 2018)”

“The number of CHN+ compounds accounts for 24%, 36% and 30% of the total organic compounds in Changchun+, Shanghai+ and Guangzhou+, respectively, whereas the peak abundance of these compounds accounts for 40%, 71% and 62%, respectively.”

“Moreover, the pie charts show that the majority (83–87% in terms of peak abundance and 72–90% in terms of peak numbers) of these CHN+ compounds can be assigned to mono- and polyaromatics with $X_c \geq 2.5$.”

“Polyaromatic compounds with $X_c \geq 2.7$ are displayed in the lower left corner of the van Krevelen diagram, accounting for 41% in terms of peak abundance (48% in terms of peak numbers) of CHN+ compounds detected in Changchun+, but merely for 9–10% in terms of peak abundance (27–31% in terms of peak numbers) in Shanghai+ and Guangzhou+.”

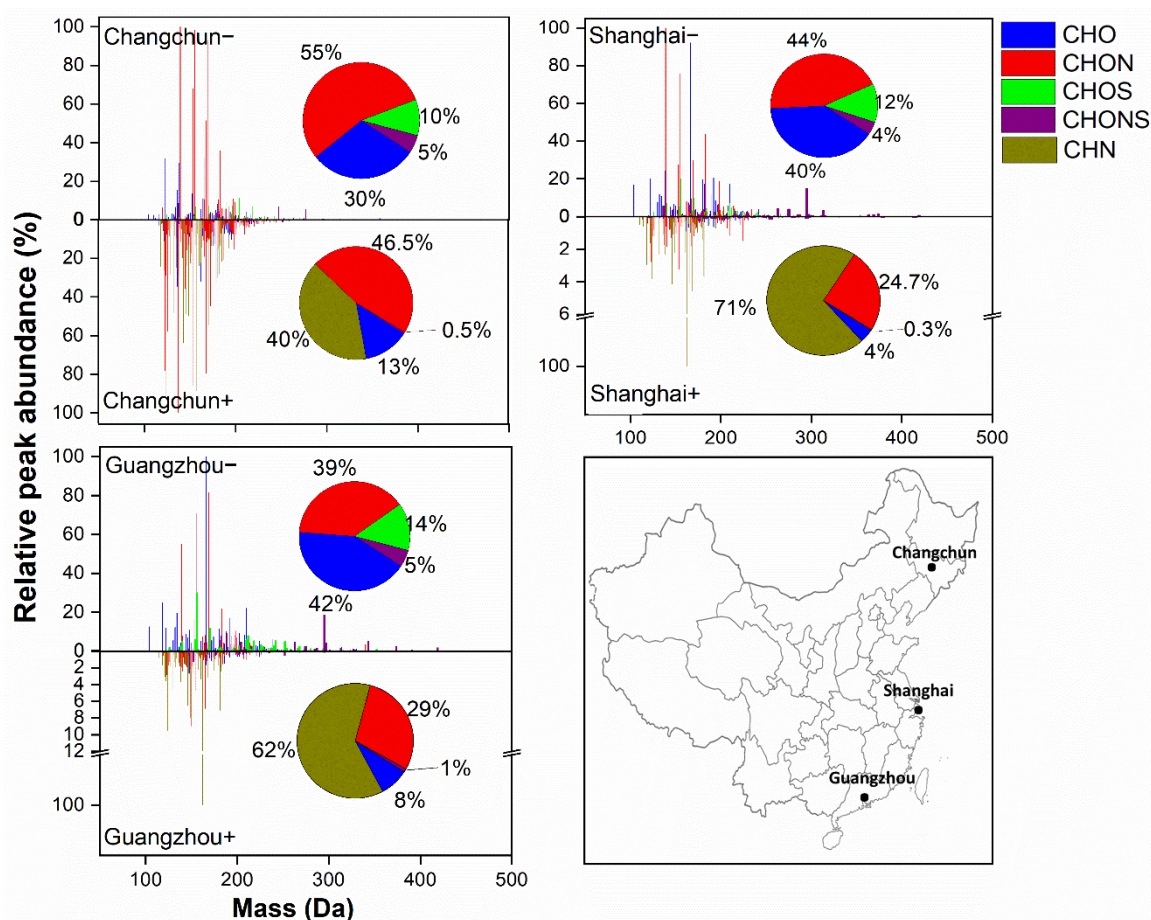


Figure 1. Mass spectra of detected organic compounds reconstructed from extracted ion chromatograms in ESI- and ESI+. The horizontal axis refers to the molecular mass (Da) of the identified species. The vertical axis refers to the relative peak abundance of each individual compound to the compound with the greatest peak abundance. The pie charts show the percentage of each organic compound subgroup (i.e. CHO, CHON, CHOS,

CHONS and CHN) in each sample in terms of peak abundance. The map in the lower right corner shows the locations of these three megacities in China.

4. The conclusion that there is more photochemical aging in the southern locations compared to the more northern location is made throughout the manuscript. However, I would argue that the differences could also be due to more fresh emissions being sampled in the northern location compared to the southern ones. This is supported by, for example, the data in Figure S1 which I think shows similar higher O/C numbers across all three, but more total lower O/C and aromatic compounds for Changchun. I recognize that van Krevelen diagrams can hide some depth (different molecular formulas with the same O/C and H/C). If this is the case here, that should be clarified in the text.

Response: This is a very good point. We have calculated the relative abundance of compounds with $O/C \geq 0.6$ (which are considered as highly oxidized compounds, please see the reference ‘Tu et al., 2016, Analytical Chemistry’) in all samples measured in negative mode. It shows that 31% of compounds in terms of peak abundance in Changchun– have O/C ratio larger than 0.6, while they are relatively higher in Shanghai– and Guangzhou– samples, accounting for 46% in Shanghai and 51% in Guangzhou. Therefore, we suggest that there is more photochemical aging process in the southern locations compared to the more northern location. This statement is now added in Page 8, line 233-235 in the revised manuscript as follows:

“Furthermore, the relative peak abundance of compounds with $O/C \geq 0.6$, which are considered as highly oxidized compounds (Tu et al., 2016), is 31% in Changchun–, and higher in Shanghai– (46%) and Guangzhou– (51%).”

Tu, P., Hall, W. A. t., and Johnston, M. V.: Characterization of Highly Oxidized Molecules in Fresh and Aged Biogenic Secondary Organic Aerosol, Anal. Chem., 88, 4495-4501, 10.1021/acs.analchem.6b00378, 2016

We also agree with the reviewer that more fresh emissions (e.g., coal combustion) were sampled in the northern location and this was stated in the Abstract section (Page 2, Line 41-43 in the revised manuscript) as “The degree of aromaticity and the number of polyaromatic compounds were substantially higher in samples from Changchun, which could be attributed to the large emissions from residential heating (i.e. coal combustion) during winter time in Northeast China.”

5. What was the photoactive radiation level at each site (were any of them cloudy)? Is there any information on the age of the air mass (back trajectories, wind speed, wind direction, etc.)? The other possible explanations for this trend should be addressed: different source types and different overall age of the OA material (i.e. longer transport for the southern locations).

Response: The daily solar radiation values (J cm^{-2}) for each city during the sampling dates are now presented in the revised Table S1 in the SI, which were taken from the World Radiation Data Centre. It shows that the solar radiation in the two Southern Chinese cities (Shanghai and Guangzhou) is 994-1329 J cm^{-2} , which is higher compared to 485-841 J cm^{-2} in the Northern city (Changchun). The related discussion is now added in Page 8, line 235-240 in the revised manuscript as follows:

“The different chemical composition of the samples is probably caused by the rather low ambient temperatures and decreased photochemical processing of organic compounds in Northeast China (indicated by the lower solar radiation in Northeast China, see Table S1), slowing down oxidation processes and leading to a larger number of PAHs, which are mainly emitted from coal burning (Huang et al., 2014; Song et al., 2018).”

48 hours back trajectories of air arriving at the three cities (Changchun, Shanghai and Guangzhou) during the sampling time is now calculated using the NOAA HYSPLIT model and they are now presented in Figure S1 in the SI (please also see Figure S1 below). It shows that air masses from Northwest of Changchun and Shanghai may affect the aerosol samples in Changchun and Shanghai, respectively, while the air masses from Northeast or North of Guangzhou may affect the aerosol samples in Guangzhou. However, in our study it is difficult to say how much effect the long transport of air masses can make on the aerosol samples. The related discussion is now stated in Page 8, line 240-242 in the revised manuscript as follows:

“In addition, long-range transport of air masses (see the 48 hours back trajectories in Fig. S1) may have a certain effect on the chemical properties of aerosol samples collected in the three cities.”

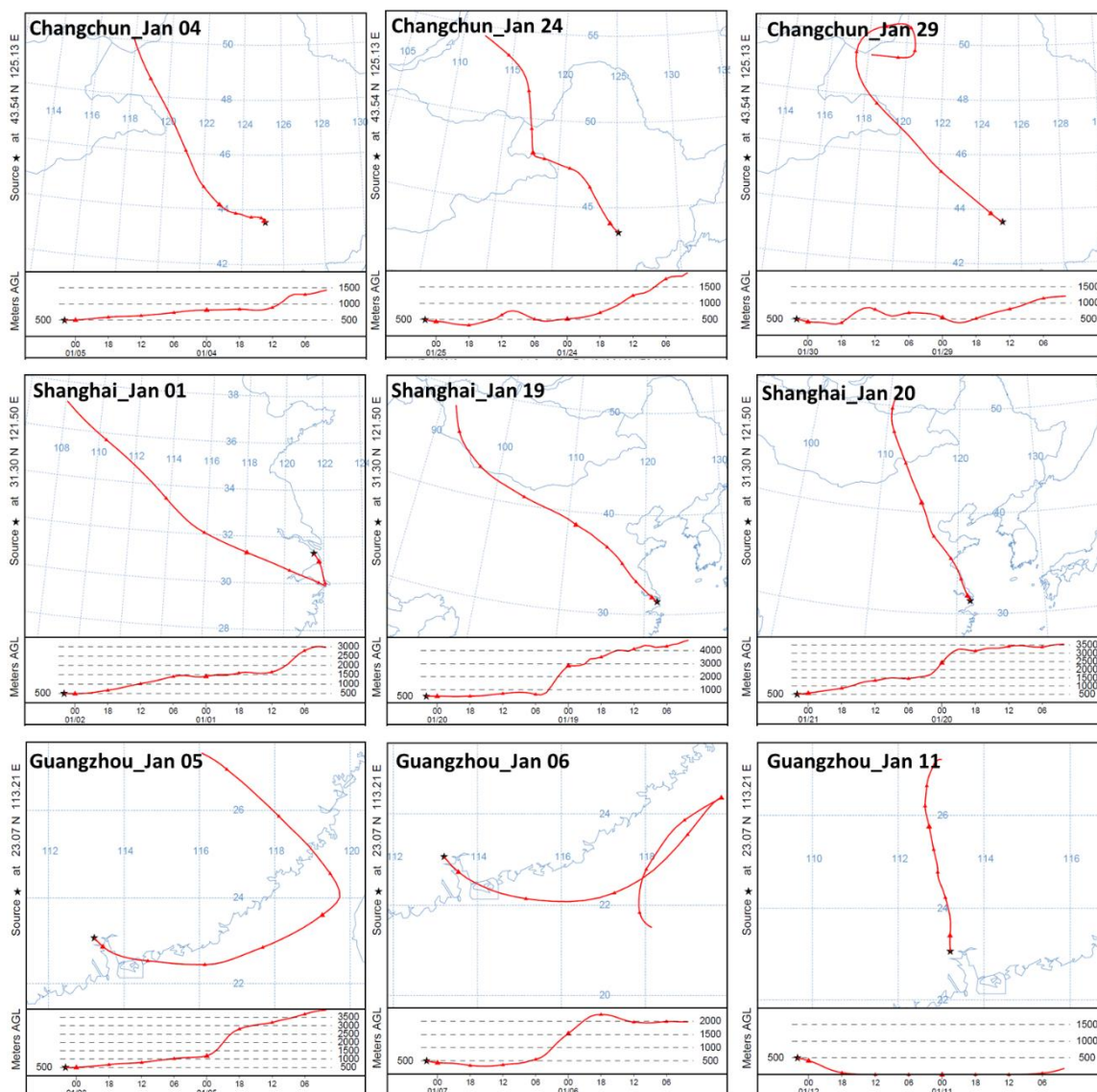


Figure S1. 48 hours back trajectories of air arriving at the three cities (Changchun, Shanghai and Guangzhou) during the sampling time calculated using the NOAA HYSPLIT model (Rolph et al., 2017).

6. For the CHON and CHN compounds, how many contained two or three nitrogen atoms? I can see evidence for a few of them in Figures 4 and S2 but it is hard to quantify. This may be a useful piece of information to include in the supplemental.

Response: In the negative ESI mode, 33-51 CHON- compounds, accounting for 1-17% of all CHON- compounds in terms of peak abundance, were assigned with formulas containing two or more than two nitrogen

atoms in the three city samples (this information is now presented in Figure S4 in the SI, also see Figure S4 below). In the positive ESI mode, 140-662 CHON⁺ compounds (accounting for 42-46% of all CHON⁺ compounds in terms of peak abundance) and 164-405 CHN⁺ compounds (accounting for 49-93% of all CHON⁺ compounds in terms of peak abundance) were assigned with formulas containing two or more than two nitrogen atoms in the three city samples (this information is now presented in Figure S5 and S9 in the SI, also see Figure S5 and S9 below).

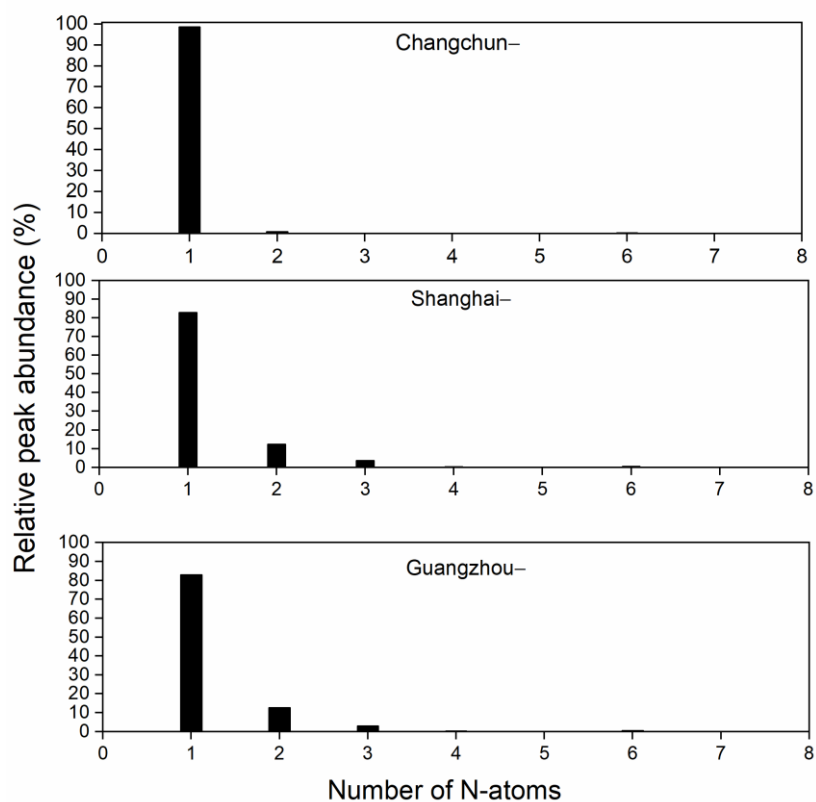


Figure S4. Classification of CHON⁻ compounds into different subgroups according to nitrogen atoms number in their formulas. The y-axis indicates the relative contribution of each subgroup to the sum of peak abundance of all CHON⁻ compounds.

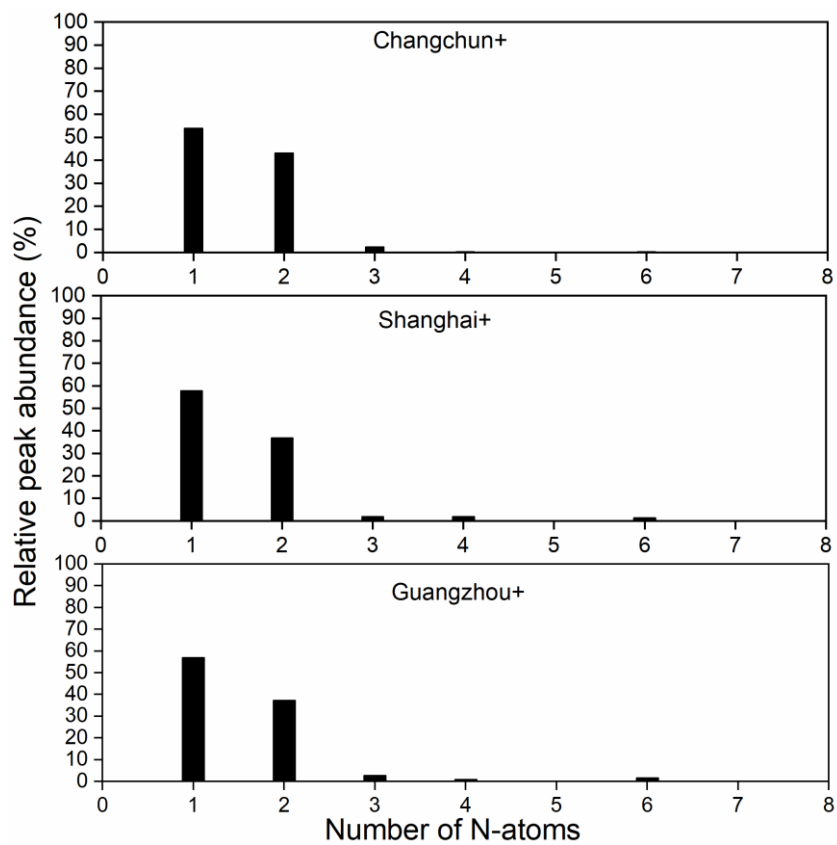


Figure S5. Classification of CHON+ compounds into different subgroups according to nitrogen atoms number in their formulas. The y-axis indicates the relative contribution of each subgroup to the sum of peak abundance of all CHON+ compounds.

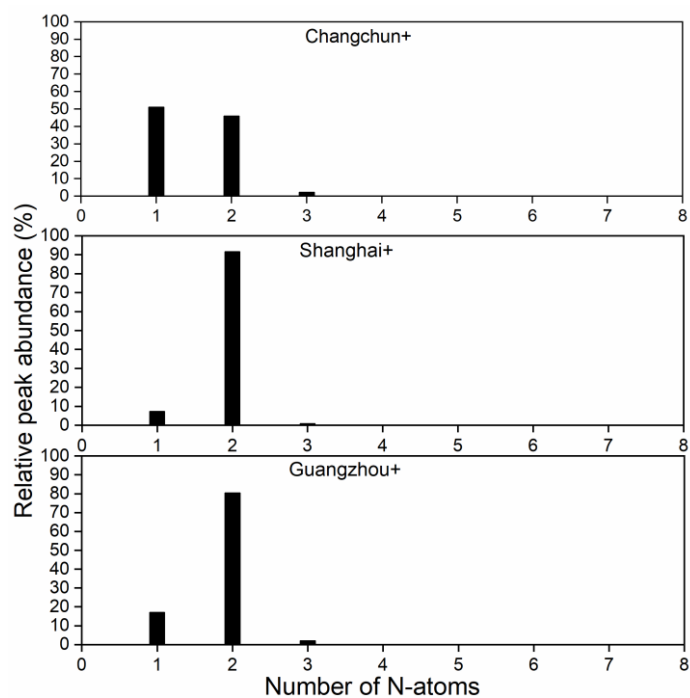


Figure S9. Classification of CHN+ compounds into different subgroups according to nitrogen atoms number in their formulas. The y-axis indicates the relative contribution of each subgroup to the sum of peak abundance of all CHN+ compounds.

7. Throughout the text, differences are stated to be significant but no significance tests are performed. I would recommend re-phrasing to avoid implying a level of analysis that was not carried out.

Response: The word 'significant' is now carefully used and the sentences related to 'significant difference' is now rephrased throughout the manuscript.

1 **Urban organic aerosol composition in Eastern China differs from North to South: Molecular**
2 **insight from a liquid chromatography-Orbitrap mass spectrometry study**

3 Kai Wang^{1,2,4}, Ru-Jin Huang¹, Martin Brüggemann³, Yun Zhang², Lu Yang¹, Haiyan Ni¹, Jie Guo¹,
4 Meng Wang¹, Jiajun Han⁵, Merete Bilde⁴, Marianne Glasius⁴, and Thorsten Hoffmann²

5 ¹State Key Laboratory of Loess and Quaternary Geology (SKLLQG), Center for Excellence in
6 Quaternary Science and Global Change, and Key Laboratory of Aerosol Chemistry and Physics,
7 Institute of Earth and Environment, Chinese Academy of Sciences, Xi'an 710061, China

8 ²Institute of Inorganic and Analytical Chemistry, Johannes Gutenberg University Mainz,
9 Duesbergweg 10–14, Mainz 55128, Germany

10 ³Atmospheric Chemistry Department (ACD), Leibniz Institute for Tropospheric Research
11 (TROPOS), Permoserstraße 15, 04318 Leipzig, Germany

12 ⁴Department of Chemistry, Aarhus University, Langelandsgade 140, DK-8000 Aarhus C, Denmark

13 ⁵Department of Chemistry, University of Toronto, 80 St. George Street, M5S3H6 Toronto, Canada

14 Corresponding Author: Ru-Jin Huang (rujin.huang@ieecas.cn) and Thorsten Hoffmann
15 (t.hoffmann@uni-mainz.de)

16

17

18

19

20

21

22

23

24

25

26

27 **Abstract:**

28 Air pollution by particulate matter in China affects human health, the ecosystem and the climate.
29 However, the chemical composition of particulate aerosol, especially of the organic fraction, is still
30 not well understood. In this study, particulate aerosol samples with a diameter of $\leq 2.5 \mu\text{m}$ ($\text{PM}_{2.5}$)
31 were collected in January 2014 in three cities located in Northeast, East and Southeast China,
32 namely Changchun, Shanghai and Guangzhou. Organic aerosol (OA) in the $\text{PM}_{2.5}$ samples was
33 analyzed by ultrahigh performance liquid chromatography (UHPLC) coupled to high-resolution
34 Orbitrap mass spectrometry in both negative mode (ESI⁻) and positive mode electrospray
35 ionization (ESI⁺). After non-target screening including the assignment of molecular formulas, the
36 compounds were classified into five groups based on their elemental composition, i.e., CHO,
37 CHON, CHN, CHOS and CHONS. The CHO, CHON and CHN groups present the dominant signal
38 abundances of 81–99.7% in the mass spectra and the majority of these compounds were assigned
39 to mono- and polyaromatics, suggesting that anthropogenic emissions are a major source of urban
40 OA in all three cities. However, the chemical characteristics of these compounds varied between
41 the different cities. The degree of aromaticity and the number of polyaromatic compounds were
42 significantly-substantially higher in samples from Changchun, which could be attributed to the large
43 emissions from residential heating (i.e., coal combustion) during winter time in Northeast China.
44 Moreover, the ESI⁻ analysis showed higher H/C and O/C ratios for organic compounds in Shanghai
45 and Guangzhou compared to samples from Changchun, indicating that OA undergoes more intense
46 photochemical oxidation processes in lower latitude regions of China and/or is affected to a larger
47 degree by biogenic sources. The majority of sulfur-containing compounds (CHOS and CHONS) in
48 all cities were assigned to aliphatic compounds with low degrees of unsaturation and aromaticity.
49 Here again, samples from Shanghai and Guangzhou show a greater chemical similarity but differ
50 largely from those from Changchun. It should be noted that the conclusions drawn in this study are
51 mainly based on comparison of molecular formulas weighted by peak abundance, and thus, are
52 associated with inherent uncertainties due to different ionization efficiencies for different organic
53 species.

54 **1. Introduction**

55 In the last decades, China has experienced rapid industrialization and urbanization accompanied by
56 severe and persistent particulate air pollution (Huang et al., 2014; Sun et al., 2014; Ding et al., 2016;
57 Song et al., 2018; Shi et al., 2019; Xu et al., 2019). These particulate air pollution extremes can not
58 only influence the regional air quality and human health in China, but also lead to a global

59 environmental problem due to long-distance transport of pollutants. To better understand the effects
60 of air pollution on air quality and human health, chemical characterization of fine particle
61 (particulate matter with an aerodynamic diameter of less than 2.5 μm , or $\text{PM}_{2.5}$) is crucial. However,
62 the chemical composition of $\text{PM}_{2.5}$ in China is still poorly understood due to a wide variety of
63 natural and anthropogenic sources as well as complex multiphase chemical reactions (Lin et al.,
64 2012a; Huang et al., 2014; Ding et al., 2016; Wang et al., 2017; Wang et al., 2018; An et al., 2019;
65 Tong et al., 2019; Wang et al., 2019a; Wang et al., 2019b). In particular, compared to the fairly
66 well understood nature of the inorganic fraction of aerosol, the organic fraction, also named organic
67 aerosol (OA), is considerably less ~~comprehended~~understood in terms of chemical composition,
68 corresponding precursors, sources and formation mechanisms (Huang et al., 2017).

69 During pollution events in China, OA accounts for as high as more than 50% of the total mass of
70 fine particle (An et al., 2019). Chemical compounds in OA cover a large complexity of species
71 including alcohols, aldehydes, carboxylic acids, imidazoles, organosulfates, organonitrates and
72 polycyclic aromatic hydrocarbons (PAHs) (Lin et al., 2012a; Rincón et al., 2012; Kourtchev et al.,
73 2014; Wang et al., 2018; Elzein et al., 2019; Wang et al., 2019a). Thus, the capacity of traditional
74 analytical techniques is limited to identify the compounds in OA and the majority (> 70%) of OA
75 has not been identified yet as specific compounds (Hoffmann et al., 2011). The insufficient
76 knowledge of chemical composition of OA hinders a better understanding of the sources, formation
77 and atmospheric processes of air pollution in China.

78 Recently, ultrahigh resolution mass spectrometry (UHRMS), such as Fourier transform ion
79 cyclotron resonance mass spectrometry (FTICR-MS) and Orbitrap-MS, coupled with soft
80 ionization sources (e.g., electrospray ionization (ESI) and atmospheric pressure chemical ionization
81 (APCI)) have been introduced to elucidate the molecular composition of OA (Nizkorodov et al.,
82 2011; Lin et al., 2012a; Lin et al., 2012b; Rincón et al., 2012; Noziere et al., 2015; Kourtchev et al.,
83 2016; Tong et al., 2016; Tu et al., 2016; Brüggemann et al., 2017; Wang et al., 2017; Fleming et
84 al., 2018; Laskin et al., 2018; Song et al., 2018; Wang et al., 2018; Brüggemann et al., 2019;
85 Daellenbach et al., 2019; Ning et al., 2019; Wang et al., 2019a). Due to the two outstanding features
86 of high resolving power and high mass accuracy, UHRMS can give precise elemental compositions
87 of individual organic compounds. However, UHRMS studies on Chinese urban OA are very limited.
88 Wang et al. (Wang et al., 2017) characterized OA in Shanghai and showed variations in chemical
89 composition among different months and between daytime and nighttime. Our recent Orbitrap MS
90 study (Wang et al., 2018) showed that wintertime OA in $\text{PM}_{2.5}$ collected in Beijing, China and
91 Mainz, Germany were very different in terms of chemical composition. In contrast, for summertime

92 OA from Germany and China, Brüggemann et al. (2019) found similar compounds and
93 concentrations of terpenoid organosulfates in PM_{10} , demonstrating that biogenic emission can
94 significantly affect OA composition at both locations. Ning et al. (2019) analyzed the OA collected
95 in a coastal Chinese city (Dalian) and found that more organic compounds were identified in haze
96 days compared to non-haze days. Nonetheless, since severe particulate pollution in China occurs
97 on a large-scale, more UHRMS studies are needed to fully elucidate the chemical composition of
98 OA in different Chinese cities.

99 In this study, $PM_{2.5}$ aerosol samples were collected in three Chinese cities, i.e., Changchun,
100 Shanghai and Guangzhou, and their organic fraction was analyzed using ultra-high-performance
101 liquid chromatography (UHPLC) coupled with Orbitrap-MS. The Chinese cities of Changchun,
102 Shanghai and Guangzhou are located in the Northeast, East and Southeast of China, which are
103 major populated regions in China with a population of 7.5, 24 and 15 million, respectively. The
104 geographic locations of these three cities cover a large latitude spanning from 23.12°N to 43.53°N
105 resulting in different meteorological conditions, including intensity and duration of sunlight,
106 average daily temperature and monsoon climate. In addition, the industrial structure, energy
107 consumption and energy sources in these three cities are different, such as much more heavy
108 industries (e.g., coal chemical industry and steelworks) in Northeast China (Zhang, 2008), which
109 can cause difference in anthropogenic emissions, and can therefore influence the chemical
110 composition of urban OA. Moreover, OA is strongly affected by residential coal combustion during
111 winter in Northeast China (Huang et al., 2014; An et al., 2019). Therefore, this study presents a
112 comprehensive overview of chemical composition of OA in three representative Chinese cities
113 during pollution episodes, which eventually can improve our understanding of OA effects on
114 climate and public health and also provide a chemical database for haze mitigation strategies in
115 China.

116 **2. Experimental**

117 **2.1 $PM_{2.5}$ samples**

118 Three 24-h integrated urban $PM_{2.5}$ samples were collected during severe haze pollution events with
119 daily average $PM_{2.5}$ mass concentration higher than $115 \mu\text{g m}^{-3}$ in each of the three Chinese cities:
120 Changchun (43.54° N, 125.13° E, 1.5 m above the ground), Shanghai (31.30° N, 121.50° E, 20 m
121 above the ground) and Guangzhou (23.07° N, 113.21° E, 53 m above the ground), which are located
122 in the Northeast, East and Southeast regions of China, respectively (see Fig. 1). Samples in
123 Changchun were collected on 4, 24 and 29 of January 2014 with $PM_{2.5}$ mass concentrations of

124 185–222 $\mu\text{g m}^{-3}$, samples in Shanghai were collected on 1, 19 and 20 of January 2014 with PM_{2.5}
125 mass concentrations of 159–172 $\mu\text{g m}^{-3}$ and samples in Guangzhou were collected on 5, 6 and 11
126 of January 2014 with PM_{2.5} mass concentrations of 138–152 $\mu\text{g m}^{-3}$. Further details (e.g., the daily
127 average concentrations of PM_{2.5}, SO₂, NO₂, CO and O₃, the average temperature and the daily solar
128 radiation value during sampling dates) are presented in Table S1, the 48 hours back trajectories of
129 air arriving at the three sampling sites during the sampling periods are shown in Fig. S1. All PM_{2.5}
130 samples were collected on prebaked quartz-fiber filters (20.3×25.4 cm) using a high-volume PM_{2.5}
131 sampler at a flow rate of 1.05 m³ min⁻¹ (Tisch Environmental, USA) and at each sampling site field
132 blanks were taken. After sample collection, filters were stored at -20 °C until analysis.

133 2.2 Sample analysis

134 Detailed description on the filter sample extraction and UHPLC–Orbitrap MS analysis can be found
135 in our previous studies (Wang et al., 2018; Wang et al., 2019a). Briefly, a part of the filters (around
136 1.13 cm², corresponding to about 600 μg particle mass in each extracted filter) was extracted three
137 times with 1.0–1.5 mL of acetonitrile-water (8/2, v/v) in an ultrasonic bath. The extracts were
138 combined, filtered through a 0.2 μm Teflon syringe filter and evaporated to almost dryness under
139 a gentle nitrogen stream. Finally, the residue was redissolved in 1000 μL acetonitrile-water (1/9,
140 v/v) to reach the total particulate mass concentration of around 600 $\mu\text{g mL}^{-1}$ for the following
141 analysis.

142 Compared to the direct infusion method applied in other UHRMS studies (Lin et al., 2012a; Lin et
143 al., 2012b; Rincón et al., 2012; Kourtchev et al., 2016; Fleming et al., 2018), the UHPLC technique
144 was used in this study, which could separate and concentrate the compounds before they entered
145 the ion source, reducing the ionization suppression and increasing the sensitive of the measurement.
146 In addition, it can provide separation of some compounds and information of retention time of the
147 compounds, which is useful for the identification of the compounds and the separation of isomers.

148 The analytes were separated using a Hypersil Gold column (C18, 50 x 2.0 mm, 1.9 μm particle size)
149 with mobile phases consisting of (A) 0.04% formic acid and 2% acetonitrile in MilliQ water and
150 (B) 2% water in acetonitrile. Gradient elution was applied with the A and B mixture at a flow rate
151 of 500 $\mu\text{L min}^{-1}$ as follows: 0–1.5 min 2% B, 1.5–2.5 min from 2% to 20% B (linear), 2.5–5.5 min
152 20% B, 5.5–6.5 min from 20% to 30% B (linear), 6.5–7.5 min from 30% to 50% B (linear), 7.5–8.5
153 min from 50% to 98% B (linear), 8.5–11.0 min 98% B, 11.0–11.05 min from 98% to 2% B (linear),
154 and 11.05–11.1 min 2% B. The Q Exactive Hybrid Quadrupole-Orbitrap MS was equipped with a
155 heated ESI source at 120 °C, applying a spray voltage of -3.3 kV and 4.0 kV for negative ESI mode

156 (ESI⁻) and positive ESI mode (ESI⁺), respectively. The mass scanning range was set from m/z 50
157 to 500 with a resolving power of 70,000 @ m/z 200. The Orbitrap MS was externally calibrated
158 before each measurement sequence using an Ultramark 1621 solution (Sigma–Aldrich, Germany)
159 providing mass accuracy of the instrument lower than 3 ppm. Each sample was measured in
160 triplicate with an injection volume of 10 µL.

161 2.3 Data processing

162 A non-target peak picking software (SIEVE[®], Thermo Fisher Scientific, Germany) was used to find
163 significant peaks in the LC-MS dataset and to calculate all mathematically possible chemical
164 formulas for ions signals with a sample-to-blank abundance ratio ≥ 10 using a mass tolerance of \pm
165 2 ppm. The permitted maximum elemental number of atoms was set as follows: ¹²C (39), ¹H (72),
166 ¹⁶O (20), ¹⁴N (7), ³²S (4), ³⁵Cl (2) and ²³Na (1) (Kind and Fiehn, 2007; Lin et al., 2012a; Wang et
167 al., 2018). To remove the chemically unreasonable formulas, further constraint was applied by
168 setting H/C, O/C, N/C, S/C and Cl/C ratios in the ranges of 0.3–3, 0–3, 0–1.3, 0–0.8 and 0–0.8
169 (Kind and Fiehn, 2007; Lin et al., 2012a; Rincón et al., 2012; Wang et al., 2018; Zielinski et al.,
170 2018), respectively. For chemical formula C_cH_hO_oN_nS_sCl_x, the double bond equivalent (DBE) was
171 calculated by the equation: $DBE = (2c + 2 - h - x + n) / 2$. The aromaticity equivalent (X_C) as a
172 modified index for aromatic compounds was obtained using the equation: $X_C = [3(DBE - (p \times o +$
173 $q \times n)) - 2] / [DBE - (p \times o + q \times n)]$, where p and q, respectively, refer to the fraction of oxygen
174 and sulfur atoms involved in the π -bond structure of a compound. As such the values of p and q
175 vary between compound categories (Yassine et al., 2014). For example, carboxylic acids and esters
176 are characterized using $p = q = 0.5$, while $p = q = 1$ and $p = q = 0$ are used for carbonyl and hydroxyl,
177 respectively. Since it is impossible to identify the structures of the hundreds of formulas observed
178 in this study, we cannot know the exact values of p and q in an individual compound. Therefore, in
179 this study, $p = q = 0.5$ was applied for compounds detected in ESI⁻ as carboxylic compounds are
180 preferably ionized in negative mode. However, because of the high complexity of the mass spectra
181 in ESI⁺, $p = q = 1$ was used in ESI⁺ to avoid an overestimation of the amount of aromatics.
182 Moreover, for $DBE \leq (p \times o + q \times n)$ or $X_C \leq 0$, X_C was defined as zero. Furthermore, in ESI⁻, for
183 odd numbers of $(p \times o + q \times n)$, the value of $(p \times o + q \times n)$ was rounded down to the lower integer.
184 $X_C \geq 2.50$ and $X_C \geq 2.71$ have been suggested as unambiguous minimum criteria for the presence
185 of monoaromatics and polyaromatics, respectively (Yassine et al., 2014).

186 Comparing the peak abundance has been used in recent UHRMS studies (Wang et al., 2017;
187 Fleming et al., 2018; Song et al., 2018; Ning et al., 2019) to illustrate the relative importance of

188 specific types of compounds. However, it should be noted that different organic compounds have
189 different signal response in the mass spectrometer due to the differences in ionization and
190 transmission efficiencies (Schmidt et al., 2006; Leito et al., 2008; Perry et al., 2008; Krueve et al.,
191 2014). Therefore, uncertainties may exist when comparing the peak areas among compounds. In
192 this work, we assume that all organic compounds have the same peak abundance response in the
193 mass spectrometer. The peak abundance-weighted average molecular mass (MM), elemental ratios,
194 DBE, and Xc for formula $C_cH_hO_oN_nS_sCl_x$ were calculated using following equations:

$$195 \quad MM_{avg} = \frac{\sum (MM_i \times A_i)}{\sum A_i}$$

$$196 \quad O/C_{avg} = \frac{\sum (O/C_i \times A_i)}{\sum A_i}$$

$$197 \quad H/C_{avg} = \frac{\sum (H/C_i \times A_i)}{\sum A_i}$$

$$198 \quad DBE_{avg} = \frac{\sum (DBE_i \times A_i)}{\sum A_i}$$

$$199 \quad Xc_{avg} = \frac{\sum (Xc_i \times A_i)}{\sum A_i}$$

200 where A_i is the peak abundance for each individual compound i .

201 **3. Results and discussion**

202 **3.1 General characteristics**

203 The main purpose of this study was to tentatively identify and compare the chemical composition
204 of organic compounds in the PM_{2.5} samples collected in the three Chinese cities: Changchun,
205 Shanghai and Guangzhou during pollution episodes. The number of organic compounds and
206 molecular formulas detected in each city, the peak abundance-weighted average values of
207 molecular mass (MM_{avg}), elemental ratios, DBE, Xc and the isomer number fraction (meaning the
208 percentage of formula numbers that have isomers among all assigned formulas) for each subgroup
209 are listed in Table 1. It should be noted that in this study we focus solely on organic compounds
210 with elevated signal abundances, and thus, presumably rather high concentrations. In contrast to
211 our previous study (Wang et al., 2018), compounds with low concentrations were excluded by
212 increasing the reconstitution volume from 500 μ L to 1000 μ L, reducing the sample injection volume
213 from 20 μ L to 10 μ L, and increasing the sample-to-blank ratio from 3 to 10 during data processing.

214 Overall, 416–769 (assigned to 272–415 molecular formulas) and 687–2943 (assigned to 383–679
215 molecular formulas) organic compounds in different samples were determined in ESI⁻ and ESI⁺,
216 respectively. The largest number of organic compounds was observed in Changchun samples in

217 both ESI⁻ and ESI⁺, indicating that OA collected during winter season in Northeast China was
218 more complex compared to urban OA in East and Southeast China. This increased number of
219 compounds can possibly be explained by the large residential coal combustion emissions in winter
220 in North China (Huang et al., 2014; Song et al., 2018; An et al., 2019). In addition, ambient
221 temperatures were lowest during the sampling period in Changchun (i.e., -14 °C to -9 °C, Table
222 S1), which likely led to a decreased boundary layer height and therefore enhanced accumulation of
223 pollutants and enhanced formation of secondary organic aerosol through for example gas-to-
224 particle partitioning.

225 As shown in Table 1, the abundance-weighted average values of MM_{avg} , ~~H/C~~ and O/C ratio of the
226 total assigned formulas for Changchun samples detected in negative mode (Changchun⁻) are 169,
227 ~~1.03~~ and 0.58, respectively, which are ~~significantly~~ lower than those for Shanghai⁻ ($MM_{avg} = 176$,
228 ~~H/C = 1.05~~ and O/C = 0.69) and for Guangzhou⁻ ($MM_{avg} = 183$, ~~H/C = 1.14~~ and O/C = 0.74). On
229 the contrary, the aromaticity equivalent X_c for organics detected in Changchun⁻, X_c(Changchun⁻)
230 = 2.13, is substantially higher than that for Shanghai⁻, X_c(Shanghai⁻) = 1.92, and Guangzhou⁻,
231 X_c(Guangzhou⁻) = 1.65. These observations indicate that urban OA in Northeast China features a
232 lower degree of oxidation and a higher degree of aromaticity compared to urban OA in East and
233 Southeast China. Furthermore, the relative peak abundance fraction of compounds with O/C ≥ 0.6,
234 which are considered as highly oxidized compounds (Tu et al., 2016), is 31% in Changchun⁻, and
235 higher in Shanghai⁻ (46%) and Guangzhou⁻ (51%). The different chemical composition of the
236 samples is probably caused by the rather low ambient temperatures and decreased photochemical
237 processing of organic compounds in Northeast China (indicated by the lower solar radiation in
238 Northeast China, see Table S1), slowing down oxidation processes and leading to a larger number
239 of PAHs, which are mainly emitted from coal burning (Huang et al., 2014; Song et al., 2018) or by
240 different biogenic/anthropogenic precursors. In addition, long-range transport of air masses (see
241 the 48 hours back trajectories in Fig. S1) may have a certain effect on the chemical properties of
242 aerosol samples collected in the three cities.

243 Figure 1 shows the reconstructed mass spectra of organic compounds detected in ESI⁻ and ESI⁺.
244 A major fraction organic species detected in ESI⁻ are attributed to CHO⁻ and CHON⁻, accounting
245 for 30–42% and 39–55% in terms of peak abundance, respectively, and comprising 39–45% and
246 23–33% in terms of peak numbers, respectively. This is consistent with previous studies on Chinese
247 urban OA by Wang et al. (2017 and 2018) and Brüggemann et al. (2019). Comparing the organic
248 compounds detected in ESI⁻ for the three cities, 139–120 formulas were observed in all cities as
249 common formulas (which refer to the compounds detected in all cities with the same molecular

250 formulas and with the same retention times (retention time difference ≤ 0.1 min)) (Fig. 2a),
251 accounting for ~~3529~~5144% and ~~7857~~8771% of all assigned formulas in terms of ~~peak-formula~~
252 numbers and peak abundance, respectively. Despite the above-mentioned differences in chemical
253 composition for OA from Changchun compared to OA from Shanghai and Guangzhou, these results
254 demonstrate that still a large number of common organic compounds exist in Chinese urban OAs
255 collected in different cities, in particular for organics with higher signal abundances. Furthermore,
256 as shown by the pie chart in Fig. 2b, these common formulas are dominated by CHON⁻ and CHO⁻,
257 accounting for ~~5962~~3330% and ~~3330~~5962% of the total common formulas in terms of peak abundance,
258 respectively.

259 As it is commonly known, ESI exhibits different ionization mechanisms in negative and positive
260 ionization modes. While ESI⁻ is especially sensitive to deprotonatable compounds (e.g., organic
261 acids), ESI⁺ is more sensitive to protonatable compounds (e.g., organic amines) (Ho et al., 2003).
262 Due to the different ionization mechanisms, clear differences were observed in the mass spectra
263 (Fig. 1) and chemical characteristics (Table 1) from ESI⁻ and ESI⁺ measurements. For example,
264 CHO compounds were preferentially detected in ESI⁻, accounting for a relatively large fraction of
265 30–42% of all detected compounds in terms of peak abundance, compared to merely 4–13% for
266 such CHO compounds in ESI⁺. In contrast, CHN compounds were only observed in ESI⁺, yielding
267 a rather large peak abundance fraction of 40–71%. In particular, as can be seen in Fig.1, several
268 peaks of CHN⁺ compounds in Shanghai⁺ and Guangzhou⁺ have much higher abundance compared
269 to other organic species, probably due to their high concentrations and/or high ionization
270 efficiencies in the positive mode. This observation indicates that most CHO compounds with high
271 concentrations are probably organic acids, whereas the majority of CHN compounds likely belong
272 to the group of organic amines, which is in good agreement with previous studies (Lin et al., 2012a;
273 Wang et al., 2017; Wang et al., 2018). Organic compounds in ESI⁺ are dominated by CHN⁺ and
274 CHON⁺ compounds in terms of both peak numbers and peak abundance and these compounds are
275 characterized by rather high H/C ratio and low O/C ratios (Table 1), indicating a low degree of
276 oxidation. The Venn diagram presented for ESI⁺ measurements in Fig. 2a shows that out of a total
277 of 383–679 formulas, ~~168~~129 formulas were found in samples from all three cities. Such common
278 formulas, thus, account for ~~2519~~4434% and ~~6530~~9075% of all assigned formulas in terms of
279 ~~peak-formula~~ numbers and peak abundance, respectively. Among these common formulas, CHN⁺
280 and CHON⁺ exhibit the highest abundance fractions of ~~6172~~3526% and ~~3526~~6172%, respectively (Fig. 2b).
281 In the following, we will compare and discuss the chemical properties in detail for the three cities,
282 including degrees of oxidation, unsaturation and aromaticity of each organic compound class (i.e.,

283 CHO, CHON, CHN, CHOS and CHONS). It should be noted that the chlorine-containing
284 compounds were not discussed in this study due to the very low MS signal abundance. In addition,
285 since peak abundances for the formula can vary by orders of magnitude, the area of the circles
286 presented in the Figure 3 and Figures 5–7 is proportional to the fourth root of the peak abundance
287 of each formula to reduce the size difference of the circles. For a more detailed comparison, figures
288 with the circle size related to the absolute peak abundances are presented in the SI.

289 3.2 CHO compounds

290 CHO compounds have been widely observed in urban OA, accounting for a substantial fraction
291 (8–67%) of OA (Rincón et al., 2012; Tao et al., 2014; Wang et al., 2017; Wang et al., 2018).
292 Previous studies have shown that a large fraction of CHO compounds in urban OA is composed of
293 organic acids, containing deprotonatable carboxyl functional groups, which are detected
294 preferentially in negative ionization mode when using ESI–MS. As shown in Table 1, a total of
295 346, 164, and 196 CHO– compounds were detected in ESI– in the OA samples collected in
296 Changchun, Shanghai and Guangzhou, accounting for 30%, 40% and 42% of the overall peak
297 abundance in each sample, respectively. Out of all assigned formulas, 52–47 common CHO–
298 formulas were observed for all cites, accounting for 1335–1752% and 7442–8868% of all identified
299 CHO– formulas in terms of formula numbers and peak abundance, respectively.

300 Despite this similarity, OA samples from Changchun– (i.e. in negative ionization mode) exhibit
301 certain differences compared to samples from Shanghai– and Guangzhou–. The average H/C
302 values for CHO– compounds are in a similar range for the three locations (i.e., 0.96–1.10), however,
303 the average O/C values for O/C(Shanghai–) = 0.59 and O/C(Guangzhou–) = 0.65 are rather high
304 compared to the average O/C ratio for Changchun–, O/C(Changchun–) = 0.41. Furthermore, the
305 relative peak abundance fraction of CHO– compounds with O/C ≥ 0.6, which are considered as
306 highly oxidized compounds (Tu et al., 2016), is 14% in Changchun and somewhat higher in
307 Shanghai– (34%) and Guangzhou– (45%). Altogether, these results indicate that CHO– compounds
308 in urban OA from East and Southeast China experienced more intense oxidation and aging
309 processes and/or were affected to a larger degree by biogenic sources.

310 Similarly, as shown in Fig. 3, the abundance-weighted average molecular formulas for CHO–
311 compounds in Changchun–, Shanghai– and Guangzhou– are C_{8.58}H_{7.86}O_{3.22} (MM_{avg}(Changchun–)
312 = 162), C_{8.01}H_{7.27}O_{4.22} (MM_{avg}(Shanghai–) = 171) and C_{7.70}H_{8.04}O_{4.48} (MM_{avg}(Guangzhou–) = 172),
313 respectively. Again, these average formulas show that CHO– in Shanghai– and Guangzhou–
314 experienced more intense oxidation processes and/or were affected to a larger degree by biogenic

315 precursors, indicated by the larger abundance-weighted MM_{avg} with a higher degree of oxygenation.
316 In contrast, CHO- compounds from OA samples in Changchun- exhibit a lower abundance-
317 weighted MM_{avg} with a decreased oxygen content.

318 Besides oxygenation, the aromaticity of the detected CHO- compounds exhibits remarkable
319 differences in these three cities. In all cities, the CHO- compounds with high peak abundance were
320 mainly assigned to monoaromatics with $2.5 \leq X_c < 2.7$ (purple circles in Fig. 3) in the region of
321 7–12 carbon atoms per compound and DBE values of 5–7. The relative peak abundance fraction
322 of monoaromatics in total CHO- compounds is 67% in Changchun, which is higher compared to
323 64% in Shanghai and 49% in Guangzhou. In addition, 14% of CHO- compounds in Changchun
324 were identified as polyaromatic compounds with $X_c \geq 2.7$ (red circles in Fig. 3), which is
325 significantly higher than the 8% in Shanghai and 4% in Guangzhou. These observations indicate
326 that CHO- compounds in the three Chinese cities are highly affected by aromatic precursors (e.g.,
327 benzene, toluene and naphthalene), in particular for the Changchun aerosol samples.

328 Besides the monoaromatics and polyaromatics, the rest of the detected CHO- compounds were
329 assigned to aliphatic compounds with an X_c lower than 2.5 (grey circles in Fig. 3). Interestingly,
330 these aliphatic compounds account for about 47% of all CHO- compounds for Guangzhou-
331 samples in terms of peak abundance, whereas samples from Changchun- and Shanghai- exhibit
332 only rather small fractions of such CHO- compounds, i.e., 19% and 28%, respectively. Such
333 aliphatic compounds are commonly derived from biogenic precursors (Kourtchev et al., 2016) and
334 vehicle emission (Tao et al., 2014; Wang et al., 2017) and/or generated by intense oxidation
335 processes of aromatic precursors, indicating the different biogenic and anthropogenic emission
336 sources and chemical reaction processes for OAs in the three cities.

337 In addition, through mass spectrometric analysis of individual compounds/formulas, we find that
338 for the Changchun- samples, formulas of $C_8H_6O_4$, $C_7H_6O_2$, $C_7H_6O_3$, $C_8H_8O_2$, and $C_8H_8O_3$ with DBE
339 values of 6, 5, 5, 5, and 5 dominate the assigned CHO formulas with respect to peak abundance.
340 According to previous studies, $C_8H_6O_4$, $C_7H_6O_2$ and $C_7H_6O_3$ are suggested to be phthalic acid,
341 benzoic acid and monohydroxy benzoic acid, respectively, which are derived from naphthalene
342 (Kautzman et al., 2010; Riva et al., 2015; Wang et al., 2017; He et al., 2018; Huang et al., 2019).
343 $C_8H_8O_2$ is likely 4-hydroxy acetophenone, which could be derived from estragole (Pereira et al.,
344 2014), while $C_8H_8O_3$ is suggested to be either 4-methoxybenzoic acid generated from estragole
345 (Pereira et al., 2014) or vanillin emitted from biomass burning (Li et al., 2014). For the Shanghai-
346 samples, besides $C_8H_6O_4$, $C_7H_6O_3$ and $C_7H_6O_2$, formulas of $C_6H_8O_7$ and $C_9H_8O_4$ with DBE values

347 of 3 and 6 were observed with high peak abundances. $C_6H_8O_7$ was identified as citric acid in the
348 pollen sample and mountain particle sample in previous studies (Fu et al., 2008; Wang et al., 2009;
349 Jung and Kawamura, 2011) and $C_9H_8O_4$ are probably homophthalic acid derived from e.g. estragole
350 (Pereira et al., 2014). For the Guangzhou- samples, besides the formulas of $C_8H_6O_4$ and $C_6H_8O_7$
351 discussed above, $C_4H_6O_4$ and $C_4H_6O_5$ with low DBE values of two were detected with high
352 abundances and are suggested to be succinic acid and malic acid, respectively (Claeys et al., 2004;
353 Wang et al., 2017).

354 3.3 CHON compounds

355 A large amount of nitrogen-containing organic compounds was detected in these three cities,
356 accounting for 39–55% and 25–47% of total peak abundance detected in ESI- and ESI+,
357 respectively. Out of all assigned formulas, 51–45 common CHON- and 89–62 common CHON+
358 formulas were observed in all cities, accounting for 9065–9682% and 6125–7544% of all CHON
359 compounds detected in ESI- and ESI+ in terms of peak abundance, respectively. It indicates that a
360 large amount of CHON compounds in all three Chinese cities show similar properties of chemical
361 composition.

362 The CHON compounds were further classified into different subgroups according to their O/N
363 ratios (Fig. 4 for CHON- and Fig. S3 for CHON+) or according to the number of nitrogen atoms
364 in their molecular formulas (see Fig. S4 for CHON- and S5 for CHON+). As shown in Fig. 4, the
365 majority (84–96% in terms of peak abundance) of CHON- compounds exhibited O/N ratios ≥ 3 ,
366 allowing the assignment of one nitro ($-NO_2$) or nitrooxy ($-ONO_2$) group for these formulas, which
367 are preferentially ionized in ESI- mode (Lin et al., 2012b; Wang et al., 2017; Song et al., 2018;
368 Wang et al., 2018). CHON- formulas with O/N ratios ≥ 4 suggest the presence of further
369 oxygenated functional groups, such as a hydroxyl group ($-OH$) or a carbonyl group ($C=O$). In
370 terms of peak abundance, 59% of CHON- compounds observed in Guangzhou- exhibited formulas
371 with O/N ratios ≥ 4 , which is significantly higher than 51% in Changchun- and 45% in Shanghai-,
372 indicating that CHON- compounds in Southeast China show a higher degree of oxidation
373 compared to those in Northeast and East China. Not surprisingly, CHON+ compounds generally
374 exhibit lower O/N ratios (Fig. S3), as they probably contain reduced nitrogen functional group (e.g.,
375 amines) which are preferably detected in ESI+. As shown in Fig. S3, CHON+ compounds with
376 O/N ratio of 1 are dominant in Changchun+, whereas CHON+ compounds in Shanghai+ and
377 Guangzhou+ show a broader range of O/N ratios from 1 to 3. Moreover, the average O/C ratios
378 (0.27–0.45) in Shanghai+ and Guangzhou+ (Table 1) are much greater than that (0.19) in

379 Changchun+. Consistent with the observations for CHO compounds, these results indicate again
380 that CHON+ compounds in the OA of East and Southeast China experienced more intensive
381 photooxidation and/or were affected to a larger degree by biogenic precursors.

382 Figure 5 shows the DBE versus C number of CHON- compounds for the three cities. The majority
383 of CHON- compounds lie in the region of 5–15 C atoms and 3–10 DBEs. 67% of CHON-
384 compounds in terms of peak abundance were assigned to mono or polyaromatics in Shanghai-,
385 which is significant-higher than 52% in Guangzhou- and 55% in Changchun-. It indicates that
386 CHON- compounds are dominated with aromatic compounds in all cities, while relatively higher
387 peak abundance weighted fraction of aromatic CHON- compounds were observed in Shanghai.

388 The peak abundance-weighted average molecular formulas for CHON- compounds in
389 Changchun-, Shanghai- and Guangzhou- are $C_{7.10}H_{6.76}O_{3.56}N_{1.03}$, $C_{7.07}H_{6.03}O_{3.80}N_{1.24}$ and
390 $C_{7.12}H_{6.36}O_{3.99}N_{1.24}$, respectively, showing that CHON- formulas in Shanghai- and Guangzhou-
391 contain more O and N atoms on average than those for Changchun-. Formulas of $C_6H_5O_3N_1$,
392 $C_6H_5O_4N_1$, $C_7H_7O_3N_1$, $C_7H_7O_4N_1$, $C_8H_9O_3N_1$, and $C_8H_9O_4N_1$ were detected with the highest
393 abundance in all cities. These molecular formulas are in line with nitrophenol or nitrocatechol
394 analogs, which have been identified in a previous urban OA study (Wang et al., 2017). Furthermore,
395 these nitrooxy-aromatic compounds were shown to enhance light absorbing properties of OA
396 (Laskin et al., 2015; Lin et al., 2015). In addition, it should be noted that the Xc values for $C_6H_5O_4N_1$,
397 $C_7H_7O_4N_1$ and $C_8H_9O_4N_1$ were calculated to be lower than 2.5, suggesting that the fraction of
398 aromatics in CHON- compounds was underestimated. This is because that for nitrocatechol
399 analogs with formulas of $C_6H_5O_4N_1$, $C_7H_7O_4N_1$ and $C_8H_9O_4N_1$, only one oxygen atom is involved
400 in the π -bond structure corresponding to the p value of 0.25 in the Xc calculation equation, which
401 is lower than the p value of 0.5 applied for the Xc calculation in this study. The diagram of DBE
402 versus C number for CHON+ compounds observed in the three locations (presented in Fig. S3-S7
403 in SI) shows that more aromatic CHON+ compounds with relatively lower degree of oxidation
404 were assigned in Changchun+ samples compared to Shanghai+ and Guangzhou+ samples.

405 **3.4 CHN+ compounds**

406 205–696 CHN+ compounds were detected in Changchun+ samples in ESI+, which is higher than
407 in Shanghai+ (253) and Guangzhou (205). These CHN+ compounds are likely assignable to amines
408 according to previous studies (Rincón et al., 2012; Wang et al., 2017; Wang et al., 2018). The
409 number of CHN+ compounds accounts for 24%, 36% and 30% of the total organic compounds in
410 Changchun+, Shanghai+ and Guangzhou+, respectively, whereas the peak abundance of these

411 compounds accounts for 40%, 71% and 62%, respectively. The majority (> 97% in terms of peak
412 abundance) of CHN+ compounds have one or two nitrogen atoms in their molecular formulas (see
413 Fig. S9). Comparing the CHN+ compounds for the three cities, 58–51 common CHN+ formulas
414 were observed in all cities, which contribute to as much as 8343–9889% of the total abundance of
415 CHN+ formulas. This large percentage indicates that CHN+ compounds with presumably high
416 concentrations in Changchun+, Shanghai+ and Guangzhou+ exhibit similar chemical composition.
417 However, again OA samples from Changchun show some distinct differences to samples from
418 Guangzhou and Shanghai.

419 A van Krevelen diagram of CHN+ compounds detected in the three samples is shown in Fig. 6,
420 illustrating H/C ratios as a function of N/C ratio. In this plot, major parts of the CHN+ compounds
421 are found in a region, which is constraint by H/C ratios between 0.5 and 2 and N/C ratios lower
422 than 0.5. Moreover, the pie charts show that the majority (83–87% in terms of peak abundance and
423 72–90% in terms of peak numbers) of these CHN+ compounds can be assigned to mono- and
424 polyaromatics with $X_c \geq 2.5$. In addition, as shown in Table 1, the average DBE and X_c values of
425 CHN+ compounds are the highest among all organic species. These observations imply that CHN+
426 compounds exhibit the highest degree of aromaticity of all organics in the Chinese urban OA
427 samples, which is consistent with previous studies (Lin et al., 2012b; Rincón et al., 2012; Wang et
428 al., 2018). Polyaromatic compounds with $X_c \geq 2.7$ are displayed in the lower left corner of the
429 van Krevelen diagram, accounting for 41% in terms of peak abundance (48% in terms of peak
430 numbers) of CHN+ compounds detected in Changchun+, but merely for 9–10% in terms of peak
431 abundance (27–31% in terms of peak numbers) in Shanghai+ and Guangzhou+. For example,
432 formulas of $C_{11}H_{11}N_1$ ($X_c = 2.7$), $C_{10}H_9N_1$ ($X_c = 2.7$), and $C_{12}H_{13}N_1$ ($X_c = 2.7$), which are assigned
433 to be naphthalene core structure-containing compounds, have relatively higher abundance in
434 Changchun+ than in Shanghai+ and Guangzhou+. Moreover, the average DBE and X_c values of
435 CHN+ compounds (see Table 1) in Changchun+ are significantly-substantially higher than those in
436 Shanghai+ and Guangzhou+, further indicating that CHN+ compounds in Changchun+ show a
437 higher degree of aromaticity, which can be caused by large coal combustion emissions in the winter
438 in Changchun. Remarkably, as can be seen in Fig. 6, the abundance of CHN+ compounds in
439 Changchun+ distributes evenly among different individual CHN+ compounds, while in Shanghai+
440 and Guangzhou+ they are dominated by the formula of $C_{10}H_{14}N_2$ (the biggest purple circle in Fig.
441 6) with DBE value of 5, which probably has high concentration and/or high ionization efficiency
442 in the positive ESI mode. According to a previous smog chamber study (Laskin et al., 2010), most
443 CHN+ aromatics are probably generated from biomass burning through the addition of reduced

444 nitrogen (e.g., NH₃) to the organic molecules via imine formation reaction, indicating that biomass
445 burning probably made a certain contribution to the formation of CHN⁺ compounds observed in
446 the three urban OA samples in our study.

447 **3.5 CHOS⁻ compounds**

448 In this study, 75–155 CHOS⁻ compounds were observed, accounting for 10%, 12% and 14% of
449 the total peak abundance of all organics in Changchun⁻, Shanghai⁻ and Guangzhou⁻, respectively.
450 Around 89–96% of these CHOS⁻ compounds were found to fulfill the O/S ≥ 4 criterion allowing
451 the assignment of at least one –OSO₃H functional group, and thus, a tentative classification to
452 organosulfates (OSs) (Lin et al., 2012a; Lin et al., 2012b; Tao et al., 2014; Wang et al., 2016; Wang
453 et al., 2017; Wang et al., 2018; Wang et al., 2019a). OSs were shown to affect the surface activity
454 and hygroscopic properties of the aerosol particles, leading to potential impacts on climate (Hansen
455 et al., 2015; Wang et al., 2019a). Out of all formulas, 28–23 common CHOS⁻ formulas were
456 detected for the three sample locations, accounting for 3928%, 6858% and 6552% of the CHOS⁻
457 peak abundance in Changchun⁻, Shanghai⁻ and Guangzhou⁻, respectively. However, 40 common
458 CHOS⁻ formulas were found between Shanghai⁻ and Guangzhou⁻, accounting for 60–65% and
459 7078–8381% in terms of the CHOS⁻ formula numbers and peak abundance, respectively. This
460 indicates that the chemical composition of the major CHOS⁻ compounds of Shanghai⁻ and
461 Guangzhou⁻ are quite similar, while they show substantial chemical differences for samples from
462 Changchun⁻.

463 Figure 7 shows the DBEs as a function of carbon number for all CHOS⁻ compounds detected for
464 the three cities. The CHOS⁻ compounds exhibit a DBE range from 0 to 10 and carbon number
465 range of 2–15. However, the majority of CHOS⁻ compounds with elevated peak abundances
466 concentrate in a region with rather low DBE values of 0–5. The average H/C ratios of CHOS⁻
467 compounds are in the range of 1.56–1.85, and thus, higher than for any other compound class,
468 whereas the average DBE values of 1.71–2.55 are the lowest among all classes. This indicates that
469 CHOS⁻ compounds in the OA from the three Chinese cities are characterized by a low degree of
470 unsaturation. Moreover, the pie charts in Fig. 7 show that aliphatic compounds with X_c ≤ 2.5 are
471 dominant in CHOS⁻ compounds with a fraction of 96–99% in terms of peak abundance, which is
472 significantly-substantially higher than that (13–48%) for CHO, CHON and CHN species. Aliphatic
473 CHOS⁻ compounds with C ≤ 10 can be formed from biogenic and/or anthropogenic precursors
474 (Hansen et al., 2014; Glasius et al., 2018; Wang et al., 2019a), such as C₂H₄O₆S₁ (derived from
475 glyoxal) (Lim et al., 2010; McNeill et al., 2012), C₃H₆O₆S₁ (derived from isoprene) (Surratt et al.,

2007) and $C_8H_{16}O_4S_1$ (derived from α -pinene). However, more CHOS⁻ compounds with $C > 10$ and with DBEs lower than 1 are observed in Changchun⁻, such as $C_{14}H_{28}O_5S_1$, $C_{13}H_{26}O_5S_1$, $C_{12}H_{24}O_5S_1$, $C_{11}H_{22}O_5S_1$ and $C_{11}H_{20}O_6S_1$. These high-carbon-number-containing CHOS⁻ compounds are likely formed from long-alkyl-chain compounds with less oxygenated functional groups, which were previously suggested to be emitted from traffic (Tao et al., 2014) or derived from sesquiterpene emissions (Brüggemann et al., 2019). However, as sesquiterpene emissions can be expected to be very low in wintertime at Changchun, the presence of these compounds further underlines the strong impact of anthropogenic emissions on CHOS⁻ formation in Changchun⁻. In this study, (O-3S)/C ratio was used instead of traditional O/C ratio to present the oxidation state of CHOS⁻ compounds, since the sulfate functional group contains three more oxygen atoms than common oxygen-containing groups (e.g., hydroxyl and carbonyl), which makes no contribution to the oxidation state of the carbon backbone of the CHOS⁻ compounds. Comparing average values for H/C, (O-3S)/C and DBEs of CHOS⁻ for the three sample locations (see Table 1), we find that the H/C ratios (1.85) and (O-3S)/C ratios (0.61–0.71) for Shanghai⁻ and Guangzhou⁻ samples are larger than those for Changchun⁻ samples (H/C = 1.56 and (O-3S)/C = 0.52), whereas the DBE values (1.71–1.79) in Shanghai⁻ and Guangzhou⁻ are lower than those for Changchun⁻ (2.55). These observations indicate that CHOS⁻ compounds in urban OA from Northeast China are less oxidized but more unsaturated compared to those in East and Southeast China, likely due to enhanced emissions from residential heating during winter in North China.

3.6 CHONS compounds

4-5% of the total organics detected in ESI⁻ were identified as CHONS⁻ compounds in terms of peak abundance. In contrast, CHONS⁺ compounds account merely for 0.3–1% of all organics detected in ESI⁺. The average MM_{avg} of the CHONS⁻ compounds for the three sample locations ranges from 214 to 293 Da, generally showing larger molecular masses than compounds of any other class because of the likely presence of both nitrate and sulfate functional groups. In total, only 8-5 common CHONS⁻ formulas were detected for all three sample locations, accounting for 84%, 58-21% and 56-20% of the CHONS⁻ peak abundance in Changchun⁻, Shanghai⁻ and Guangzhou⁻, respectively. As already observed for other compound classes, these percentages imply that the CHONS⁻ compounds in urban OA of Shanghai⁻ and Guangzhou⁻ exhibit a rather similar chemical composition, whereas such compounds are significantly different for Changchun⁻.

In the OA samples of Shanghai⁻ and Guangzhou⁻, 78–87% of CHONS⁻ compounds in terms of peak abundance have 7 or more O atoms in their formulas, allowing the assignment of one $-OSO_3H$

508 and one -NO₃ functional groups in the molecular structures, thus, classifying them as potential
509 nitrooxy-organosulfates. In contrast to Shanghai- and Guangzhou-, only 26% of CHONS-
510 compounds were assigned to such nitrooxy-organosulfates for Changchun-, indicating that most
511 of the N atoms in the CHONS- compounds are present in a reduced oxidation state, e.g., in the
512 form of amines. The average DBE and X_c values of CHONS- compounds in Shanghai- and
513 Guangzhou- are 3.3–3.45 and 0.43–0.44, respectively. Again these values differ ~~significantly~~
514 for the Changchun- samples with an increased average DBE of 3.75 and an average X_c of 1.06,
515 indicating that CHONS- compounds in Changchun- possess on average a higher degree of
516 unsaturation and aromaticity compared to such compounds in Shanghai- and Guangzhou- samples.
517 Interestingly, the compound with formula C₁₀H₁₇O₇NS has the highest relative peak abundance
518 (32%) in Shanghai- and Guangzhou-, whereas in Changchun- the compound with formula
519 C₂H₃O₄NS is dominant. C₁₀H₁₇O₇NS has previously been identified as ~~pinanediol~~-mononitrate
520 organosulfate generated from α/β-pinene (Iinuma et al., 2007; Surratt et al., 2008; Lin et al., 2012b;
521 Wang et al., 2017), while C₂H₃O₄NS may be assigned as a cyanogroup-containing sulfate. This
522 observation is comparable to our previous study (Wang et al., 2019a), which found that C₁₀H₁₇O₇NS
523 was dominant for CHONS- compounds in low-concentration aerosol samples collected in Beijing
524 (China) and Mainz (Germany). Consistently, a C₂H₃O₄NS compound had the highest abundance
525 among CHONS- compounds in polluted Beijing aerosol samples. This agreement can be explained
526 by the adjacent locations of Beijing (39.99°N, 116.39°E) and Changchun (43.54°N, 125.13°E) and
527 similar residential heating patterns by coal combustion during wintertime. In conclusion, these
528 results further demonstrate that the precursors for CHONS- compounds in Shanghai- and
529 Guangzhou- are different from those in Changchun-, which is probably due to differences in
530 anthropogenic emissions.

531 **4 Conclusion**

532 The molecular composition of the organic fraction of PM_{2.5} samples collected in three Chinese
533 megacities (Changchun, Shanghai and Guangzhou) was investigated using a UHPLC-Orbitrap
534 mass spectrometer. In total, 416–769 (ESI-) and 687–2943 (ESI+) organic compounds were
535 observed and separated into five subgroups: CHO, CHN, CHON, CHOS and CHONS. Specifically,
536 ~~139-120~~ common formulas were detected in ESI- and ~~168-129~~ common formulas in ESI+ for all
537 sample locations, accounting for ~~7857-8771~~% and ~~6530-9075~~% in terms of peak abundance,
538 respectively. Overall, we found that urban OA in Changchun, Shanghai and Guangzhou shows a
539 quite similar chemical composition for organic compounds of high concentrations. The majority of
540 these organic species was assigned to mono-aromatic or poly-aromatic compounds, indicating that

541 anthropogenic emissions are the major source for urban OA in all three cities.

542 Despite the chemical similarity of the three sample locations for ~~major~~ organic compounds in urban
543 OA, remarkable differences were found in chemical composition of the remaining particle
544 constituents, in particular for OA samples from Changchun. In general, a larger amount of
545 polyaromatics was observed for Changchun samples, most likely due to emissions from coal
546 combustion during wintertime residential heating period. Moreover, the peak abundance-weighted
547 average DBE and average Xc values of the total organic compounds in Changchun were found to
548 be larger than those for Shanghai and Guangzhou, showing that organic compounds in Changchun
549 possess a higher degree of unsaturation and aromaticity. For average H/C and O/C ratios a similar
550 trend was observed. While average H/C and O/C ratios detected in ESI⁻ were found to be highest
551 for Guangzhou samples, ~~significantly-relatively~~ lower values were observed for Shanghai and
552 Changchun samples, indicating that OA collected in lower latitude regions of China experiences
553 more intense photochemical oxidation processes and/or are affect to a larger degree by biogenic
554 sources.

555 **5 Limitations**

556 In this study, we used the peak abundance-weighted method to illustrate the difference in chemical
557 formulas assigned by Orbitrap mass spectrometry. This comparison was made based on the
558 assumption that the measured organic compounds have same peak abundance response in the mass
559 spectrometer. However, this assumption can bring some uncertainties because the ionization
560 efficiencies vary between different compounds (Schmidt et al., 2006; Leito et al., 2008; Perry et al.,
561 2008; Krueve et al., 2014). For example, the ionization efficiencies of nitrophenol species detected
562 in negative ESI mode can vary by a large degree depending on the position of the substituents at
563 the nitrobenzene ring (Schmidt et al., 2006; Krueve et al., 2014) and the ionization efficiencies of
564 carboxylic acids can also vary by several orders of magnitude depending on the structures (Krueve
565 et al., 2014). Nonetheless, it is a challenging analytical task to identify and quantify all compounds
566 in ambient OA due to the high chemical complexity of OA and the limits in authentic standards of
567 OA. Despite the inherent uncertainties, the peak abundance-weighted comparison of molecular
568 formulas provides an overview of the difference in chemical composition of OA in these three
569 representative Chinese cities. In particular, the chemical formulas assigned in this study can be
570 validated in future studies by authentic standards and the difference in ionization efficiencies can
571 be further evaluated.

572

573 **Author contributions.** RJH, TH and KW conducted the study design. LY, HN, JG and MW
574 collected the PM_{2.5} filter samples. KW and YZ carried out the experimental work and data analysis.
575 KW wrote the manuscript. KW, TH, RJH, M. Brüggemann, YZ, JH, M. Bilde and MG interpreted
576 data and edited the manuscript. All authors commented on and discussed the manuscript.

577 **Competing interests.** The authors declare that they have no conflict of interest.

578 **Acknowledgements.** This study was supported by the National Natural Science Foundation of
579 China (NSFC, Grant No. 41925015, No. 91644219 and No. 41877408), the Chinese Academy of
580 Sciences (No. ZDBS-LY-DQC001), the National Key Research and Development Program of
581 China (No. 2017YFC0212701), and the German Research Foundation (Deutsche
582 Forschungsgemeinschaft, DFG) under Grant No. INST 247/664-1 FUGG. K. Wang and Y. Zhang
583 acknowledge the scholarship from Chinese Scholarship Council (CSC) and Max Plank Graduate
584 Center with Johannes Gutenberg University of Mainz (MPGC) and thanks Prof. Ulrich Pöschl, Dr.
585 Christopher J. Kampf and Dr. Yafang Cheng for their helpful suggestion on this study. K. Wang
586 also thanks Dr. Huanfeng Dong from Zhejiang University for the great support on the programming
587 of data process.

588
589
590
591
592
593
594
595
596
597
598
599
600
601
602
603
604
605
606
607
608
609
610
611
612
613
614
615
616

617

618

619

References

620 An, Z., Huang, R. J., Zhang, R., Tie, X., Li, G., Cao, J., Zhou, W., Shi, Z., Han, Y., Gu, Z., and Ji, Y.: Severe
621 haze in northern China: A synergy of anthropogenic emissions and atmospheric processes, *Proc Natl Acad*
622 *Sci U S A*, 116, 8657-8666, 10.1073/pnas.1900125116, 2019.

623 Brüggemann, M., Poulain, L., Held, A., Stelzer, T., Zuth, C., Richters, S., Mutzel, A., van Pinxteren, D.,
624 Inuma, Y., Katkevica, S., Rabe, R., Herrmann, H., and Hoffmann, T.: Real-time detection of highly
625 oxidized organosulfates and BSOA marker compounds during the F-BEACH 2014 field study, *Atmos.*
626 *Chem. Phys.*, 17, 1453-1469, 10.5194/acp-17-1453-2017, 2017.

627 Brüggemann, M., van Pinxteren, D., Wang, Y., Yu, J. Z., and Herrmann, H.: Quantification of known and
628 unknown terpenoid organosulfates in PM10 using untargeted LC-HRMS/MS: contrasting summertime
629 rural Germany and the North China Plain, *Environmental Chemistry*, -, <https://doi.org/10.1071/EN19089>,
630 2019.

631 Claeys, M., Graham, B., Vas, G., Wang, W., Vermeylen, R., Pashynska, V., Cafmeyer, J., Guyon, P., Andre,
632 M., Artaxo, P., and Maenhaut, W.: Formation of secondary organic aerosol through photooxidation of
633 isoprene, *Science*, 303, 1173-1175, 10.1126/science.1092805, 2004.

634 Daellenbach, K. R., Kourtchev, I., Vogel, A. L., Bruns, E. A., Jiang, J., Petäjä, T., Jaffrezou, J.-L., Aksoyoglu,
635 S., Kalberer, M., Baltensperger, U., El Haddad, I., and Prévôt, A. S. H.: Impact of anthropogenic and
636 biogenic sources on the seasonal variation in the molecular composition of urban organic aerosols: a field
637 and laboratory study using ultra-high-resolution mass spectrometry, *Atmospheric Chemistry and Physics*,
638 19, 5973-5991, 10.5194/acp-19-5973-2019, 2019.

639 Ding, X., Zhang, Y.-Q., He, Q.-F., Yu, Q.-Q., Shen, R.-Q., Zhang, Y., Zhang, Z., Lyu, S.-J., Hu, Q.-H., Wang,
640 Y.-S., Li, L.-F., Song, W., and Wang, X.-M.: Spatial and seasonal variations of secondary organic aerosol
641 from terpenoids over China, *J. geophys. Res.-Atoms.*, 121, 14661-14678, doi:10.1002/2016JD025467,
642 2016.

643 Elzein, A., Dunmore, R. E., Ward, M. W., Hamilton, J. F., and Lewis, A. C.: Variability of polycyclic
644 aromatic hydrocarbons and their oxidative derivatives in wintertime Beijing, China, *Atmospheric*
645 *Chemistry and Physics*, 19, 8741-8758, 10.5194/acp-19-8741-2019, 2019.

646 Fleming, L. T., Lin, P., Laskin, A., Laskin, J., Weltman, R., Edwards, R. D., Arora, N. K., Yadav, A.,
647 Meinardi, S., Blake, D. R., Pillarisetti, A., Smith, K. R., and Nizkorodov, S. A.: Molecular composition
648 of particulate matter emissions from dung and brushwood burning household cookstoves in Haryana,
649 India, *Atmos. Chem. Phys.*, 18, 2461-2480, 10.5194/acp-18-2461-2018, 2018.

650 Fu, P., Kawamura, K., Okuzawa, K., Aggarwal, S. G., Wang, G., Kanaya, Y., and Wang, Z.: Organic
651 molecular compositions and temporal variations of summertime mountain aerosols over Mt. Tai, North
652 China Plain, *J. Geophys. Res.*, 113, 10.1029/2008jd009900, 2008.

653 Glasius, M., Hansen, A. M. K., Claeys, M., Henzing, J. S., Jedynska, A. D., Kasper-Giebl, A., Kistler, M.,
654 Kristensen, K., Martinsson, J., Maenhaut, W., Nøjgaard, J. K., Spindler, G., Stenström, K. E., Swietlicki,
655 E., Szidat, S., Simpson, D., and Yttri, K. E.: Composition and sources of carbonaceous aerosols in
656 Northern Europe during winter, *Atmos. Environ.*, 173, 127-141, 10.1016/j.atmosenv.2017.11.005, 2018.

657 Hansen, A. M. K., Kristensen, K., Nguyen, Q. T., Zare, A., Cozzi, F., Noejgaard, J. K., Skov, H., Brandt, J.,
658 Christensen, J. H., Strom, J., Tunved, P., Krejci, R., and Glasius, M.: Organosulfates and organic acids in
659 Arctic aerosols: speciation, annual variation and concentration levels, *Atmos. Chem. Phys.*, 14, 7807-
660 7823, <https://doi.org/10.5194/acp-14-7807-2014>, 2014.

661 Hansen, A. M. K., Hong, J., Raatikainen, T., Kristensen, K., Ylisirniö, A., Virtanen, A., Petäjä, T., Glasius,
662 M., and Prisle, N. L.: Hygroscopic properties and cloud condensation nuclei activation of limonene-
663 derived organosulfates and their mixtures with ammonium sulfate, *Atmos. Chem. Phys.*, 15, 14071-14089,
664 <https://doi.org/10.5194/acp-15-14071-2015>, 2015.

665 He, X., Huang, X. H. H., Chow, K. S., Wang, Q., Zhang, T., Wu, D., and Yu, J. Z.: Abundance and Sources
666 of Phthalic Acids, Benzene-Tricarboxylic Acids, and Phenolic Acids in PM2.5 at Urban and Suburban
667 Sites in Southern China, *ACS Earth and Space Chemistry*, 2, 147-158,
668 10.1021/acsearthspacechem.7b00131, 2018.

669 Ho, C. S., Lam, C. W. K., Chan, M. H. M., Cheung, R. C. K., Law, L. K., Suen, M. W. M., and Tai, H. L.:
670 Electrospray ionisation mass spectrometry: principles and clinical application, *Clin. Biochem. Rev.*, 24,
671 10, 2003.

672 Hoffmann, T., Huang, R. J., and Kalberer, M.: Atmospheric analytical chemistry, *Anal. Chem.*, 83, 4649-
673 4664, 10.1021/ac2010718, 2011.

674 Huang, G., Liu, Y., Shao, M., Li, Y., Chen, Q., Zheng, Y., Wu, Z., Liu, Y., Wu, Y., Hu, M., Li, X., Lu, S.,
675 Wang, C., Liu, J., Zheng, M., and Zhu, T.: Potentially Important Contribution of Gas-Phase Oxidation of
676 Naphthalene and Methylanthalene to Secondary Organic Aerosol during Haze Events in Beijing,
677 *Environ Sci Technol*, 53, 1235-1244, 10.1021/acs.est.8b04523, 2019.

678 Huang, R. J., Zhang, Y., Bozzetti, C., Ho, K. F., Cao, J. J., Han, Y., Daellenbach, K. R., Slowik, J. G., Platt,
679 S. M., Canonaco, F., Zotter, P., Wolf, R., Pieber, S. M., Bruns, E. A., Crippa, M., Ciarelli, G., Piazzalunga,
680 A., Schwikowski, M., Abbaszade, G., Schnelle-Kreis, J., Zimmermann, R., An, Z., Szidat, S.,
681 Baltensperger, U., El Haddad, I., and Prevot, A. S.: High secondary aerosol contribution to particulate
682 pollution during haze events in China, *Nature*, 514, 218-222, 10.1038/nature13774, 2014.

683 Huang, R. J., Cao, J. J., and Worsnop, D.: Sources and Chemical Composition of Particulate Matter During
684 Haze Pollution Events in China, in: *Air pollution in Eastern Asia: an integrated perspective*, edited by
685 Bouarar, I., Wang, X. M., and Brasseur, G. P., Springer, Cham, Switzerland, 49-68, 2017.

686 Inuma, Y., Müller, C., Berndt, T., Böge, O., Claeys, M., and Herrmann, H.: Evidence for the existence of
687 organosulfates from β -pinene ozonolysis in ambient secondary organic aerosol, *Environ. Sci. Technol.*,
688 41, 6678-6683, 10.1021/es070938t, 2007.

689 Jung, J., and Kawamura, K.: Enhanced concentrations of citric acid in spring aerosols collected at the Gosan
690 background site in East Asia, *Atmos. Environ.*, 45, 5266-5272, 10.1016/j.atmosenv.2011.06.065, 2011.

691 Kautzman, K. E., Surratt, J. D., Chan, M. N., Chan, A. W., Hersey, S. P., Chhabra, P. S., Dalleska, N. F.,
692 Wennberg, P. O., Flagan, R. C., and Seinfeld, J. H.: Chemical composition of gas- and aerosol-phase
693 products from photooxidation of naphthalene, *J. Phys. Chem. A*, 114, 913-934, 10.1021/jp908530s, 2010.

694 Kind, T., and Fiehn, O.: Seven Golden Rules for heuristic filtering of molecular formulas obtained by
695 accurate mass spectrometry, *BMC Bioinformatics*, 8, 10.1186/1471-2105-8-105, 2007.

696 Kourtchev, I., O'Connor, I. P., Giorio, C., Fuller, S. J., Kristensen, K., Maenhaut, W., Wenger, J. C., Sodeau,
697 J. R., Glasius, M., and Kalberer, M.: Effects of anthropogenic emissions on the molecular composition of
698 urban organic aerosols: An ultrahigh resolution mass spectrometry study, *Atmo. Environ.*, 89, 525-532,
699 10.1016/j.atmosenv.2014.02.051, 2014.

700 Kourtchev, I., Godoi, R. H. M., Connors, S., Levine, J. G., Archibald, A. T., Godoi, A. F. L., Paralovo, S. L.,
701 Barbosa, C. G. G., Souza, R. A. F., Manzi, A. O., Seco, R., Sjostedt, S., Park, J.-H., Guenther, A., Kim,
702 S., Smith, J., Martin, S. T., and Kalberer, M.: Molecular composition of organic aerosols in central
703 Amazonia: an ultra-high-resolution mass spectrometry study, *Atmos. Chem. Phys.*, 16, 11899-11913,
704 <https://doi.org/10.5194/acp-16-11899-2016>, 2016.

705 Kruve, A., Kaupmees, K., Liigand, J., and Leito, I.: Negative electrospray ionization via deprotonation:
706 predicting the ionization efficiency, *Anal Chem*, 86, 4822-4830, 10.1021/ac404066v, 2014.

707 Laskin, A., Laskin, J., and Nizkorodov, S. A.: Chemistry of atmospheric brown carbon, *Chem. Rev.*, 115,
708 4335-4382, 10.1021/cr5006167, 2015.

709 Laskin, J., Laskin, A., Roach, P. J., Slysz, G. W., Anderson, G. A., Nizkorodov, S. A., Bones, D. L., and
710 Nguyen, L. Q.: High-Resolution Desorption Electrospray Ionization Mass Spectrometry for Chemical
711 Characterization of Organic Aerosols, *Anal. Chem.*, 82, 2048-2058, 10.1021/ac902801f, 2010.

712 Laskin, J., Laskin, A., and Nizkorodov, S. A.: Mass Spectrometry Analysis in Atmospheric Chemistry, *Anal.*
713 *Chem.*, 90, 166-189, 10.1021/acs.analchem.7b04249, 2018.

714 Lee, A., Goldstein, A. H., Kroll, J. H., Ng, N. L., Varutbangkul, V., Flagan, R. C., and Seinfeld, J. H.: Gas-
715 phase products and secondary aerosol yields from the photooxidation of 16 different terpenes, *J. Geophys.*
716 *Res.*, 111, 10.1029/2006jd007050, 2006.

717 Leito, I., Herodes, K., Huopolainen, M., Virro, K., Kunnapas, A., Kruve, A., and Tanner, R.: Towards the
718 electrospray ionization mass spectrometry ionization efficiency scale of organic compounds, *Rapid*
719 *Commun Mass Spectrom*, 22, 379-384, 10.1002/rcm.3371, 2008.

720 Li, Y. J., Huang, D. D., Cheung, H. Y., Lee, A. K. Y., and Chan, C. K.: Aqueous-phase photochemical
721 oxidation and direct photolysis of vanillin – a model compound of methoxy phenols from biomass burning,
722 *Atmospheric Chemistry and Physics*, 14, 2871-2885, 10.5194/acp-14-2871-2014, 2014.

723 Lim, Y. B., Tan, Y., Perri, M. J., Seitzinger, S. P., and Turpin, B. J.: Aqueous chemistry and its role in
724 secondary organic aerosol (SOA) formation, *Atmos. Chem. Phys.*, 10, 10521-10539, 10.5194/acp-10-
725 10521-2010, 2010.

726 Lin, P., Rincon, A. G., Kalberer, M., and Yu, J. Z.: Elemental composition of HULIS in the Pearl River Delta

727 Region, China: results inferred from positive and negative electrospray high resolution mass
728 spectrometric data, *Environ. Sci. Technol.*, 46, 7454-7462, 10.1021/es300285d, 2012a.

729 Lin, P., Yu, J. Z., Engling, G., and Kalberer, M.: Organosulfates in humic-like substance fraction isolated
730 from aerosols at seven locations in East Asia: a study by ultra-high-resolution mass spectrometry, *Environ.*
731 *Sci. Technol.*, 46, 13118-13127, 10.1021/es303570v, 2012b.

732 Lin, P., Laskin, J., Nizkorodov, S. A., and Laskin, A.: Revealing Brown Carbon Chromophores Produced in
733 Reactions of Methylglyoxal with Ammonium Sulfate, *Environ. Sci. Technol.*, 49, 14257-14266,
734 10.1021/acs.est.5b03608, 2015.

735 McNeill, V. F., Woo, J. L., Kim, D. D., Schwier, A. N., Wannell, N. J., Sumner, A. J., and Barakat, J. M.:
736 Aqueous-phase secondary organic aerosol and organosulfate formation in atmospheric aerosols: a
737 modeling study, *Environ Sci Technol*, 46, 8075-8081, 10.1021/es3002986, 2012.

738 Ning, C., Gao, Y., Zhang, H., Yu, H., Wang, L., Geng, N., Cao, R., and Chen, J.: Molecular characterization
739 of dissolved organic matters in winter atmospheric fine particulate matters (PM_{2.5}) from a coastal city of
740 northeast China, *Sci Total Environ*, 689, 312-321, 10.1016/j.scitotenv.2019.06.418, 2019.

741 Nizkorodov, S. A., Laskin, J., and Laskin, A.: Molecular chemistry of organic aerosols through the
742 application of high resolution mass spectrometry, *Phys. Chem. Chem. Phys.*, 13, 3612-3629,
743 10.1039/c0cp02032j, 2011.

744 Noziere, B., Kalberer, M., Claeys, M., Allan, J., D'Anna, B., Decesari, S., Finessi, E., Glasius, M., Grgic, I.,
745 Hamilton, J. F., Hoffmann, T., Iinuma, Y., Jaoui, M., Kahnt, A., Kampf, C. J., Kourchev, I., Maenhaut,
746 W., Marsden, N., Saarikoski, S., Schnelle-Kreis, J., Surratt, J. D., Szidat, S., Szmigielski, R., and
747 Wisthaler, A.: The molecular identification of organic compounds in the atmosphere: state of the art and
748 challenges, *Chem. Rev.*, 115, 3919-3983, 10.1021/cr5003485, 2015.

749 Pereira, K. L., Hamilton, J. F., Rickard, A. R., Bloss, W. J., Alam, M. S., Camredon, M., Muñoz, A., Vázquez,
750 M., Borrás, E., and Ródenas, M.: Secondary organic aerosol formation and composition from the photo-
751 oxidation of methyl chavicol (estragole), *Atmos. Chem. Phys.*, 14, 5349-5368, 10.5194/acp-14-5349-
752 2014, 2014.

753 Perry, R. H., Cooks, R. G., and Noll, R. J.: ORBITRAP MASS SPECTROMETRY: INSTRUMENTATION,
754 ION MOTION AND APPLICATIONS, *Mass Spectrometry Reviews*, 27, 661-699, 10.1002/mas.20186,
755 2008.

756 Rincón, A. G., Calvo, A. I., Dietzel, M., and Kalberer, M.: Seasonal differences of urban organic aerosol
757 composition - an ultra-high resolution mass spectrometry study, *Environ. Chem.*, 9, 298,
758 10.1071/en12016, 2012.

759 Riva, M., Tomaz, S., Cui, T., Lin, Y.-H., Perraudin, E., Gold, A., Stone, E. A., Villenave, E., and Surratt, J.
760 D.: Evidence for an Unrecognized Secondary Anthropogenic Source of Organosulfates and Sulfonates:
761 Gas-Phase Oxidation of Polycyclic Aromatic Hydrocarbons in the Presence of Sulfate Aerosol, *Environ.*
762 *Sci. Technol.*, 49, 6654-6664, 10.1021/acs.est.5b00836, 2015.

763 Schmidt, A. C., Herzsuh, R., Matysik, F. M., and Engewald, W.: Investigation of the ionisation and
764 fragmentation behaviour of different nitroaromatic compounds occurring as polar metabolites of
765 explosives using electrospray ionisation tandem mass spectrometry, *Rapid Commun Mass Spectrom*, 20,
766 2293-2302, 10.1002/rcm.2591, 2006.

767 Shi, Z., Vu, T., Kotthaus, S., Harrison, R. M., Grimmond, S., Yue, S., Zhu, T., Lee, J., Han, Y., Demuzere,
768 M., Dunmore, R. E., Ren, L., Liu, D., Wang, Y., Wild, O., Allan, J., Acton, W. J., Barlow, J., Barratt, B.,
769 Beddows, D., Bloss, W. J., Calzolari, G., Carruthers, D., Carslaw, D. C., Chan, Q., Chatzidiakou, L., Chen,
770 Y., Crilley, L., Coe, H., Dai, T., Doherty, R., Duan, F., Fu, P., Ge, B., Ge, M., Guan, D., Hamilton, J. F.,
771 He, K., Heal, M., Heard, D., Hewitt, C. N., Hollaway, M., Hu, M., Ji, D., Jiang, X., Jones, R., Kalberer,
772 M., Kelly, F. J., Kramer, L., Langford, B., Lin, C., Lewis, A. C., Li, J., Li, W., Liu, H., Liu, J., Loh, M.,
773 Lu, K., Lucarelli, F., Mann, G., McFiggans, G., Miller, M. R., Mills, G., Monk, P., Nemitz, E., amp, apos,
774 Connor, F., Ouyang, B., Palmer, P. I., Percival, C., Popoola, O., Reeves, C., Rickard, A. R., Shao, L., Shi,
775 G., Spracklen, D., Stevenson, D., Sun, Y., Sun, Z., Tao, S., Tong, S., Wang, Q., Wang, W., Wang, X.,
776 Wang, X., Wang, Z., Wei, L., Whalley, L., Wu, X., Wu, Z., Xie, P., Yang, F., Zhang, Q., Zhang, Y.,
777 Zhang, Y., and Zheng, M.: Introduction to the special issue "In-depth study of air pollution sources and
778 processes within Beijing and its surrounding region (APHH-Beijing)", *Atmospheric Chemistry and*
779 *Physics*, 19, 7519-7546, 10.5194/acp-19-7519-2019, 2019.

780 Song, J., Li, M., Jiang, B., Wei, S., Fan, X., and Peng, P.: Molecular Characterization of Water-Soluble
781 Humic like Substances in Smoke Particles Emitted from Combustion of Biomass Materials and Coal

782 Using Ultrahigh-Resolution Electrospray Ionization Fourier Transform Ion Cyclotron Resonance Mass
783 Spectrometry, *Environ. Sci. Technol.*, 52, 2575-2585, 10.1021/acs.est.7b06126, 2018.

784 Sun, Y., Jiang, Q., Zhang, Z., Fu, P., Li, J., Yang, T., and Yin, Y.: Investigation of the sources and evolution
785 processes of severe haze pollution in Beijing in January 2013, *J. Geophys. Res.-Atmos.*, 119, 4380-4389,
786 10.1002/, 2014.

787 Surratt, J. D., Gomez-Gonzalez, Y., Chan, A. W., Vermeylen, R., Shahgholl, M., Kleindienst, T. E., Jaoui,
788 M., Maenhaut, W., Claeys, M., Flagan, R. C., and Seinfeld, J. H.: Evidence for Organosulfate in
789 Secondary Organic Aerosol, *Environ. Sci. Technol.*, 41, 517-527, 10.1021/es062081q, 2007.

790 Surratt, J. D., Gómez-González, Y., Chan, A. W., Vermeylen, R., Shahgholi, M., Kleindienst, T. E., Edney,
791 E. O., Offenberg, J. H., Lewandowski, M., Jaoui, M., Maenhaut, W., Claeys, M., Flagan, R. C., and
792 Seinfeld, J. H.: Organosulfate Formation in Biogenic Secondary Organic Aerosol, *J. Phys. Chem. A*, 112,
793 8345-8378, 2008.

794 Tao, S., Lu, X., Levac, N., Bateman, A. P., Nguyen, T. B., Bones, D. L., Nizkorodov, S. A., Laskin, J., Laskin,
795 A., and Yang, X.: Molecular Characterization of Organosulfates in Organic Aerosols from Shanghai and
796 Los Angeles Urban Areas by Nanospray-Desorption Electrospray Ionization High-Resolution Mass
797 Spectrometry, *Environ. Sci. Technol.*, 48, 10993-11001, 10.1021/es5024674, 2014.

798 Tong, H., Kourtchev, I., Pant, P., Keyte, I. J., O'Connor, I. P., Wenger, J. C., Pope, F. D., Harrison, R. M.,
799 and Kalberer, M.: Molecular composition of organic aerosols at urban background and road tunnel sites
800 using ultra-high resolution mass spectrometry, *Faraday Discuss.*, 189, 51-68, 10.1039/c5fd00206k, 2016.

801 Tong, H., Zhang, Y., Filippi, A., Wang, T., Li, C., Liu, F., Leppla, D., Kourtchev, I., Wang, K., Keskinen, H.
802 M., Levula, J. T., Arangio, A. M., Shen, F., Ditas, F., Martin, S. T., Artaxo, P., Godoi, R. H. M.,
803 Yamamoto, C. I., de Souza, R. A. F., Huang, R. J., Berkemeier, T., Wang, Y., Su, H., Cheng, Y., Pope,
804 F. D., Fu, P., Yao, M., Pohlker, C., Petaja, T., Kulmala, M., Andreae, M. O., Shiraiwa, M., Poschl, U.,
805 Hoffmann, T., and Kalberer, M.: Radical Formation by Fine Particulate Matter Associated with Highly
806 Oxygenated Molecules, *Environ Sci Technol*, 53, 12506-12518, 10.1021/acs.est.9b05149, 2019.

807 Tu, P., Hall, W. A. t., and Johnston, M. V.: Characterization of Highly Oxidized Molecules in Fresh and
808 Aged Biogenic Secondary Organic Aerosol, *Anal. Chem.*, 88, 4495-4501,
809 10.1021/acs.analchem.6b00378, 2016.

810 Wang, G., Kawamura, K., Umemoto, N., Xie, M., Hu, S., and Wang, Z.: Water-soluble organic compounds
811 in PM_{2.5} and size-segregated aerosols over Mount Tai in North China Plain, *J. Geophys. Res.*, 114,
812 10.1029/2008jd011390, 2009.

813 Wang, K., Zhang, Y., Huang, R.-J., Cao, J., and Hoffmann, T.: UHPLC-Orbitrap mass spectrometric
814 characterization of organic aerosol from a central European city (Mainz, Germany) and a Chinese
815 megacity (Beijing), *Atmos. Environ.*, 189, 22-29, 10.1016/j.atmosenv.2018.06.036, 2018.

816 Wang, K., Zhang, Y., Huang, R.-J., Wang, M., Ni, H., Kampf, C. J., Cheng, Y., Bilde, M., Glasius, M., and
817 Hoffmann, T.: Molecular characterization and source identification of atmospheric particulate
818 organosulfates using ultrahigh resolution mass spectrometry, *Environ. Sci. Technol.*,
819 10.1021/acs.est.9b02628, 2019a.

820 Wang, M., Huang, R.-J., Cao, J., Dai, W., Zhou, J., Lin, C., Ni, H., Duan, J., Wang, T., Chen, Y., Li, Y.,
821 Chen, Q., Haddad, I. E., and Hoffmann, T.: Determination of n-alkanes, PAHs and hopanes in
822 atmospheric aerosol: evaluation and comparison of thermal desorption GC-MS and solvent extraction
823 GC-MS approaches, *Atmos. Meas. Tech. Discuss.*, 1-21, 10.5194/amt-2019-4, 2019b.

824 Wang, X. K., Rossignol, S., Ma, Y., Yao, L., Wang, M. Y., Chen, J. M., George, C., and Wang, L.: Molecular
825 characterization of atmospheric particulate organosulfates in three megacities at the middle and lower
826 reaches of the Yangtze River, *Atmos. Chem. Phys.*, 16, 2285-2298, [https://doi.org/10.5194/acp-16-2285-](https://doi.org/10.5194/acp-16-2285-2016)
827 [2016](https://doi.org/10.5194/acp-16-2285-2016), 2016.

828 Wang, X. K., Hayeck, N., Brüggemann, M., Yao, L., Chen, H. F., Zhang, C., Emmelin, C., Chen, J. M.,
829 George, C., and Wang, L.: Chemical characterization of organic aerosol in: A study by Ultrahigh-
830 Performance Liquid Chromatography Coupled with Orbitrap Mass Spectrometry, *J. Geophys. Res.-Atmos.*,
831 122, 703-722, <https://doi.org/10.1002/2017JD026930>, 2017.

832 Xu, W., Sun, Y., Wang, Q., Zhao, J., Wang, J., Ge, X., Xie, C., Zhou, W., Du, W., Li, J., Fu, P., Wang, Z.,
833 Worsnop, D. R., and Coe, H.: Changes in Aerosol Chemistry From 2014 to 2016 in Winter in Beijing:
834 Insights From High-Resolution Aerosol Mass Spectrometry, *J. Geophys. Res.-Atmos.*, 124, 1132-1147,
835 10.1029/2018jd029245, 2019.

836 Yassine, M. M., Harir, M., Dabek-Zlotorzynska, E., and Schmitt-Kopplin, P.: Structural characterization of

837 organic aerosol using Fourier transform ion cyclotron resonance mass spectrometry: aromaticity
838 equivalent approach, *Rapid Commun. Mass Spectrom.*, 28, 2445-2454, 10.1002/rcm.7038, 2014.
839 Zhang, P.: Revitalizing old industrial base of Northeast China: Process, policy and challenge, *Chin. Geogra.*
840 *Sci.*, 18, 109-118, 10.1007/s11769-008-0109-2, 2008.
841 Zielinski, A. T., Kourtchev, I., Bortolini, C., Fuller, S. J., Giorio, C., Popoola, O. A. M., Bogialli, S., Tapparo,
842 A., Jones, R. L., and Kalberer, M.: A new processing scheme for ultra-high resolution direct infusion
843 mass spectrometry data, *Atmos. Environ.*, 178, 129-139, 10.1016/j.atmosenv.2018.01.034, 2018.

844

845

846

847

848

849

850

851

852

853

854

855

856

857

858

859

860

861

862

863

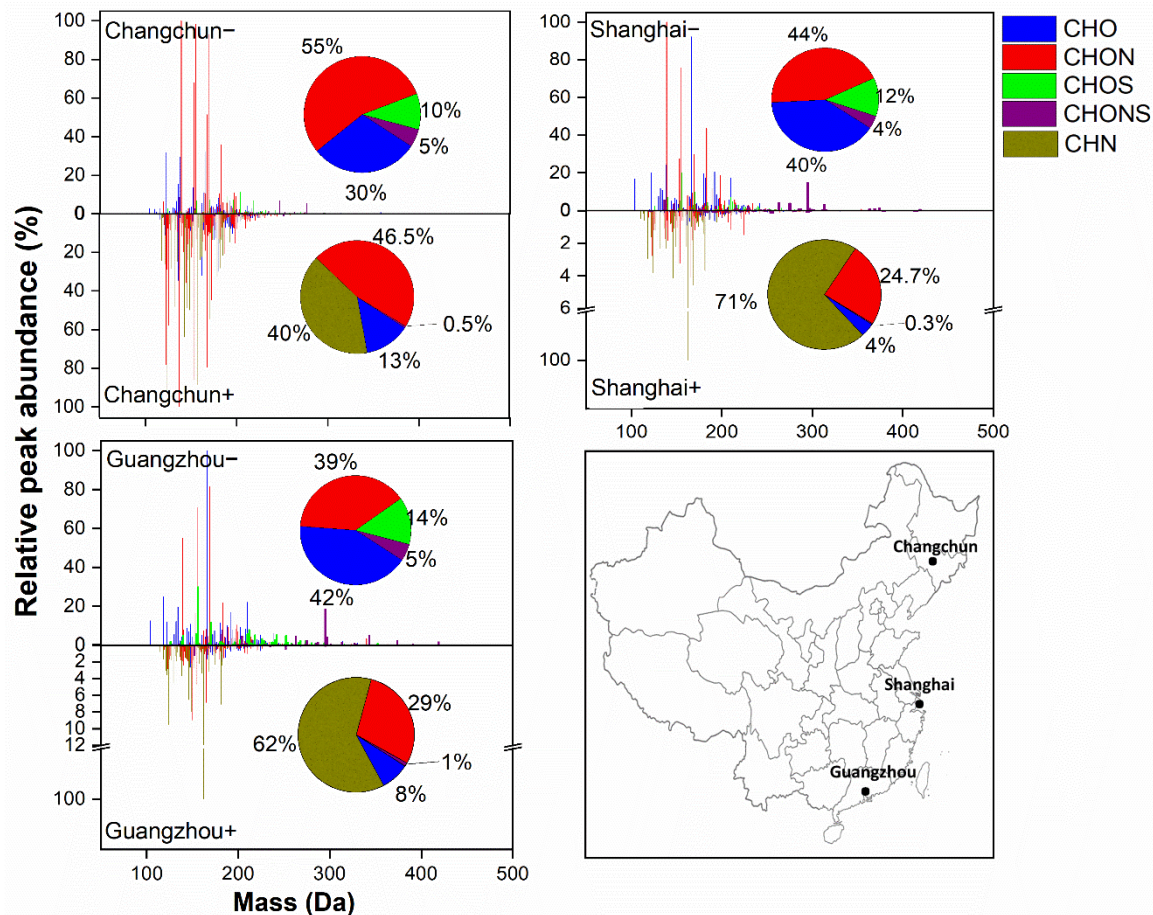
864

865 Table 1. Number of organic compounds and molecular formulas in each subgroup and the peak
 866 abundance-weighted average values of molecular mass (MM_{avg}), elemental ratios, double bond
 867 equivalent (DBE), aromaticity equivalent (X_c) and isomer number fraction (meaning the
 868 percentage of formula numbers that have isomers among all assigned formulas) for detected
 869 organic compounds in ESI⁻ and ESI⁺ in the three Chinese cities.

Sample ID	Subgroup	Number of compounds*	Relative abundance (%)	MM_{avg}	H/C	O/C**	DBE	X_c	Isomer number fraction (%)
Changchun ⁻	total	769(415)	100	169	1.03	0.58	5.02	2.13	34
	CHO ⁻	346(136)	30	162	0.96	0.41	5.65	2.28	52
	CHON ⁻	180(96)	55	163	0.94	0.51	5.24	2.44	36
	CHOS ⁻	155(105)	10	198	1.56	1.17(0.52)	2.55	0.50	28
	CHONS ⁻	88(78)	5	214	1.35	1.07(-1.4)	3.75	1.06	8
Shanghai ⁻	total	416(272)	100	176	1.05	0.69	4.99	1.92	31
	CHO ⁻	164(90)	40	171	0.97	0.59	5.37	1.94	41
	CHON ⁻	135(89)	44	169	0.86	0.56	5.67	2.47	37
	CHOS ⁻	75(62)	12	190	1.85	1.41(0.61)	1.79	0.34	15
	CHONS ⁻	42(31)	4	266	1.56	1.00(0.11)	3.30	0.44	13
Guangzhou ⁻	total	488(304)	100	183	1.14	0.74	4.55	1.65	34
	CHO ⁻	196(110)	42	172	1.10	0.65	4.68	1.57	44
	CHON ⁻	161(98)	39	173	0.89	0.58	5.56	2.41	35
	CHOS ⁻	86(67)	14	201	1.85	1.48(0.71)	1.71	0.21	21
	CHONS ⁻	45(29)	5	293	1.56	0.82(0.06)	3.45	0.43	28
Changchun ⁺	total	2943(679)	100	160	1.21	0.13	5.58	2.36	56
	CHO ⁺	609(162)	13	174	0.94	0.28	6.55	2.22	50
	CHN ⁺	696(126)	40	154	1.22	0.00	5.84	2.60	77
	CHON ⁺	1594(352)	46.5	161	1.27	0.19	5.11	2.22	55
	CHONS ⁺	44(39)	0.5	196	1.91	0.70	2.64	0.09	13
Shanghai ⁺	total	704(383)	100	162	1.37	0.09	4.91	2.32	32
	CHO ⁺	87(67)	4	184	1.13	0.43	5.46	1.46	19
	CHN ⁺	253(84)	71	159	1.38	0.00	5.08	2.55	54
	CHON ⁺	350(218)	24.7	167	1.40	0.27	4.34	1.81	30
	CHONS ⁺	14(14)	0.3	241	1.17	0.61	5.32	0.91	0
Guangzhou ⁺	total	687(412)	100	161	1.41	0.17	4.58	2.07	30
	CHO ⁺	125(87)	8	185	1.12	0.42	5.19	1.20	26
	CHN ⁺	205(78)	62	156	1.42	0.00	4.80	2.47	54
	CHON ⁺	336(227)	29	165	1.47	0.45	4.00	1.51	26
	CHONS ⁺	21(20)	1	209	1.84	0.71	3.05	0.31	5

870 *The values in brackets indicate the number of unique molecular formulas. **The values in brackets indicate the
 871 (O-3S)/C and (O-3S-2N)/C ratios for CHOS and CHONS compounds, respectively, detected in ESI⁻ mode

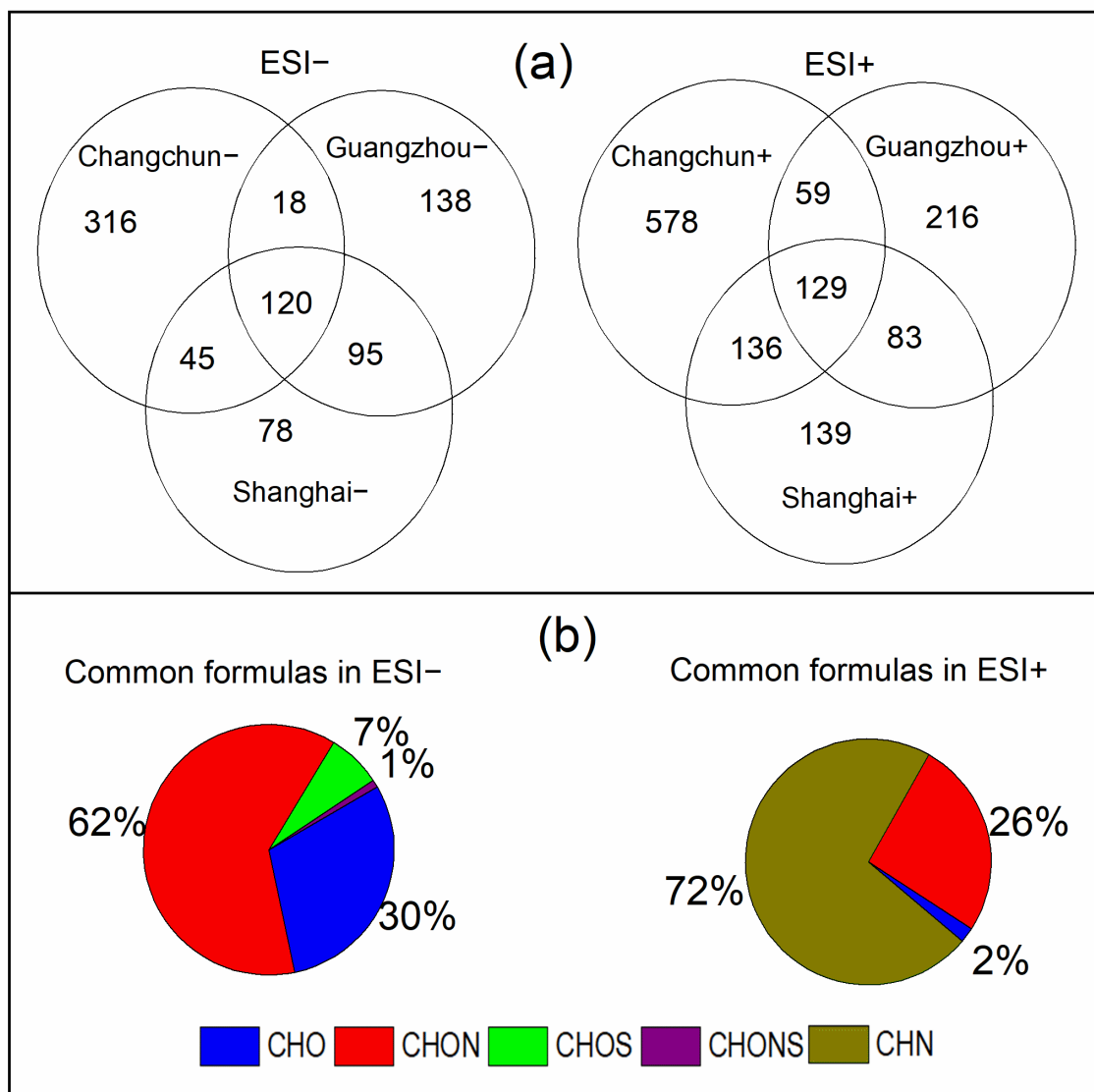
872



873

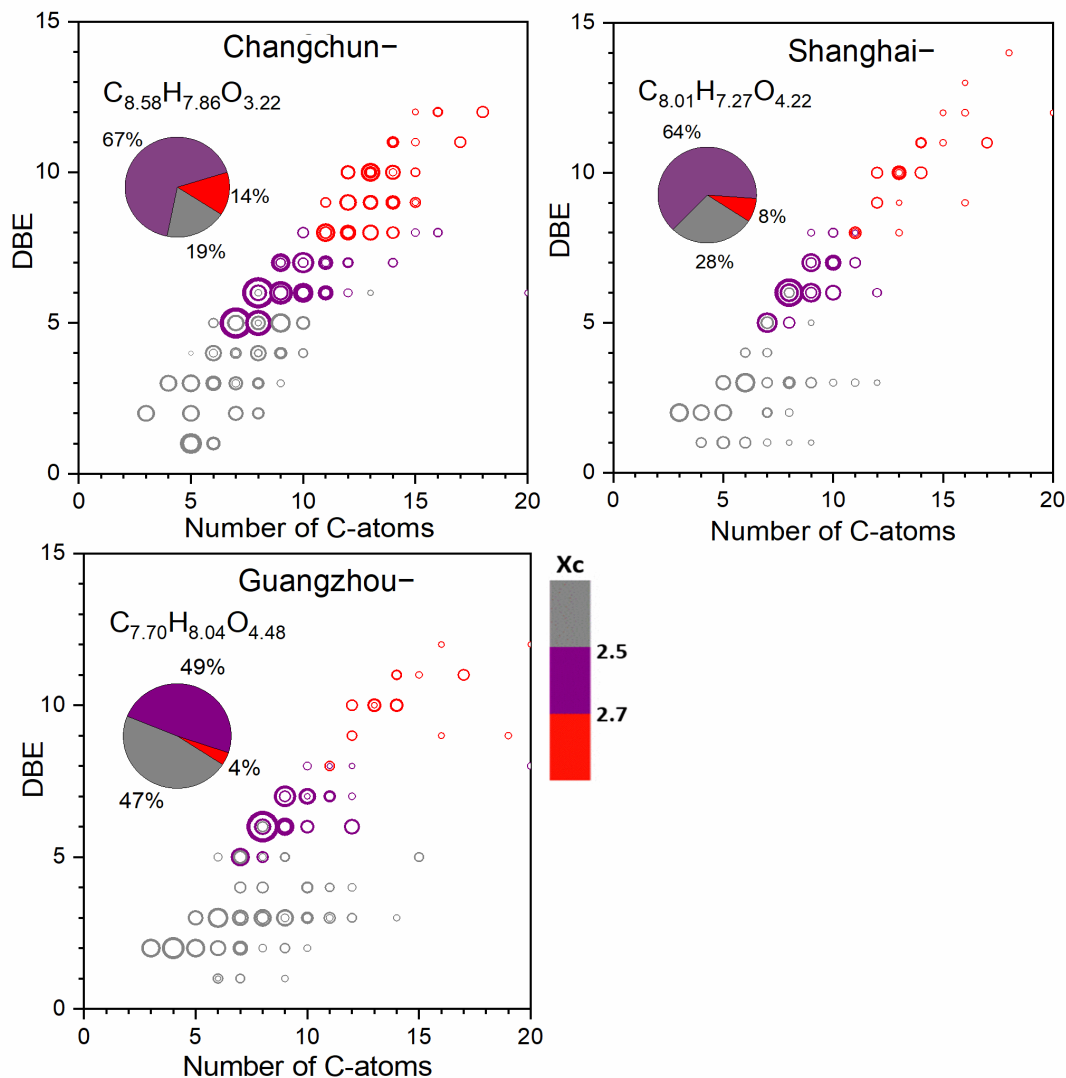
874 Figure 1. Mass spectra of detected organic compounds reconstructed from extracted ion
 875 chromatograms in ESI⁻ and ESI⁺. The horizontal axis refers to the molecular mass (Da) of the
 876 identified species. The vertical axis refers to the relative peak abundance of each individual
 877 compound to the compound with the greatest peak abundance. The pie charts show the percentage
 878 of each organic compound subgroup (i.e., CHO, CHON, CHOS, CHONS and CHN) in each sample
 879 in terms of peak abundance. The map in the lower right corner shows the locations of these three
 880 megacities in China.

881



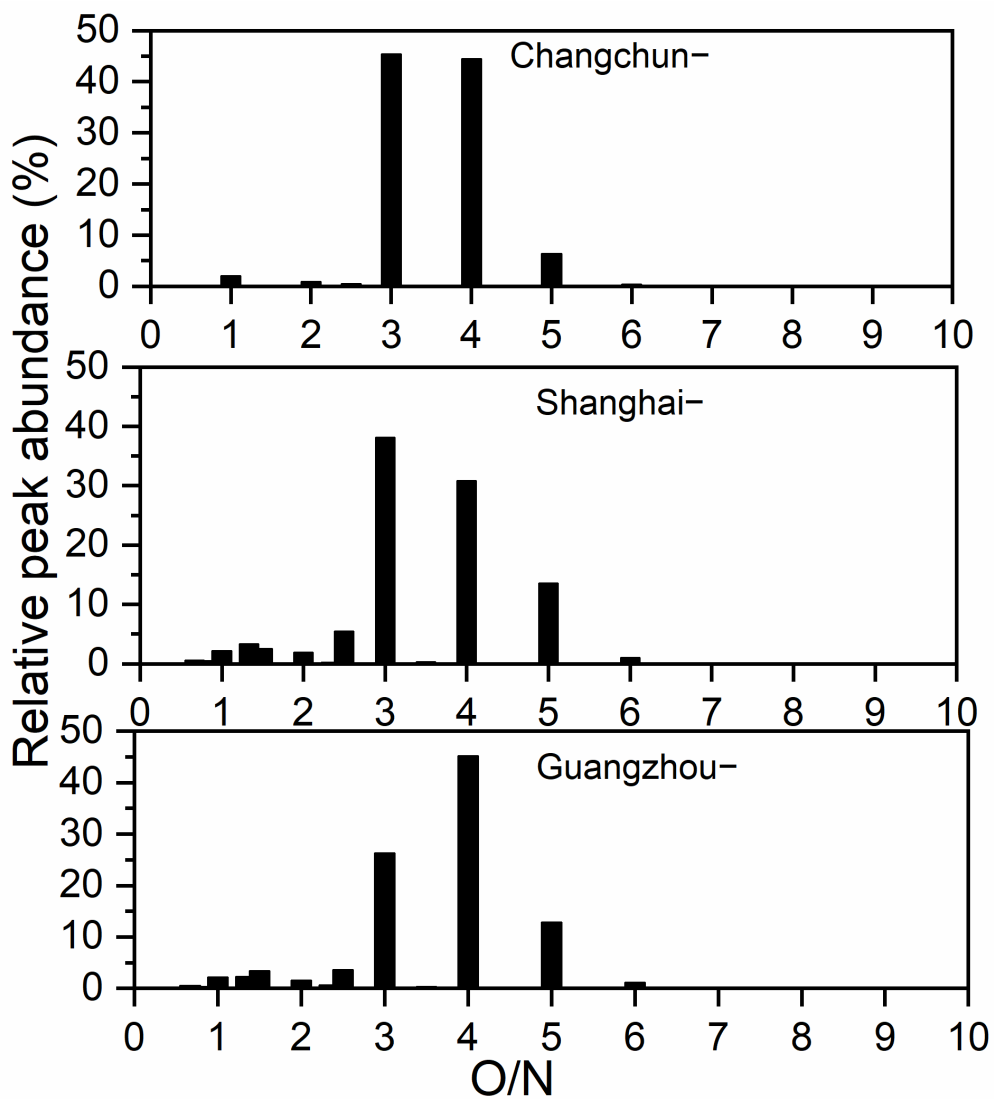
882

883 Figure 2. (a) Venn diagrams showing the number distribution of all molecular formulas detected in
 884 ESI- and ESI+ for all sample locations. The overlapping molecular formulas refer to the
 885 compounds detected in each city with the same molecular formulas and with the same retention
 886 times (retention time difference ≤ 0.1 min). (b) Peak abundance contribution of each elemental
 887 formula category to the total common formulas.



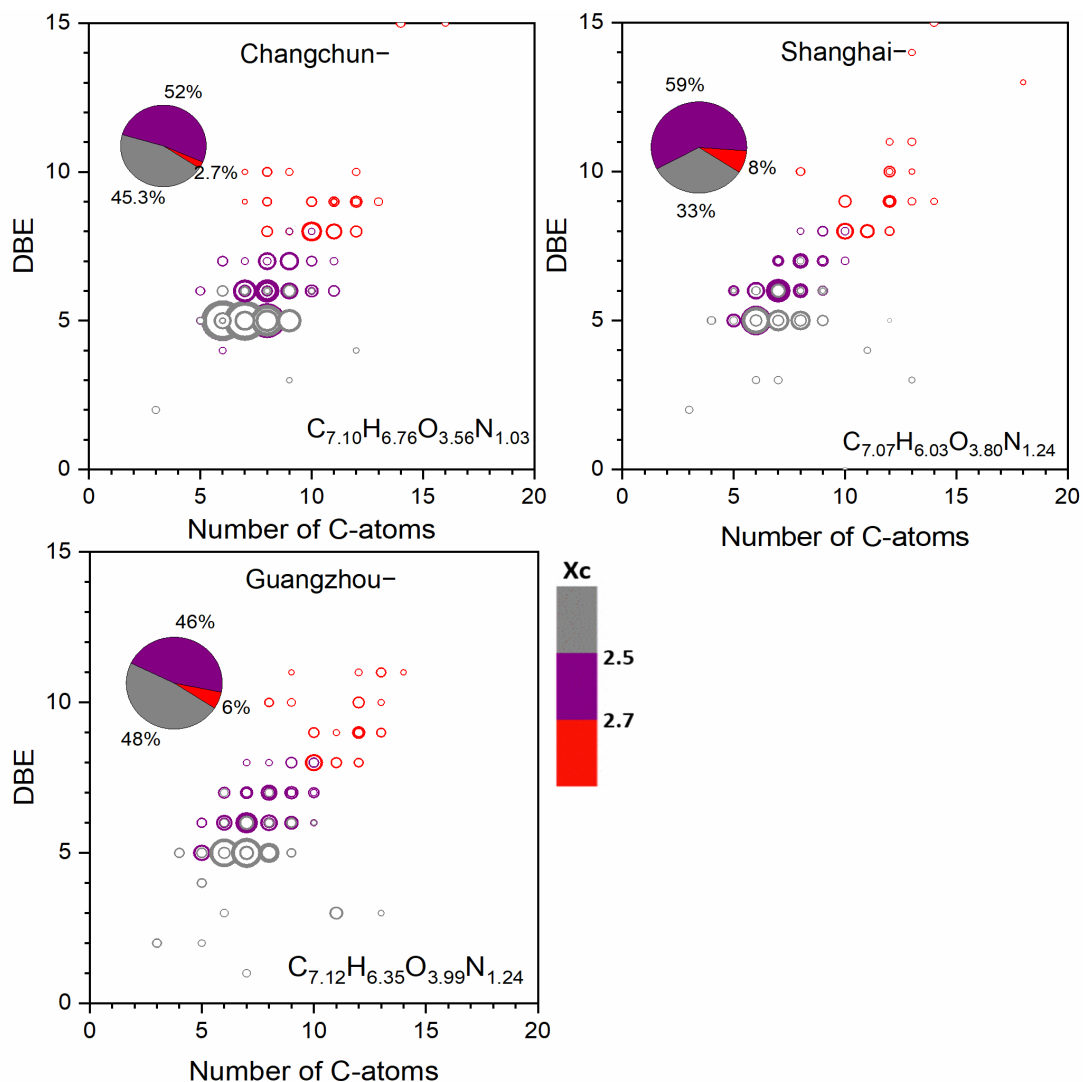
888

889 Figure 3. Double bond equivalent (DBE) versus carbon number for all CHO⁻ compounds for all
 890 sample locations. The molecular formula represents the abundance-weighted average CHO⁻
 891 formula and the area of the circles is proportional to the fourth root of the peak abundance of an
 892 individual compound (a diagram with circle areas related to the absolute peak abundances is
 893 presented in Fig. S2). The color bar denotes the aromaticity equivalent (gray with Xc < 2.50, purple
 894 with 2.50 ≤ Xc < 2.70 and red with Xc ≥ 2.70). The pie charts show the percentage of each Xc
 895 category (i.e., gray color-coded compounds, purple color-coded compounds and red color-coded
 896 compounds) in each sample in terms of peak abundance.



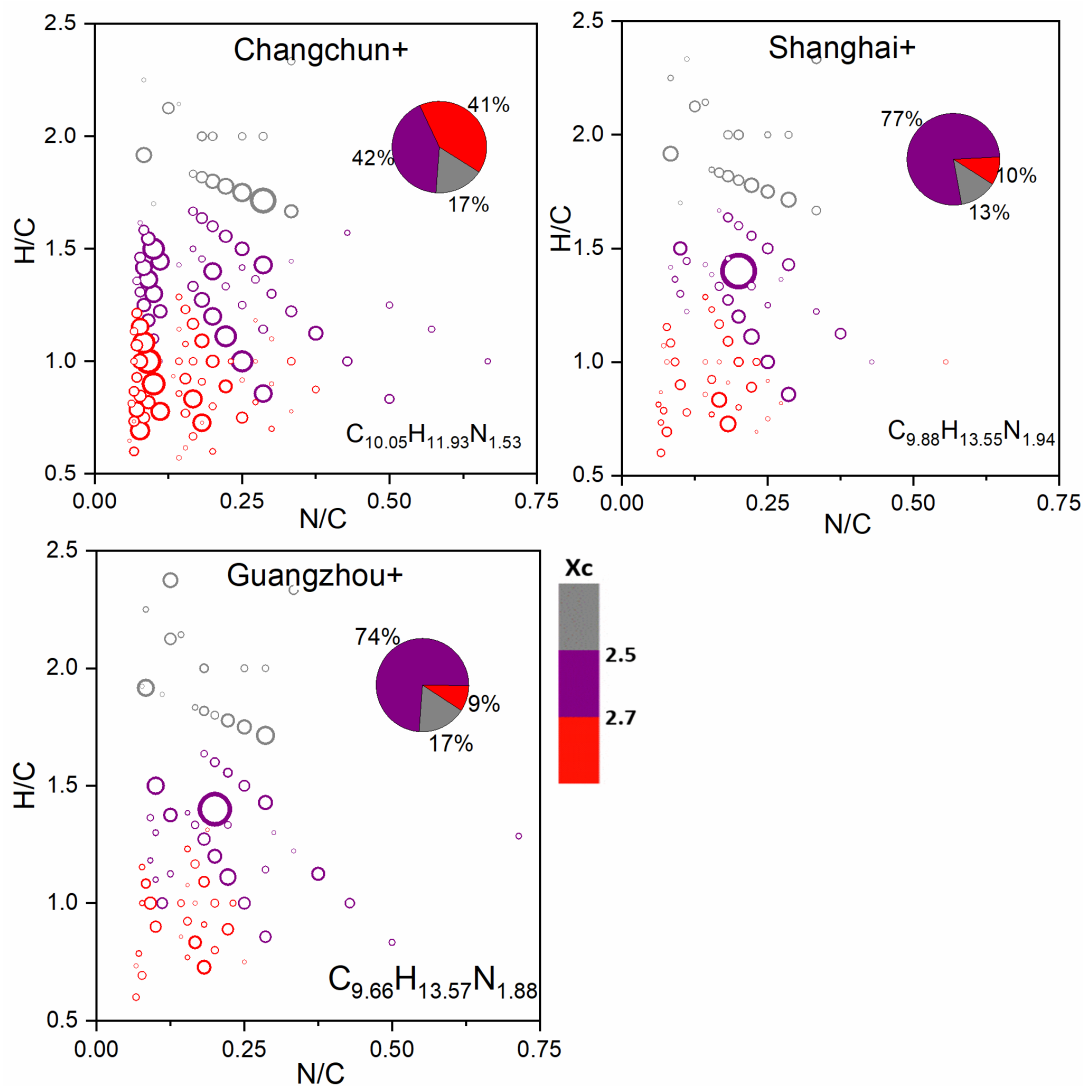
897

898 Figure 4. Classification of CHON⁻ compounds into different subgroups according to O/N ratios in
 899 their formulas. The y-axis indicates the relative contribution of each specific O/N ratio subgroup to
 900 the sum of peak abundances of CHON⁻ compounds.



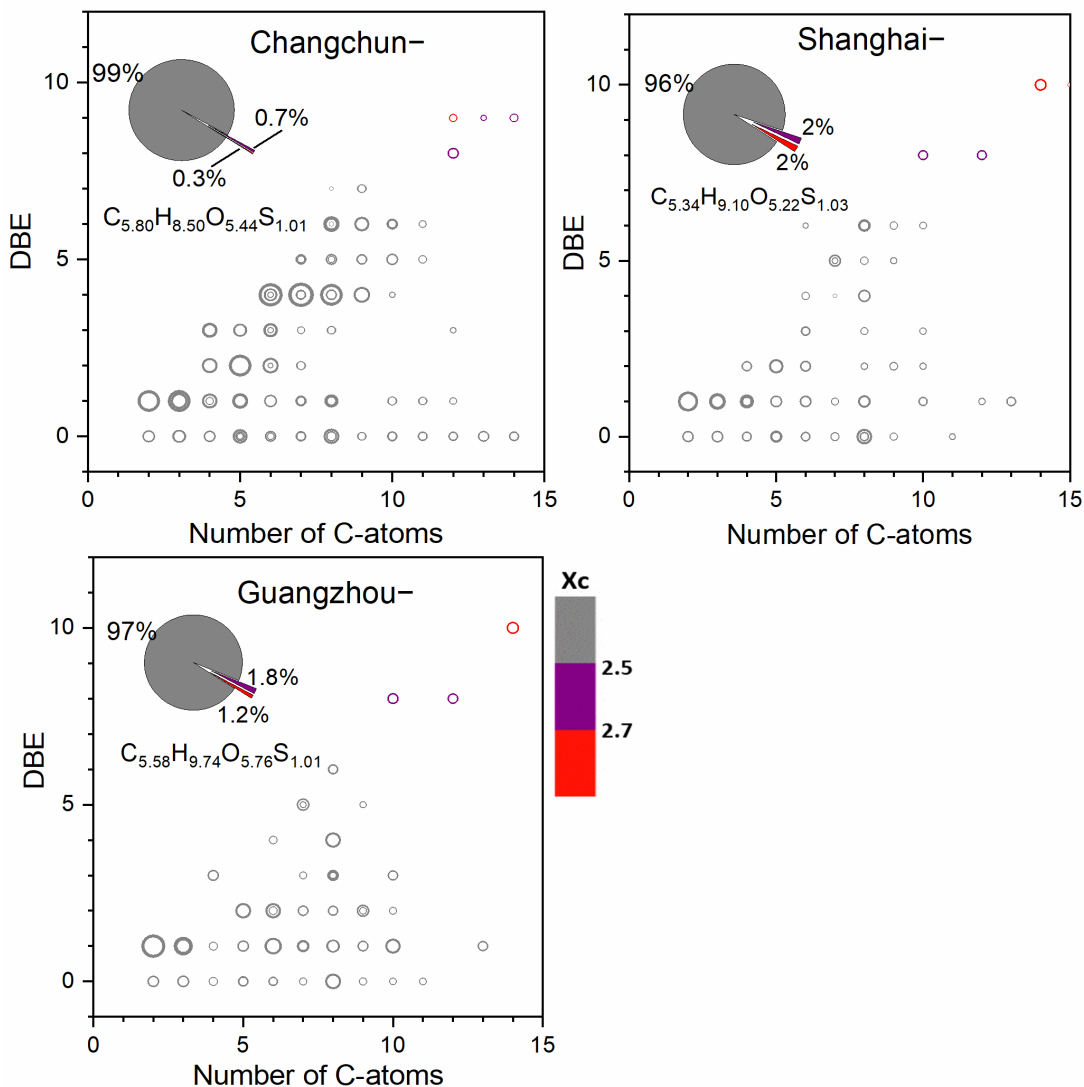
901

902 Figure 5. Double bond equivalent (DBE) versus carbon number for all CHON-
 903 compounds for all sample locations. The molecular formula represents the abundance-weighted average CHON-
 904 formula and the area of circles is proportional to the fourth root of the peak abundance of an
 905 individual compound ([a diagram with circle areas related to absolute peak abundances is presented
 906 in Fig. S6](#)). The color bar denotes the aromaticity equivalent (gray with $X_c < 2.50$, purple with 2.50
 907 $\leq X_c < 2.70$ and red with $X_c \geq 2.70$). The pie charts show the percentage of each X_c category (i.e.,
 908 gray color-coded compounds, purple color-coded compounds and red color-coded compounds) in
 909 each sample in terms of peak abundance.



910

911 Figure 6. Van Krevelen diagrams for CHN+ compounds in Changchun, Shanghai and Guangzhou
 912 samples. The area of circles is proportional to the fourth root of the peak abundance of an individual
 913 compound (a diagram with circle areas related to absolute peak abundances is presented in Fig.
 914 S10) and the color bar denotes the aromaticity equivalent (gray with $X_c < 2.50$, purple with $2.50 \leq$
 915 $X_c < 2.70$ and red with $X_c \geq 2.70$). The pie charts show the percentage of each Xc category (i.e.,
 916 gray color-coded compounds, purple color-coded compounds and red color-coded compounds) in
 917 each sample in terms of peak abundance.



918

919 Figure 7. Double bond equivalent (DBE) versus carbon number for all CHOS- compounds for all
 920 sample locations. The molecular formula represents the abundance-weighted average CHOS-
 921 formula and the area of circles is proportional to the fourth root of the peak abundance of an
 922 individual compound ([a diagram with circle areas related to absolute peak abundances is presented](#)
 923 [in Fig. S11](#)). The color bar denotes the aromaticity equivalent (gray with $X_c < 2.50$, purple with
 924 $2.50 \leq X_c < 2.70$ and red with $X_c \geq 2.70$). The pie charts show the percentage of each X_c category
 925 (i.e., gray color-coded compounds, purple color-coded compounds and red color-coded compounds)
 926 in each sample in terms of peak abundance.

927

928

929

1 **Supplement material**

2 **Urban organic aerosol composition in Eastern China differs from North to South: Molecular**
3 **insight from a liquid chromatography-Orbitrap mass spectrometry study**

4 **Kai Wang et al.**

5 Corresponding Author: Ru-Jin Huang (rujin.huang@ieecas.cn) and Thorsten Hoffmann
6 (t.hoffmann@uni-mainz.de)

7

8

9

10

11

12

13

14

15

16

17

18

19

20

21

22

23

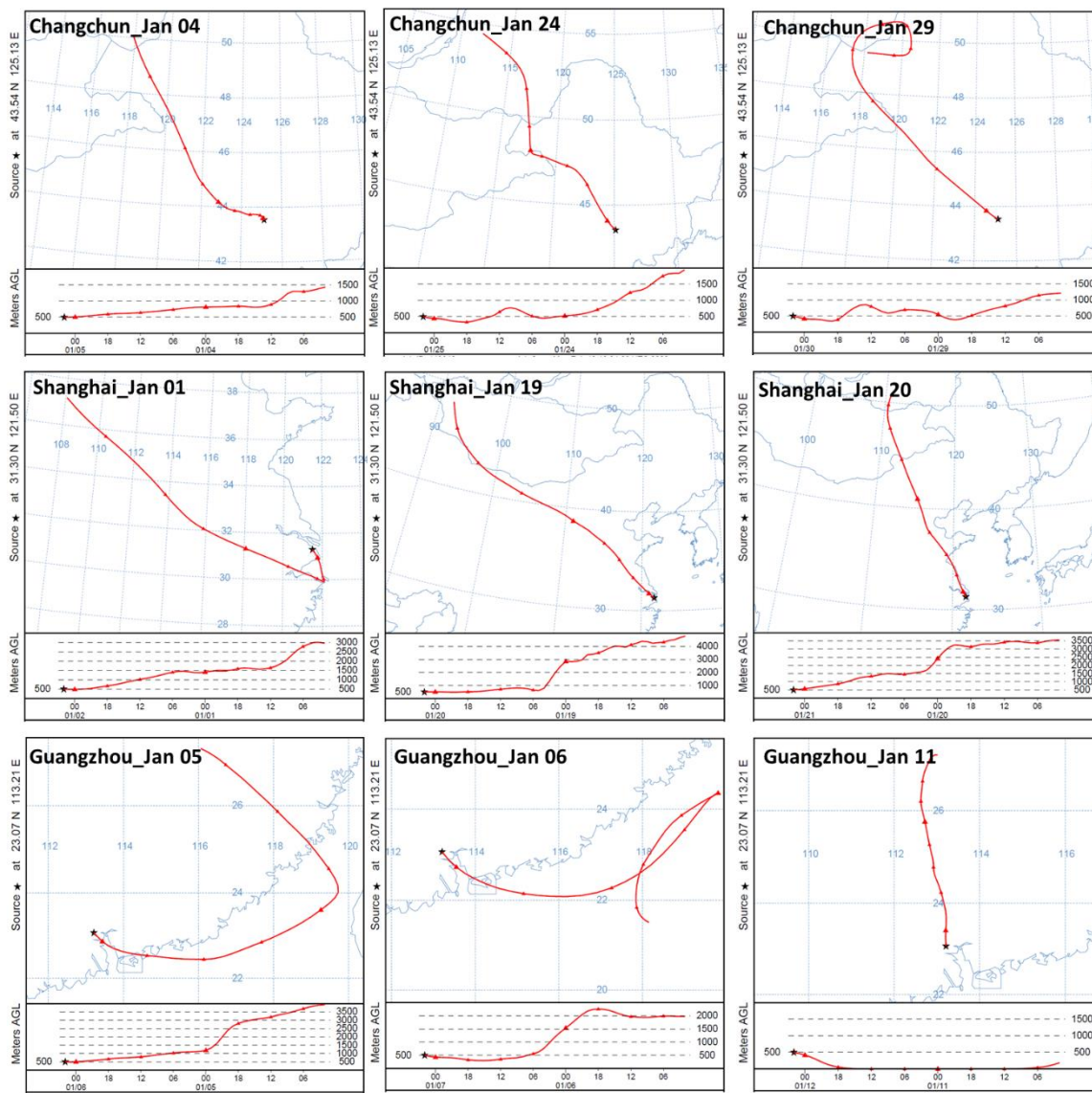
24

25 Table S1: The daily average concentrations of PM_{2.5}, SO₂, NO₂, CO and O₃, average
 26 temperature (T) and daily solar radiation in Changchun, Shanghai and Guangzhou during filter
 27 sampling dates.

Sample ID	Sampling Date	PM _{2.5} ($\mu\text{g m}^{-3}$)	SO ₂ ($\mu\text{g m}^{-3}$)	NO ₂ ($\mu\text{g m}^{-3}$)	CO (mg m^{-3})	O ₃ ($\mu\text{g m}^{-3}$)	T (°C)	<u>Solar radiation</u> (J cm^{-2})
Changchun	04-01-2014	222	72	63	1.5	43	-14	<u>841*</u>
	24-01-2014	162	77	51	1.4	70	-11	<u>485*</u>
	29-01-2014	185	70	29	0.9	58	-9	<u>576*</u>
Shanghai	01-01-2014	171	63	99	1.7	61	10	<u>1133*</u>
	19-01-2014	159	33	61	1.3	74	7	<u>1307</u>
	20-01-2014	172	59	76	1.8	42	6	<u>994</u>
Guangzhou	05-01-2014	152	39	89	1.4	113	16	<u>1372</u>
	06-01-2014	138	42	109	1.7	117	15	<u>1164</u>
	11-01-2014	138	24	80	1.6	69	16	<u>1329</u>

28 The data of SO₂, NO₂, CO, O₃ and T have been taken from an open air quality database (www.aqistudy.cn), while
 29 the data of solar radiation were provided by the World Radiation Data Centre
 30 (http://wrdc.mgo.rssi.ru/wrdc_en_new.htm). * Since the data of solar radiation for Changchun (43.54°N, 125.13°E)
 31 are not available, here we present the daily solar radiation data observed for Shengyang (41.44°N, 123.31°E),
 32 which is located quite close to Changchun.

33
 34
 35
 36
 37
 38
 39
 40
 41
 42
 43
 44
 45



47

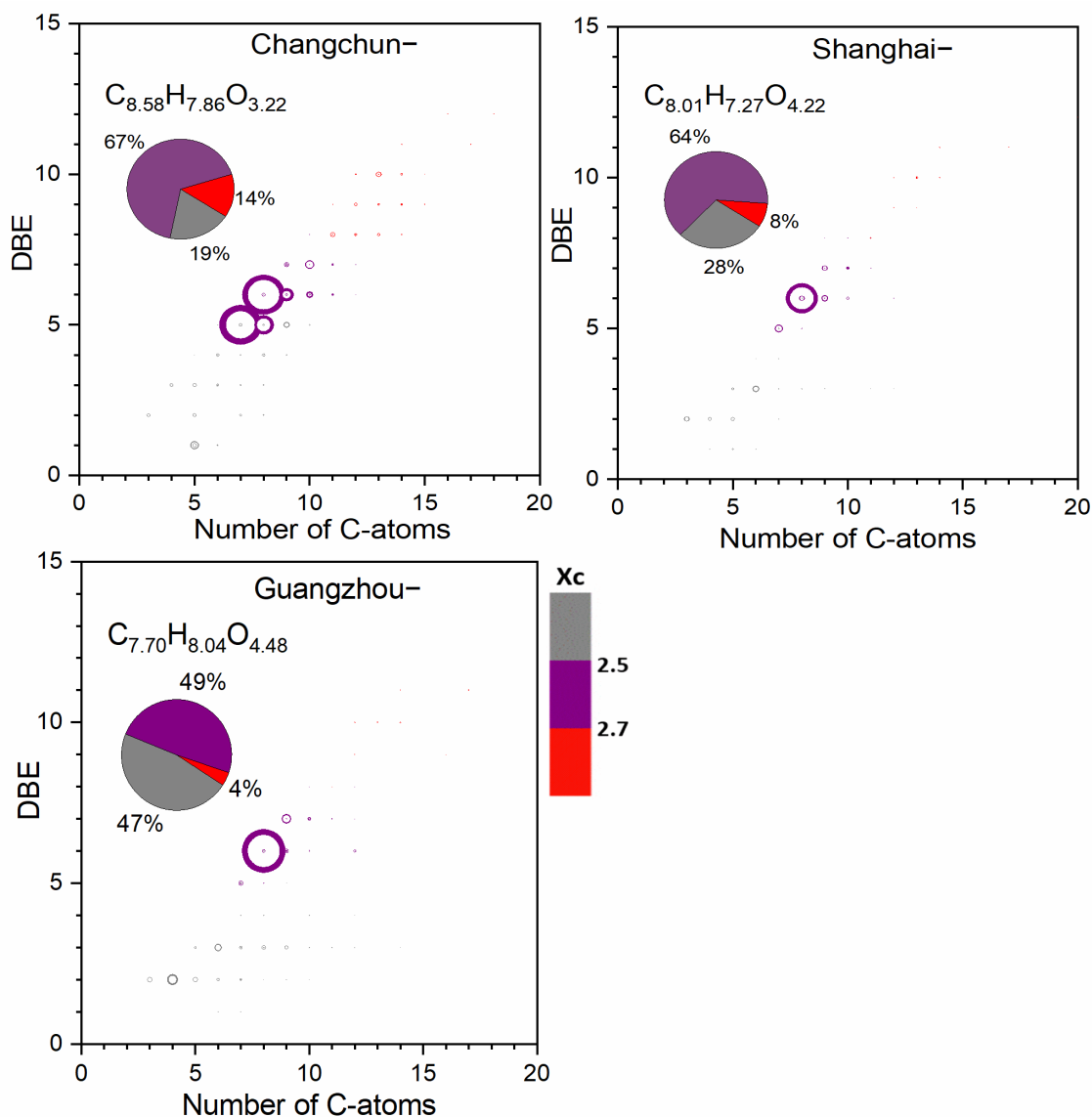
48 Figure S1. 48 hours back trajectories of air arriving at the three cities (Changchun, Shanghai and
 49 Guangzhou) during the sampling time calculated using the NOAA HYSPLIT model (Rolph et al.,
 50 2017).

51

52

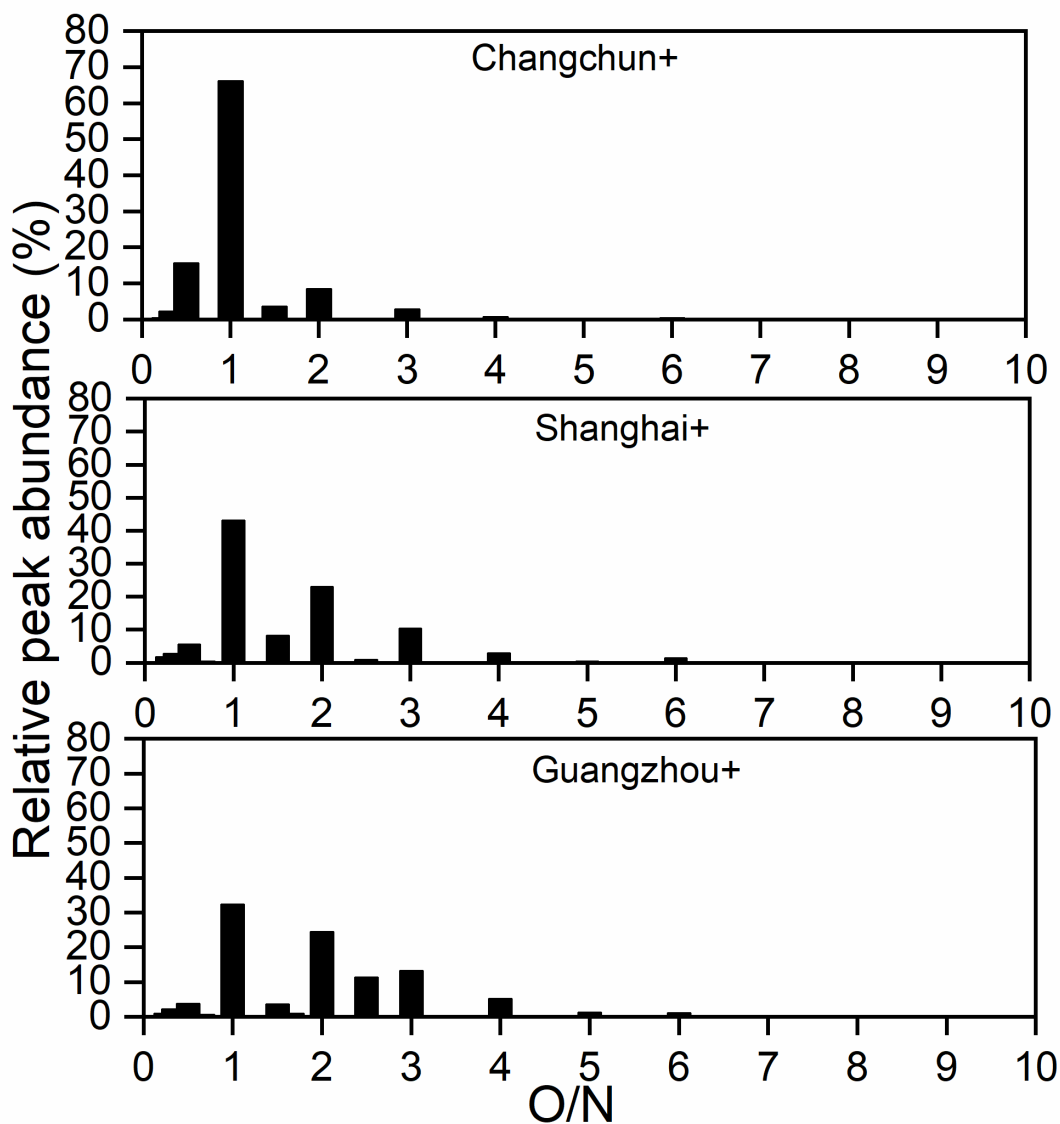
53

54



56

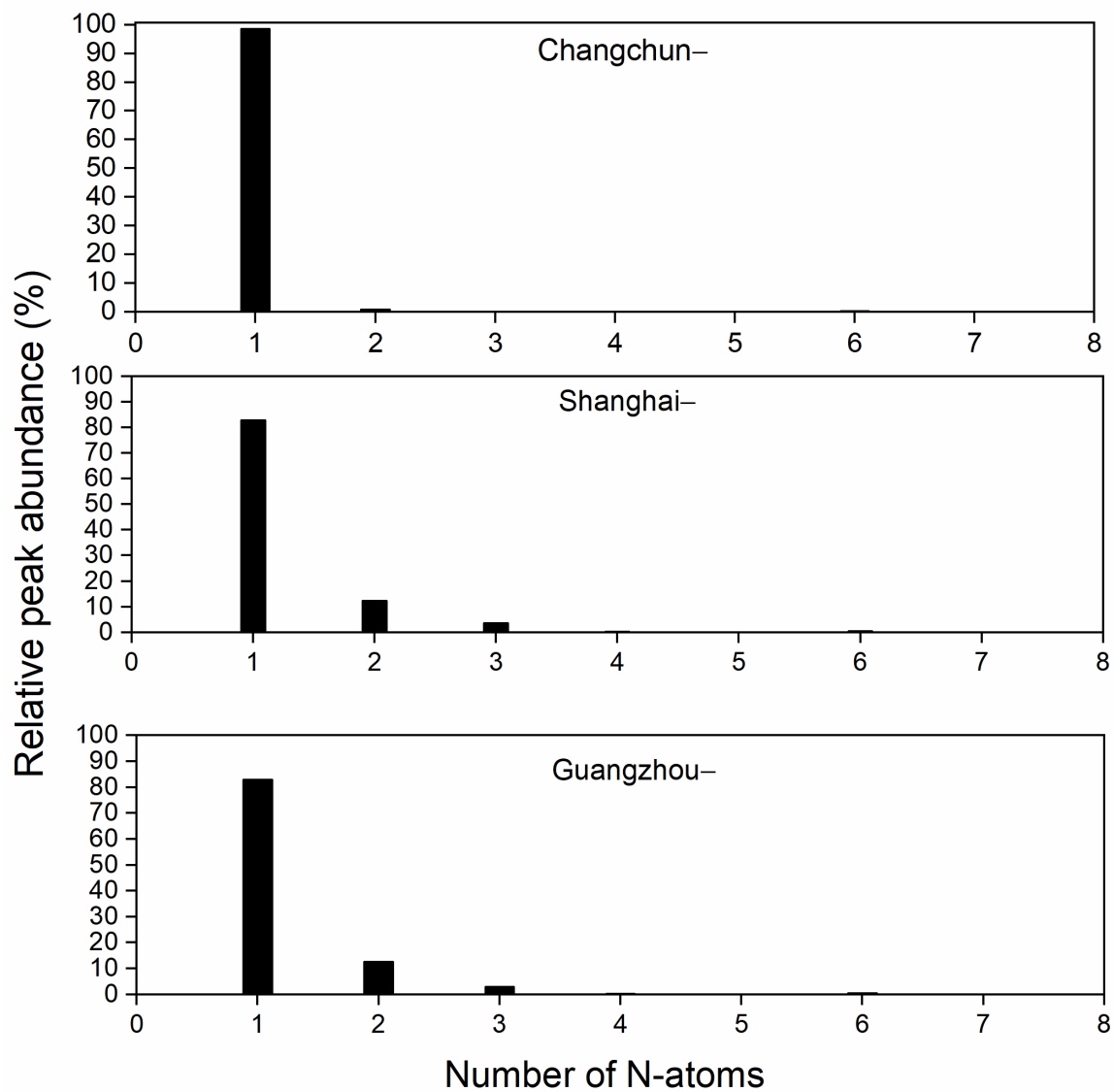
57 Figure S2. Double bond equivalent (DBE) versus carbon number for all CHO- compounds for all
 58 sample locations. The molecular formula represents the abundance-weighted average CHO-
 59 formula and the area of the circles is proportional to the absolute peak abundance of an individual
 60 compound. The color bar denotes the aromaticity equivalent (gray with $X_c < 2.50$, purple with 2.50
 61 $\leq X_c < 2.70$ and red with $X_c \geq 2.70$). The pie charts show the percentage of each X_c category (i.e.,
 62 gray color-coded compounds, purple color-coded compounds and red color-coded compounds) in
 63 each sample in terms of peak abundance.



64

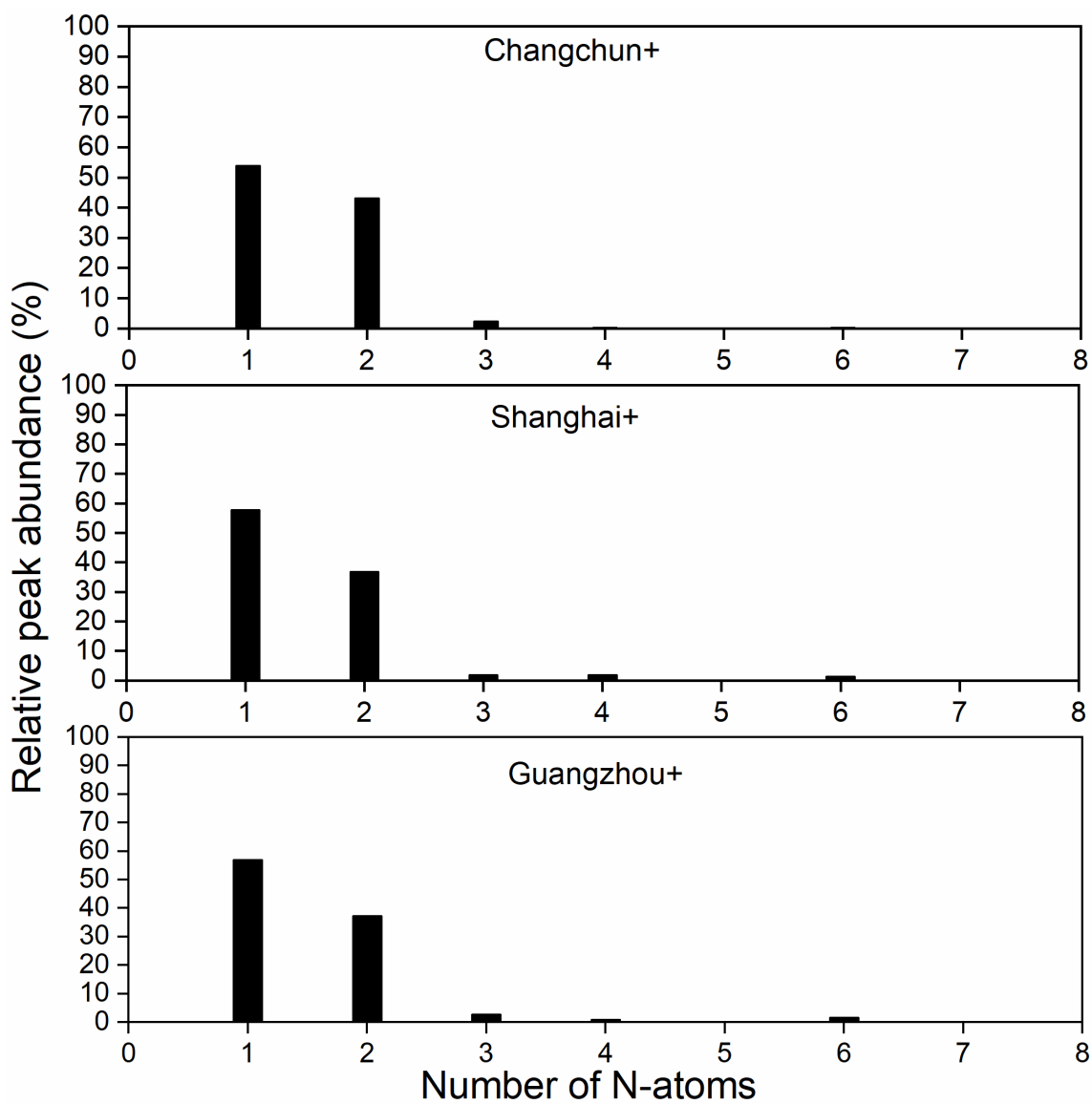
65 Figure S3. Classification of CHON+ compounds into different subgroups according to O/N ratios
 66 in their formulas. The y-axis indicates the relative contribution of each subgroup to the sum of peak
 67 abundance of CHON+ compounds.

68



69

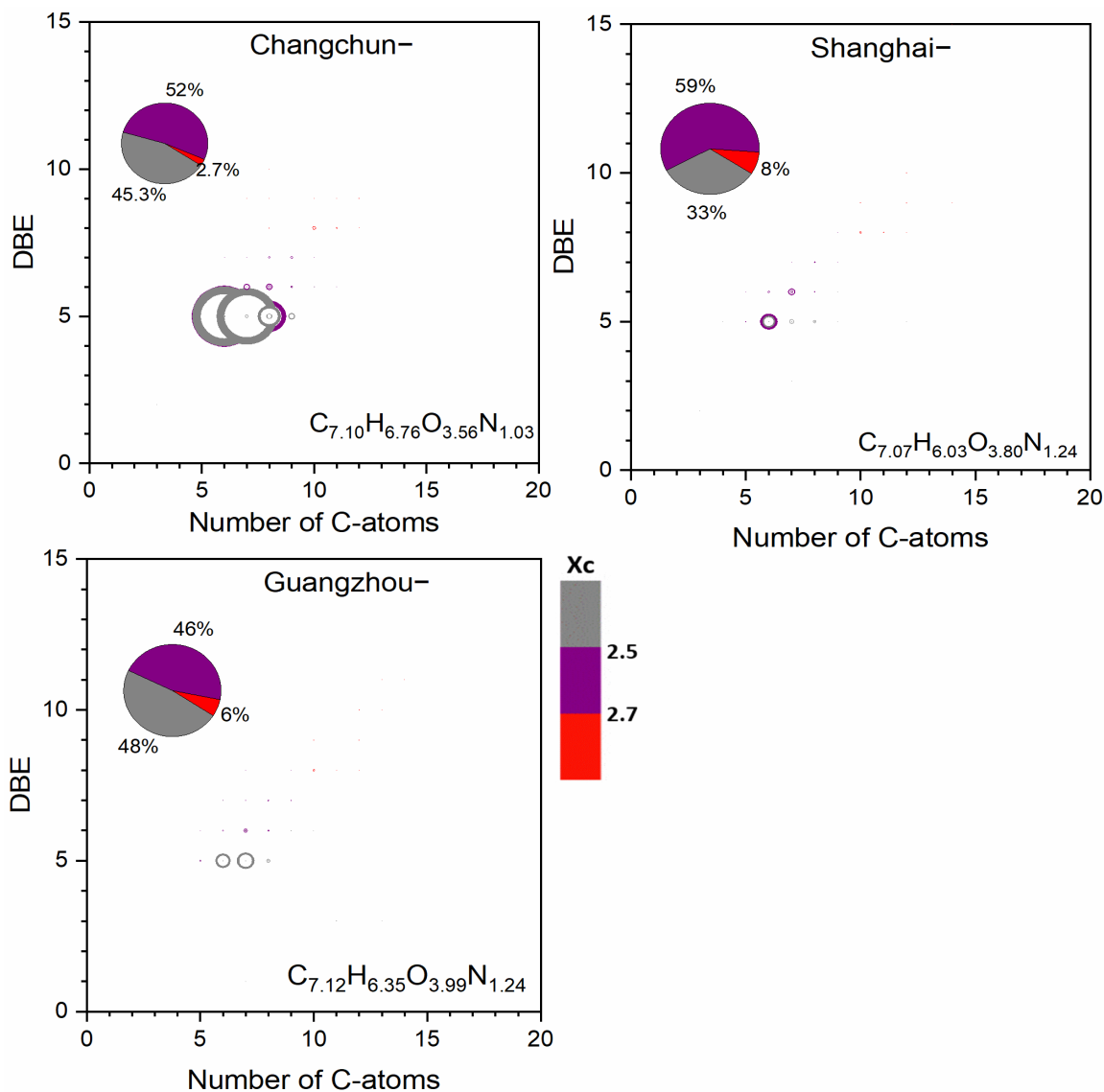
70 Figure S4. Classification of CHON⁻ compounds into different subgroups according to nitrogen
 71 atoms number in their formulas. The y-axis indicates the relative contribution of each subgroup to
 72 the sum of peak abundance of all CHON⁻ compounds.



73

74 Figure S5. Classification of CHON+ compounds into different subgroups according to nitrogen
 75 atoms number in their formulas. The y-axis indicates the relative contribution of each subgroup to
 76 the sum of peak abundance of all CHON+ compounds.

77

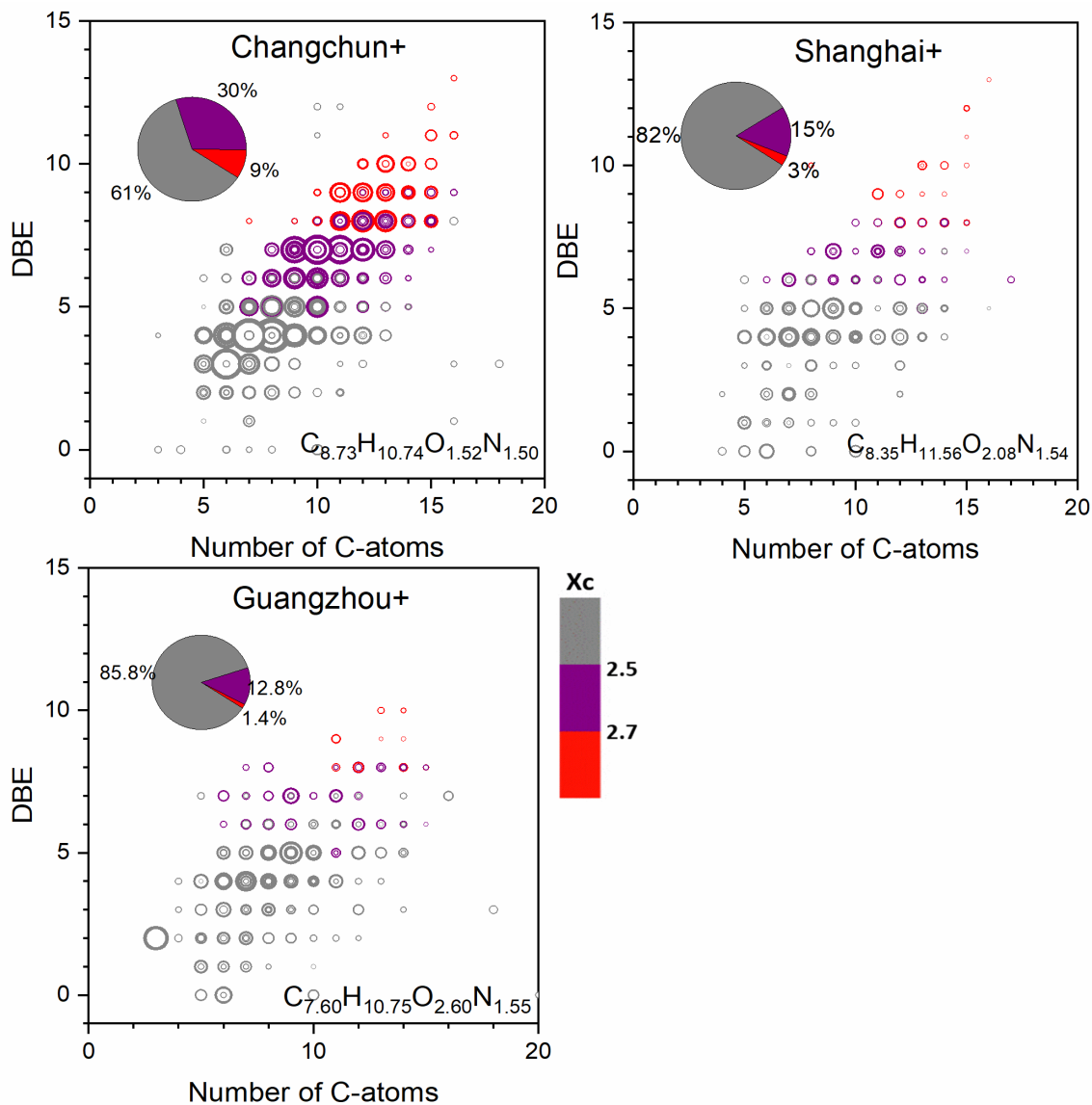


78

79 Figure S6. Double bond equivalent (DBE) versus carbon number for all CHON⁻ compounds for
 80 all sample locations. The molecular formula represents the abundance-weighted average CHON-
 81 formula and the area of circles is proportional to the absolute peak abundance of an individual
 82 compound. The color bar denotes the aromaticity equivalent (gray with $X_c < 2.50$, purple with 2.50
 83 $\leq X_c < 2.70$ and red with $X_c \geq 2.70$). The pie charts show the percentage of each X_c category (i.e.,
 84 gray color-coded compounds, purple color-coded compounds and red color-coded compounds) in
 85 each sample in terms of peak abundance.

86

87



88

89 Figure S7. Double bond equivalent (DBE) vs C number for all CHON+ compounds of all samples.

90 The molecular formula represents the abundance-weighted average CHON+ formula and the area

91 of the circles is proportional to the fourth root of the peak abundance of an individual compound

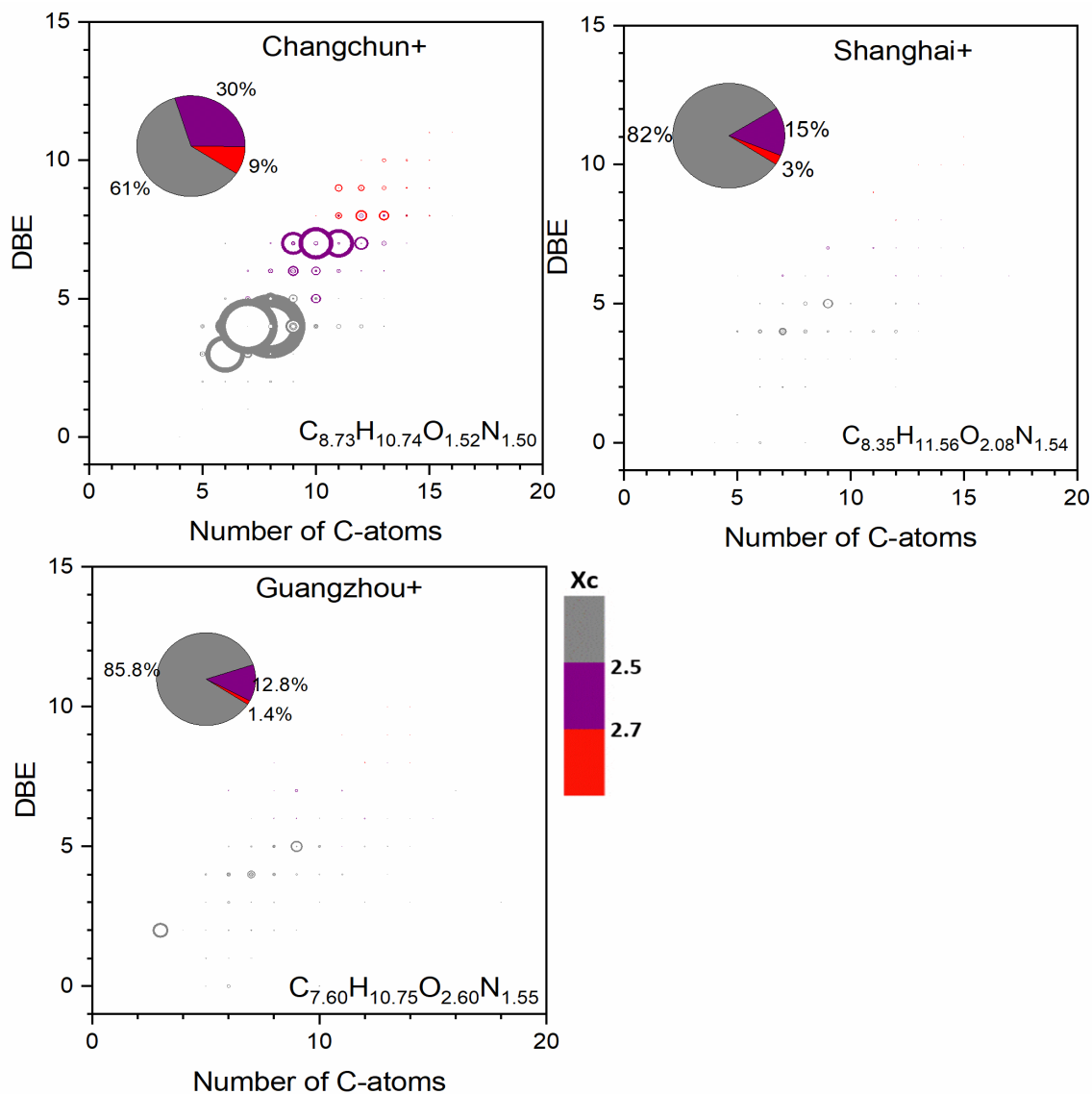
92 [\(the diagram with circle area related to absolute peak abundance is presented in Fig. S8\)](#). The color

93 bar denotes the aromaticity equivalent (gray with $X_c < 2.50$, purple with $2.50 \leq X_c < 2.70$ and red

94 with $X_c \geq 2.70$). The pie charts show the percentage of each X_c category (i.e., gray color-coded

95 compounds, purple color-coded compounds and red color-coded compounds) in each sample in

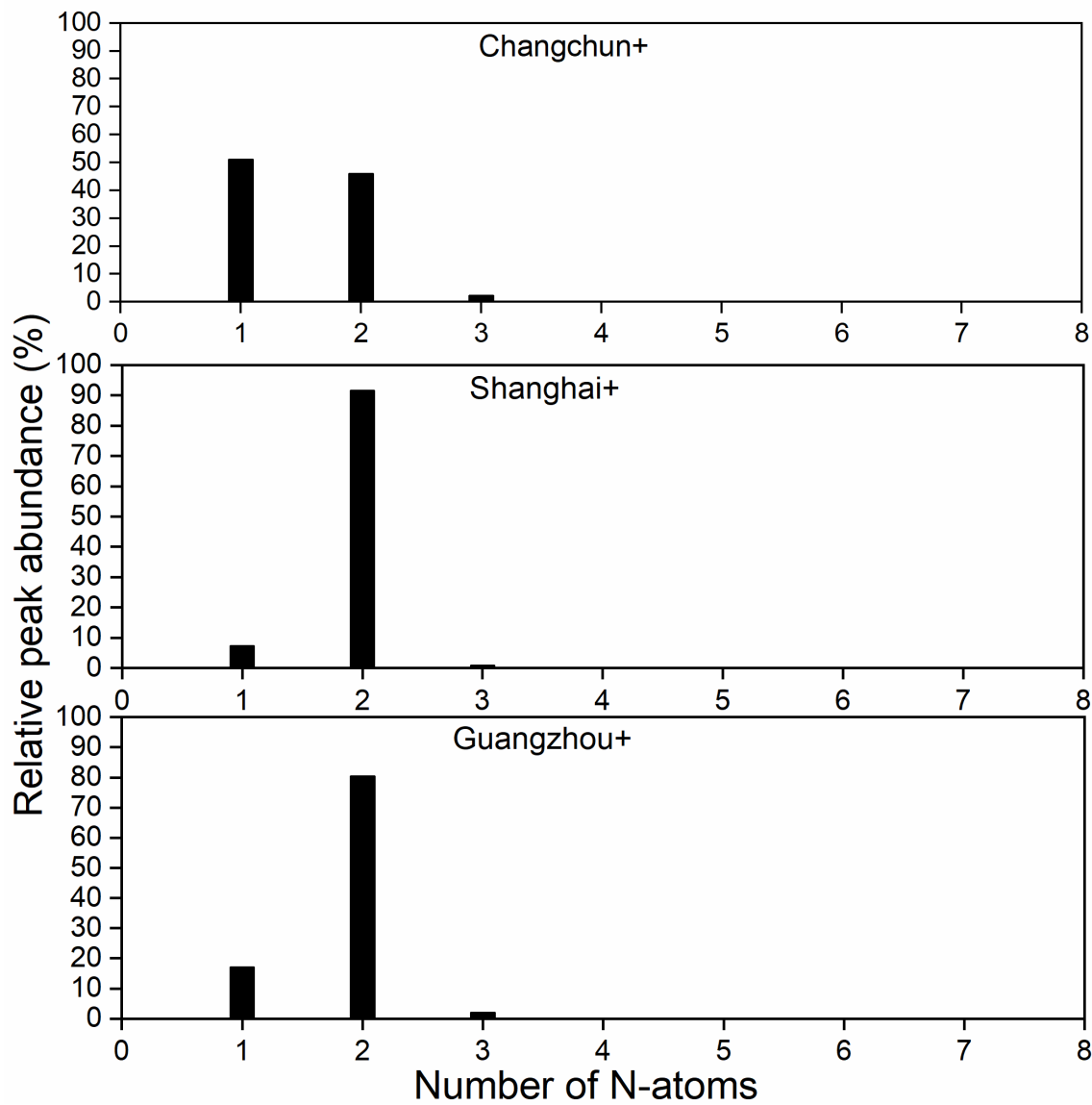
96 terms of peak abundance.



97

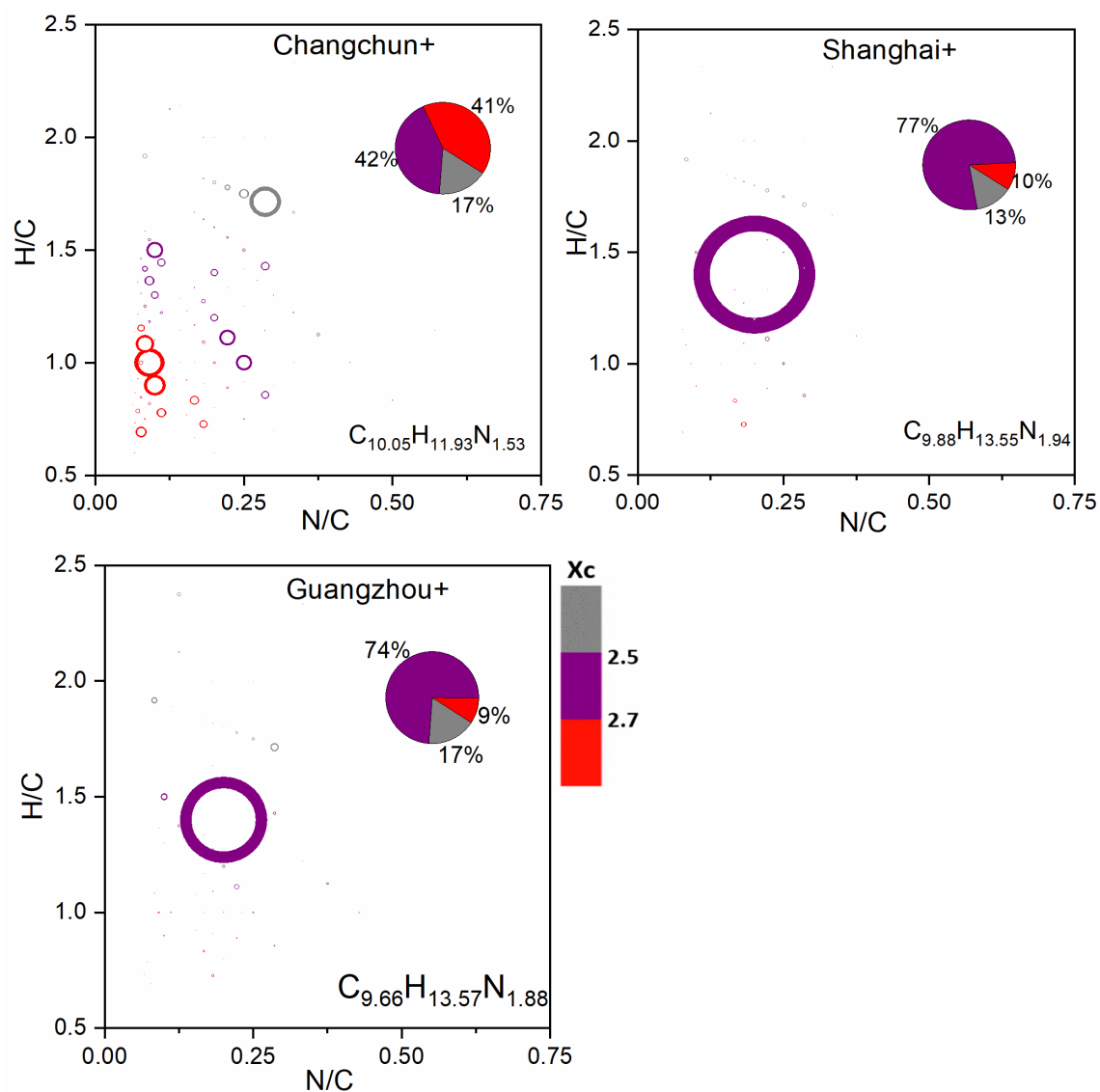
98 Figure S8. Double bond equivalent (DBE) vs C number for all CHON+ compounds of all samples.
 99 The molecular formula represents the abundance-weighted average CHON+ formula and the area
 100 of the circles is proportional to the absolute peak abundance of an individual compound. The color
 101 bar denotes the aromaticity equivalent (gray with $X_c < 2.50$, purple with $2.50 \leq X_c < 2.70$ and red
 102 with $X_c \geq 2.70$). The pie charts show the percentage of each X_c category (i.e., gray color-coded
 103 compounds, purple color-coded compounds and red color-coded compounds) in each sample in
 104 terms of peak abundance.

105



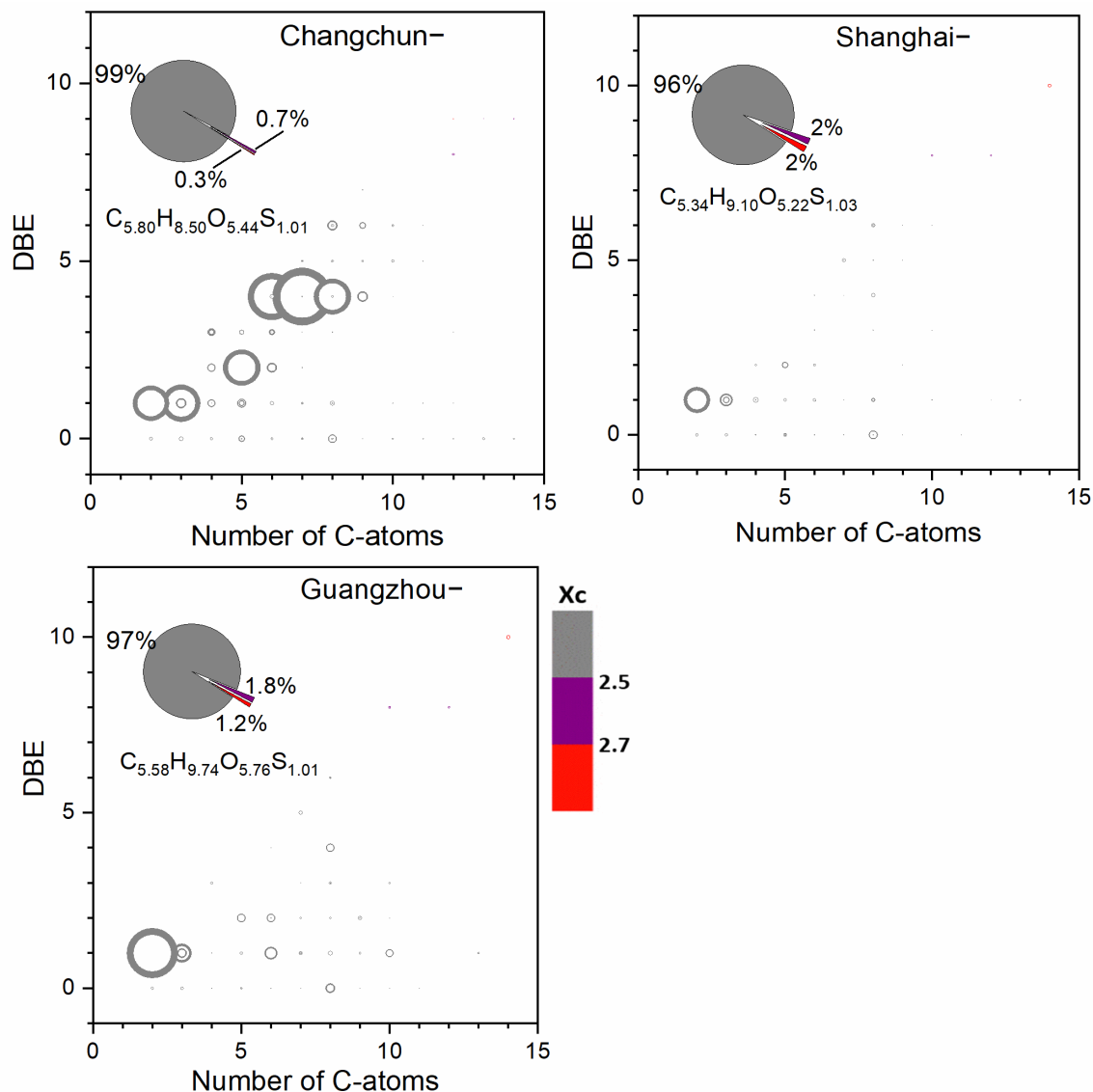
106

107 Figure S9. Classification of CHN+ compounds into different subgroups according to nitrogen
 108 atoms number in their formulas. The y-axis indicates the relative contribution of each subgroup to
 109 the sum of peak abundance of all CHN+ compounds.



110

111 Figure S10. Van Krevelen diagrams for CHN+ compounds in Changchun, Shanghai and
 112 Guangzhou samples. The area of circles is proportional to the absolute peak abundance of an
 113 individual compound and the color bar denotes the aromaticity equivalent (gray with Xc < 2.50,
 114 purple with 2.50 ≤ Xc < 2.70 and red with Xc ≥ 2.70). The pie charts show the percentage of each
 115 Xc category (i.e., gray color-coded compounds, purple color-coded compounds and red color-
 116 coded compounds) in each sample in terms of peak abundance.



117

118 Figure S11. Double bond equivalent (DBE) versus carbon number for all CHOS- compounds for
 119 all sample locations. The molecular formula represents the abundance-weighted average CHOS-
 120 formula and the area of circles is proportional to the absolute peak abundance of an individual
 121 compound. The color bar denotes the aromaticity equivalent (gray with $X_c < 2.50$, purple with 2.50
 122 $\leq X_c < 2.70$ and red with $X_c \geq 2.70$). The pie charts show the percentage of each X_c category (i.e.,
 123 gray color-coded compounds, purple color-coded compounds and red color-coded compounds) in
 124 each sample in terms of peak abundance.

125

126

127

References

- 128 Kind, T., and Fiehn, O.: Seven Golden Rules for heuristic filtering of molecular formulas obtained by
129 accurate mass spectrometry, *BMC Bioinformatics*, 8, 10.1186/1471-2105-8-105, 2007.
- 130 Kourtchev, I., Godoi, R. H. M., Connors, S., Levine, J. G., Archibald, A. T., Godoi, A. F. L., Paralovo, S. L.,
131 Barbosa, C. G. G., Souza, R. A. F., Manzi, A. O., Seco, R., Sjostedt, S., Park, J.-H., Guenther, A., Kim,
132 S., Smith, J., Martin, S. T., and Kalberer, M.: Molecular composition of organic aerosols in central
133 Amazonia: an ultra-high-resolution mass spectrometry study, *Atmos. Chem. Phys.*, 16, 11899-11913,
134 <https://doi.org/10.5194/acp-16-11899-2016>, 2016.
- 135 Lin, P., Rincon, A. G., Kalberer, M., and Yu, J. Z.: Elemental composition of HULIS in the Pearl River Delta
136 Region, China: results inferred from positive and negative electrospray high resolution mass
137 spectrometric data, *Environ. Sci. Technol.*, 46, 7454-7462, 10.1021/es300285d, 2012.
- 138 Rincón, A. G., Calvo, A. I., Dietzel, M., and Kalberer, M.: Seasonal differences of urban organic aerosol
139 composition - an ultra-high resolution mass spectrometry study, *Environ. Chem.*, 9, 298,
140 10.1071/en12016, 2012.
- 141 Rolph, G., Stein, A., and Stunder, B.: Real-time Environmental Applications and Display sYstem: READY,
142 *Environ. Model. Softw.*, 95, 210-228, 10.1016/j.envsoft.2017.06.025, 2017.
- 143 Wang, K., Zhang, Y., Huang, R.-J., Cao, J., and Hoffmann, T.: UHPLC-Orbitrap mass spectrometric
144 characterization of organic aerosol from a central European city (Mainz, Germany) and a Chinese
145 megacity (Beijing), *Atmos. Environ.*, 189, 22-29, 10.1016/j.atmosenv.2018.06.036, 2018.
- 146 Wang, X. K., Hayeck, N., Brüggemann, M., Yao, L., Chen, H. F., Zhang, C., Emmelin, C., Chen, J. M.,
147 George, C., and Wang, L.: Chemical characterization of organic aerosol in: A study by Ultrahigh-
148 Performance Liquid Chromatography Coupled with Orbitrap Mass Spectrometry, *J. Geophys. Res.-Atmos.*,
149 122, 703-722, <https://doi.org/10.1002/2017JD026930>, 2017.
- 150 Yassine, M. M., Harir, M., Dabek-Zlotorzynska, E., and Schmitt-Kopplin, P.: Structural characterization of
151 organic aerosol using Fourier transform ion cyclotron resonance mass spectrometry: aromaticity
152 equivalent approach, *Rapid Commun. Mass Spectrom.*, 28, 2445-2454, 10.1002/rcm.7038, 2014.
- 153 Zielinski, A. T., Kourtchev, I., Bortolini, C., Fuller, S. J., Giorio, C., Popoola, O. A. M., Bogialli, S., Tapparo,
154 A., Jones, R. L., and Kalberer, M.: A new processing scheme for ultra-high resolution direct infusion
155 mass spectrometry data, *Atmos. Environ.*, 178, 129-139, 10.1016/j.atmosenv.2018.01.034, 2018.

156